

AWARD NUMBER: W81XWH-16-1-0244

TITLE: Epicatechin as a Therapeutic Strategy to Mitigate the Development of Cardiac Remodeling and Fibrosis

PRINCIPAL INVESTIGATOR: Francisco Villarreal

CONTRACTING ORGANIZATION: University of California, San Diego
La Jolla, CA 92093-0613

REPORT DATE: SEPTEMBER 2019

TYPE OF REPORT: ANNUAL

PREPARED FOR: U.S. Army Medical Research and Materiel Command
Fort Detrick, Maryland 21702-5012

DISTRIBUTION STATEMENT: Approved for Public Release;
Distribution Unlimited

The views, opinions and/or findings contained in this report are those of the author(s) and should not be construed as an official Department of the Army position, policy or decision unless so designated by other documentation.

REPORT DOCUMENTATION PAGE

Form Approved
OMB No. 0704-0188

Public reporting burden for this collection of information is estimated to average 1 hour per response, including the time for reviewing instructions, searching existing data sources, gathering and maintaining the data needed, and completing and reviewing this collection of information. Send comments regarding this burden estimate or any other aspect of this collection of information, including suggestions for reducing this burden to Department of Defense, Washington Headquarters Services, Directorate for Information Operations and Reports (0704-0188), 1215 Jefferson Davis Highway, Suite 1204, Arlington, VA 22202-4302. Respondents should be aware that notwithstanding any other provision of law, no person shall be subject to any penalty for failing to comply with a collection of information if it does not display a currently valid OMB control number. **PLEASE DO NOT RETURN YOUR FORM TO THE ABOVE ADDRESS.**

1. REPORT DATE SEPTEMBER 2019		2. REPORT TYPE Annual		3. DATES COVERED 10 Aug 2018 – 9 Aug 2019	
4. TITLE AND SUBTITLE Epicatechin as a Therapeutic Strategy to Mitigate the Development of Cardiac Remodeling and Fibrosis				5a. CONTRACT NUMBER W81XWH-16-1-0244	
				5b. GRANT NUMBER PR150090	
				5c. PROGRAM ELEMENT NUMBER	
6. AUTHOR(S) Francisco Villarreal E-Mail: fvillarr@ucsd.edu				5d. PROJECT NUMBER	
				5e. TASK NUMBER	
				5f. WORK UNIT NUMBER	
7. PERFORMING ORGANIZATION NAME(S) AND ADDRESS(ES) University of California, San Diego 9500 Gilman Dr. Dept. 621 La Jolla, CA 92093-0621				8. PERFORMING ORGANIZATION REPORT NUMBER	
9. SPONSORING / MONITORING AGENCY NAME(S) AND ADDRESS(ES) U.S. Army Medical Research and Materiel Command Fort Detrick, Maryland 21702-5012				10. SPONSOR/MONITOR'S ACRONYM(S)	
				11. SPONSOR/MONITOR'S REPORT NUMBER(S)	
12. DISTRIBUTION / AVAILABILITY STATEMENT Approved for Public Release; Distribution Unlimited					
13. SUPPLEMENTARY NOTES					
14. ABSTRACT Heart failure with preserved ejection fraction (HFpEF) continues to increase and little is known about its pathophysiology. About 2/3 of patients are women and risk factors include aging, hypertension and metabolic syndrome. A feature of the disease is cardiac fibrosis. Currently, no drugs target HFpEF and the development of animal models can assist in therapy evaluation. We developed a female rat model of aging, estrogen depletion and metabolic syndrome to evaluate the role of these factors in altering cardiac structure/function. Aged female Fischer F344 rats were allocated into an aging group, aging + ovariectomy and aging + ovariectomy + 10% fructose in drinking water. At 22 months of age, animals were anesthetized and left ventricular (LV) function was evaluated. Histological measures were also obtained. Intraventricular pressure-volume loop analysis evidenced significant decreases in stroke work cardiac output and increases in myocardial stiffness with ovariectomy. Histological analysis indicated increasing levels of inflammatory infiltration, perivascular and interstitial fibrosis with ovariectomy and with fructose supplementation. In conclusion, with aging, estrogen deprivation, markedly deteriorates myocardial microstructure which may facilitate the loss of diastolic and systolic function. This model may serve to understand the role that aging and menopause may have in the development of HFpEF.					
15. SUBJECT TERMS fibrosis, myocardium, heart failure, stiffness, estrogen, aging, metabolic syndrome					
16. SECURITY CLASSIFICATION OF:			17. LIMITATION OF ABSTRACT	18. NUMBER OF PAGES	19a. NAME OF RESPONSIBLE PERSON USAMRMC
a. REPORT	b. ABSTRACT	c. THIS PAGE			19b. TELEPHONE NUMBER (include area code)
Unclassified	Unclassified	Unclassified	Unclassified	49	

Table of Contents

	<u>Page</u>
1. Introduction.....	2
2. Keywords.....	2
3. Accomplishments.....	2
4. Impact.....	12
5. Changes/Problems.....	12
6. Products.....	13
7. Participants & Other Collaborating Organizations.....	15
8. Special Reporting Requirements.....	15
9. Appendices.....	16

INTRODUCTION

The project proposes that treatment with the flavanol (-)-epicatechin (Epi) will ameliorate adverse tissue remodeling and cardiac fibrosis in female animal models developing diastolic dysfunction as seen in women with heart failure with preserved ejection fraction (HFpEF). The project's 3 specific aims are (1) to determine if early use of Epi in female animal models of fibrotic hearts will reduce collagen deposition and preserve function, (2) to determine if late use of Epi in female animal models of fibrotic hearts will reduce collagen deposition and recover function, and (3) to investigate if the beneficial effects of Epi are due to its action on the cardiac fibroblast which are the cells mainly responsible for the production of fibrillar collagens. The mechanism(s) and functional outcomes of oral Epi preventive and therapeutic treatments will be defined in a relevant female animal model of diastolic dysfunction and can potentially lead to the design and implementation of clinical trials for the treatment for myocardial fibrosis leading to improved function.

KEYWORDS

Fibrosis, myocardium, heart failure, aging, estrogen, metabolic syndrome, stiffness, collagen, compliance, remodeling, epicatechin, flavanols, left ventricle.

ACCOMPLISHMENTS

I. Major goals of the project

Major Goals (Aims): The following are the **major tasks** identified in the Statement of Work associated with each aim.

Aim 1 related: Early preventive treatment with (-)-epicatechin (Epi) prevents myocardial fibrosis

1. Characterize effects of aging on myocardial fibrosis in untreated animals (completed)
2. Characterize effects of early Epi treatment on myocardial fibrosis in a model of estrogen depletion and aging (90% completed)
3. Characterize effects of early Epi treatment on myocardial fibrosis in a model of estrogen depletion, aging and fructose supplementation (90% completed)

Aim 2 related: Late treatment with Epi reverses myocardial fibrosis

4. Characterize long-term baseline effects of aging on myocardial fibrosis (completed)
5. Characterize the reversal of myocardial fibrosis by late Epi treatment in a model of estrogen depletion and aging (completed)
6. Characterize effects of estrogen depletion, aging and fructose supplementation on myocardial fibrosis and its reversal by late Epi treatment (completed)

Aim 3 related: The anti-fibrotic effects of (-)-epicatechin are mediated by TGF- β 1 inhibition

7. Cardiac fibroblast phenotype characterization (40% completed)
8. Effects of profibrotic phenotype stimulation/inhibition (40% completed)
9. Gene expression modulation (ongoing)

II. Accomplishments

Aim 1 related

A. Characterizing the effects of aging, estrogen depletion and excess weight on left ventricular (LV) remodeling

During year 2, a large part of the project's effort related to completing the implementation and assessment of the female model of aging driven cardiac remodeling and fibrosis that was to be compounded by ovariectomy (estrogen depletion) and fructose supplementation (yielding excess weight gain). We completed the characterization of changes in cardiac structure/function that develop as a function of aging (alone), aging + ovariectomy and aging + ovariectomy + fructose supplementation. A highly detailed and extensive characterization of the models has been published (see bibliography list). We are actively using data gathered from these in vivo studies to implement computer models that will allow us to simulate the impact that structural changes have on diastolic function (mechanical properties).

As listed in the proposed project plans, we completed the following tasks/subtasks:

- Assessed serial changes in cardiac structure/function using echocardiography
- Implemented terminal studies and recorded detailed carotid and intraventricular hemodynamics
- Performed ex vivo pressure-volume curves to examine changes in global left ventricular (LV) compliance
- Performed ex vivo pressure-strain curves to examine changes in free wall LV epicardial strains
- Fixed hearts, measured and recorded detailed histomorphometric parameters
- Compiled and summarized all data and performed a rigorous statistical evaluation, wrote reports and shared data
- Analyze by histological methods the role that inflammation may play in modulating the process of aging/ovariectomy/weight gain associated LV remodeling
- Analyze by multiplex immunoassays the role that select circulating proinflammatory cytokines may play in the remodeling process

Methods utilized include echocardiography to measure in vivo changes in heart morphology, diastolic and systolic function. In vivo carotid and LV hemodynamics utilized a Millar pressure conductance catheter. At the time of the terminal study, an ex vivo assessment of LV pressure volume and strain was implemented using an inflatable balloon as well as video recording of the inflating hearts to monitor the displacement of epicardial markers and calculate two-dimensional strains. Finally, hearts were fixed and sectioned for detailed histological analysis using hematoxylin and eosin and Sirius Red staining. Once stained, sections were visualized using standard microscopy and images analyzed for LV morphometry and collagen density by using a high resolution digital system (HALO system). We have also utilized immunohistochemistry, tunnel assays, multiplex immunodetection of pro-inflammatory cytokines in plasma samples. All data was summarized in databases and subjected to rigorous statistical analysis using GraphPad software.

Aim 1 results have led to the publication of an extensive research article in the *Journal of Physiology*. The following is the abstract of the submitted manuscript:

Unmasking of Estrogen Dependent Left Ventricular Dysfunction in Aged Female Rats: A Potential Model for pre-HFpEF

Two-thirds of patients with heart failure with preserved ejection fraction (HFpEF) are older women and risk factors include hypertension and excess weight/obesity. Pathophysiological factors that drive early disease development (before heart failure ensues) remain obscure and female animal models are lacking. The study evaluated the intersecting roles of aging, estrogen depletion and excess weight on altering cardiac structure/function. Female, 18 month old, Fischer F344 rats were divided into aging group, aging + ovariectomy (OVX) and aging + ovariectomy plus 10% fructose (OVF) in drinking water (n=8-16/group) to induce weight gain. Left ventricular (LV) structure/function was monitored by echocardiography. At 22 months of age, animals were anesthetized and catheter-based hemodynamics evaluated, followed by histological measures of chamber morphometry and collagen density. All aged animals developed hypertension. OVF animals increased body weight. Echocardiography only detected mild chamber remodeling with aging while intraventricular pressure-volume loop analysis showed significant ($p<0.05$) decreases vs. aging in stroke volume (13% OVX and 15% for OVF), stroke work (34% and 52%), cardiac output (29% and 27%), and increases in relaxation time (10% OVX) with preserved ejection fraction. Histology indicated papillary and interstitial fibrosis with aging, which was higher in the endocardium of OVX and OVF groups. With aging, ovariectomy leads to the loss of diastolic and global LV function while preserving ejection fraction. This model recapitulates many cardiovascular features present in HFpEF patients and may help understand the roles that aging and estrogen depletion play in early (pre-HFpEF) disease development. [**end of abstract**].

Details pertaining to each of the findings can be found in the attached (appendix) manuscript.

B. Characterizing the effects of early Epi treatment on aging, estrogen depletion and excess weight associated LV remodeling/fibrosis

During year 2 and 3 of the project, we successfully implemented all of the required in vivo studies to assess the effects of early Epi treatment on aging associated cardiac remodeling in the absence or presence of estrogens and excess weight as per fructose supplementation. Altogether, we completed 90% of the project and we are only waiting to receive the results of the histological analysis of tissue samples for determinations of fibrosis. No major issues arose during the studies and we expect to be 100% completed with the next 2 months. In the interest of report length, and since we have completed aim 2 studies (reported in a summarized version below) we will refrain from presenting these results until the final report is provided next year. However, a preliminary analysis of structural and functional data is encouraging.

Aim 2 related

Characterizing the effects of late Epi treatment on aging, estrogen depletion and excess weight associated LV remodeling/fibrosis

During the last year, we completed all of the in vivo studies assessing the effects of late Epi treatment on aging associated cardiac remodeling in the absence or presence of estrogens and/or excess weight. A summary of results is presented below for studies performed in aged female rats subjected to ovariectomy + fructose supplementation (OVF) vs. those treated with epicatechin (OVFE) for a period of 1 month prior to their terminal study.

Echocardiography

As shown in figure 1, results reveal comparable modest changes in OVF +/- epicatechin groups. Anterior wall thickness in diastole (AWThD) decreased modestly as a function of time (A). For posterior wall diastolic wall thickness (PWThD) there was also a minor decrease in thickness over time without differences between groups (B). There was a significant time dependent increase in LV diastolic and systolic chamber diameters (C, D) in all groups. Heart rate (HR), ejection fraction (EF) and fractional shortening (FS) were also not different between OVF groups (data not shown).

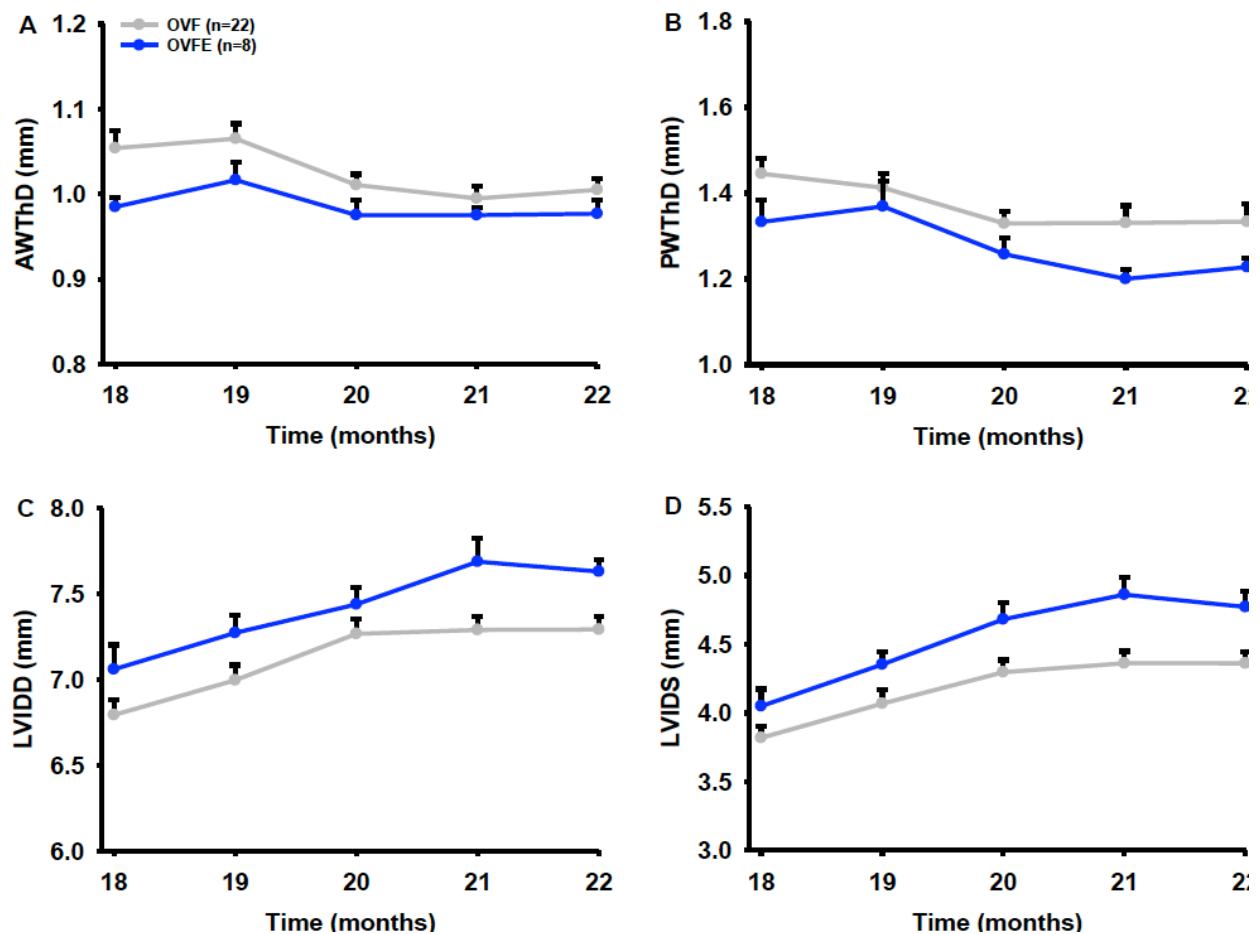


Figure 1. Left ventricular (LV) remodeling as serially tracked by echocardiography. (A) Anterior wall thickness in diastole (AWThD). (B) Posterior wall thickness in diastole (PWThD). (C) LV internal diameter diastole (LVIDD). (D) LV internal diameter in systole (LVIDS). For panels C and D, $p < 0.001$ for time dependent changes in all groups. OVF: ovariectomized + fructose. OVFE: supplemented with epicatechin. Values are mean \pm SEM.

Hemodynamic measurements

As shown in figure 2, for systolic aortic pressure (Pao) there were not differences between OVF and epicatechin treated animals. Cardiac index (output normalized to body weight), stroke volume index and ejection fraction were also comparable. Figure 3 depicts isovolumic relaxation time constant (IVRT) also known as “Tau” and arterial elastance (Ea) respectively. No differences were noted between OVF and epicatechin groups (OVFE).

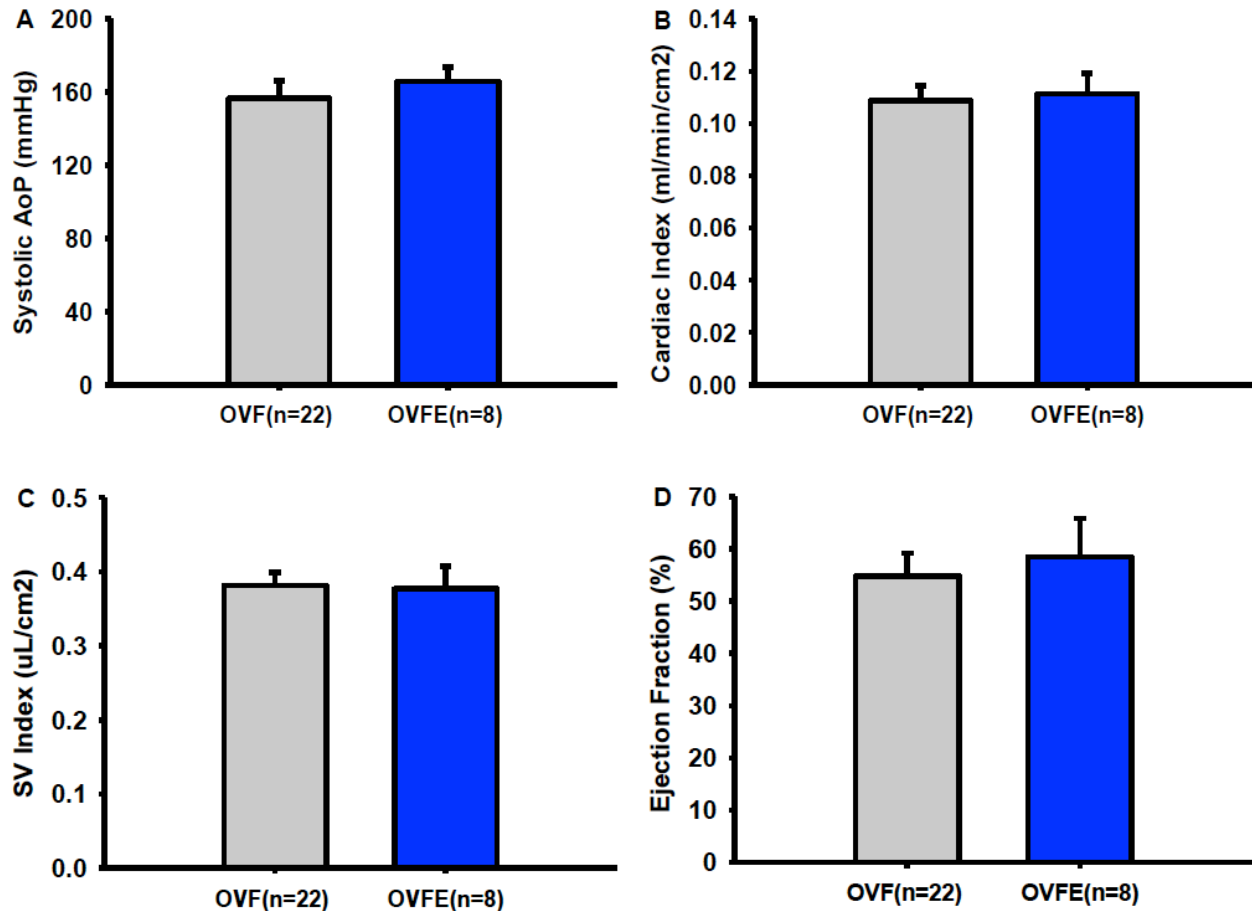


Figure 2. Hemodynamic values derived from arterial and left ventricular (LV) conductance catheter measurements during the terminal study. (A) Systolic aortic pressure. (B) Cardiac index, (C) Stroke volume (SV) index and, (D) Ejection fraction. OVFE: supplemented with epicatechin. Values are mean \pm SEM.

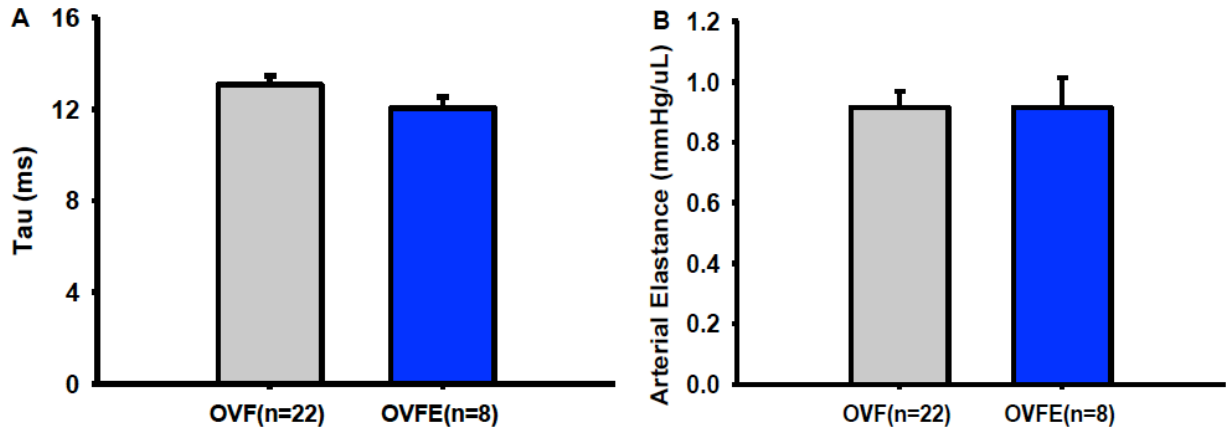


Figure 3. Hemodynamic values derived from arterial and left ventricular (LV) conductance catheter measurements during the terminal study. (A) LV isovolumic relaxation time constant (Tau), (B) Arterial elastance. OVF: ovariectomized + fructose, OVFE: supplemented with epicatechin. Values are mean \pm SEM.

Ex-vivo LV mechanics

As shown in figure 4, analysis of LV PV curves (A) demonstrate a significant right shift in epicatechin vs. OVF while chamber stiffness (B) remained similar at the pressures examined. Epicardial circumferential strain analysis revealed no differences in E_{11} between OVF and OVFE groups or in longitudinal strains (E_{22}).

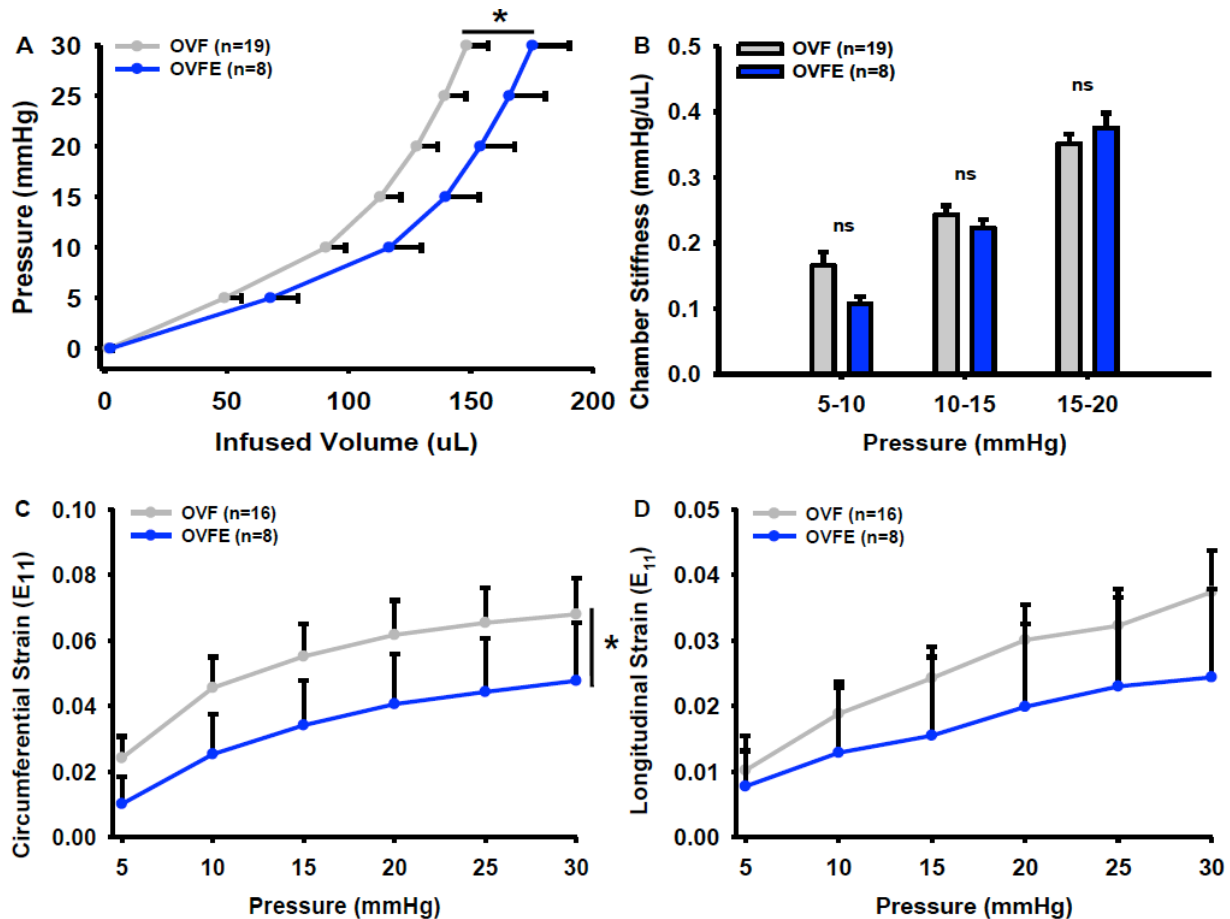


Figure 4. Ex-vivo analysis of left ventricular (LV) mechanics. (A) Passive LV pressure-volume (PV) curves for all groups at 21 months of age ($p < 0.05$ aged, OVF vs. OVFE). (B) analysis of chamber stiffness at different pressures. Two-dimensional circumferential (E_{11}) and longitudinal (E_{22}) LV epicardial strains at incremental LV pressures (C, D). OVF: ovariectomized + fructose. OVFE: supplementec with epicatechin. Values are mean \pm SEM.

Histological analysis and collagen quantification

Representative Sirius Red stained cross-sections of hearts from select animals of the different groups at low and high magnifications are shown in figure 5. Images similar to those shown in the panel were used to quantify collagen abundance in the LV by segments (12 free wall and 6 septal). Results from morphometry and histology are summarized in figure 6. Animals treated with epicatechin exhibited significantly decreased LV collagen area, % free wall ($p = 0.06$), septal and total LV collagen vs. OVF. Thus, late epicatechin treatment appears to exert an antifibrotic effect.

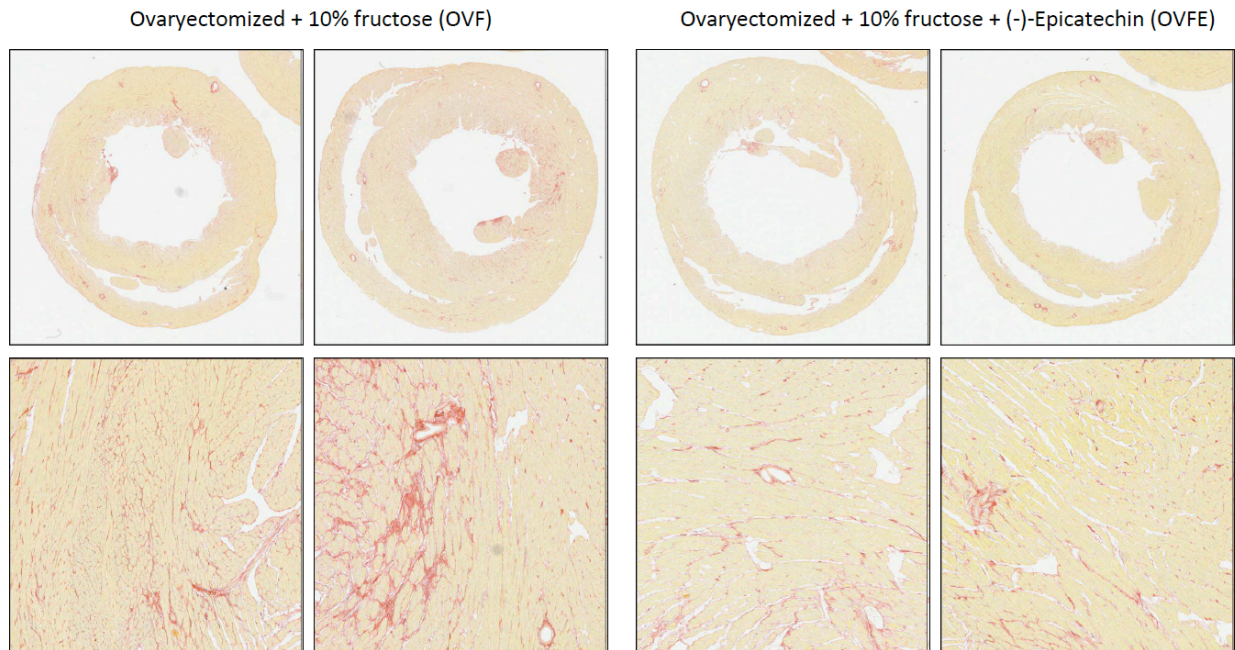


Figure 5. Representative images 2 and 20 X magnification from Sirius Red staining of hearts from all groups. Histomorphometric analysis of LV tissue sections.

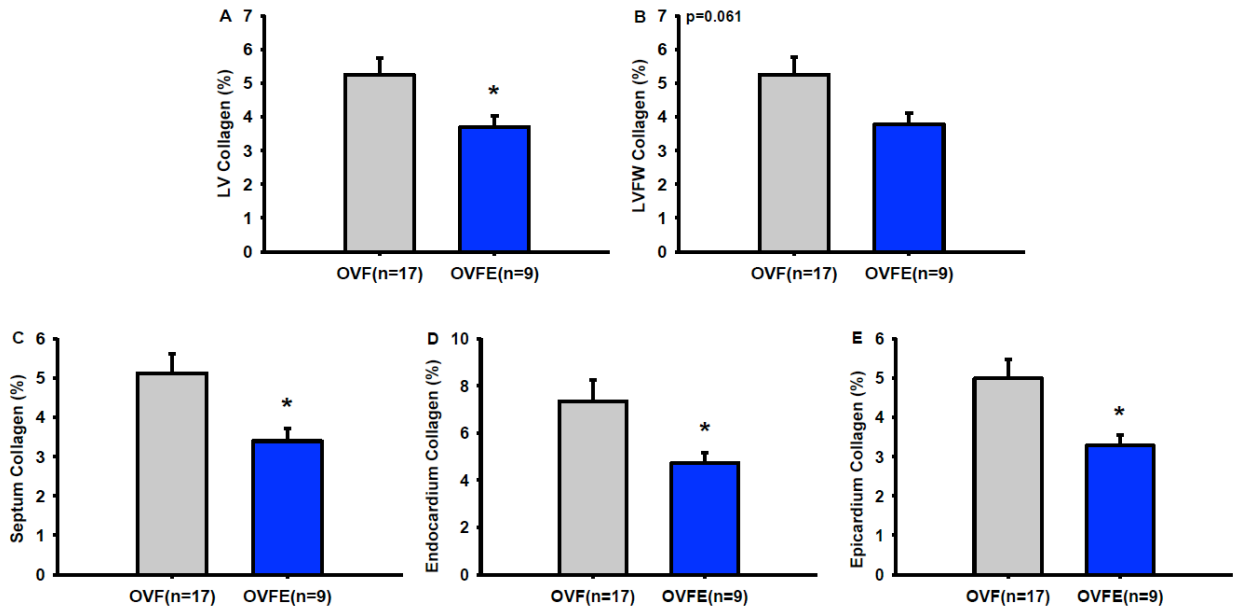


Figure 6. Histomorphometric analysis of LV tissue sections. (A) LV collagen area, (B) LV collagen area free wall % collagen, (C) septum % collagen, (D) endocardium, (E) epicardium collagen ratio. Values are mean \pm SEM. * $p < 0.05$ vs. OVF by unpaired t-test.

Major findings from this study can be summarized as follows:

- As per echo results, all groups developed slowly over time and in a similar magnitude, modest eccentric LV remodeling (i.e. chamber dilation)
- With late epicatechin treatment, half-time for diastolic relaxation and increases in arterial elastance remained unchanged vs. OVF
- All groups demonstrate unaltered systolic hypertension
- Systolic and diastolic function measures remained unaltered with epicatechin treatment
- Ex vivo LV pressure-volume curves indicate a right shift in animals treated with epicatechin suggesting greater tissue compliance which did not reach statistical significance
- An notable presence of LV fibrosis occurs in OVF rats that is significantly reduced with epicatechin treatment

Conclusions and Clinical Perspectives

The results presented here are comparable to those previously published by us in aged rats subjected to ovariectomy and fructose supplementation. Late (1 month) treatment with epicatechin was effective in altering the ex vivo passive mechanical properties of the LV while also suppressing fibrosis throughout the myocardial walls. While these results are encouraging as per the potential of epicatechin to reduced tissue fibrosis, it had a minor impact on LV structure and function suggesting that earlier and longer treatment is likely required. In this regards, studies to be reported from aim 1 which are 90% completed should be able to shed light into this possibility. Once the analysis is complete we will be able to gauge the potential to act as an effective reducer of fibrosis that positively impact LV function which can then be explored for its potential clinical use in patients with HFpEF.

Aim 1 and 2 related: Mathematical modeling studies

Fibrillar collagen plays a major role in the passive material properties of the myocardium. Hearts with severe fibrosis have significantly higher tissue stiffness, which can affect overall filling mechanics of the ventricular chamber. It has been shown that cardiac fibrosis is not a homogenous process, and we are employing modeling approaches of diastolic ventricular function to examine the significance of these regional differences in fibrosis. Many studies have modeled infarct zones using finite-element methods, generally by drastically increasing the stiffness of the infarct scar and border zone. To model the pathophysiology of cardiac fibrosis, a similar approach was used in our preliminary studies to model rat LV during passive inflation. Utilizing realistic ventricular geometry, muscle fiber structure and collagen distribution, the goals of the model include quantifying the local material properties, deformations and stresses, and overall passive filling function. Passive material properties are important to diastolic function, and can be used to quantify the efficacy of treatments for heart failure in animal models. A transverse isotropic constitutive law with respect to the local fiber axis was used for this initial model. Experimental results from aim 1 studies showed increased collagen area fraction in the subendocardium vs. epicardium. Simulations using a bulk measurement of collagen versus a transmural variation were compared. These preliminary results show only modest differences between models with a single material vs. those with transmurally varying properties. We are currently awaiting the completion of aim 1 studies to determine if greater differences in tissue fibrosis become evident and what their impact may be in LV material properties.

In collaboration with senior expert from UCSD's department of Bioengineering we are currently also working on developing a testable hypothesis for the potential cause of HFpEF in female patients. As this hypothesis is to be put forward we will be able to propose a series of modeling studies using data derived from these experiments and others. We anticipate to be able to generate a manuscript on this concept within the next 3 months for submission in late 2019.

Aim 3 related

The anti-fibrotic effects of (-)-epicatechin are mediated by TGF- β 1 inhibition

Over the course of the last year and a half, we implemented the culturing of cardiac fibroblasts isolated from young and aged female hearts. However, after many "logical" adjustments to the isolation protocol, we consistently detected a lower yield of cells vs. male hearts. Furthermore, in attempting to challenge the cells to develop a pro-fibrotic phenotype using high glucose media or angiotensin II, we noted a limited responsiveness to the stimulation vs. our historical strong response from male derived cells. On these basis, we proceeded to utilize male rat derived cells from our frozen allotments of cells. In figure 7 below, we summarize ELISA results for the determination of TGF β -1 levels in cell lysates and cell culture media for male cardiac fibroblasts obtained from young hearts stimulated with high glucose for 48 h while figure 8 reports on changes in total collagen levels as per hydroxyproline assays.

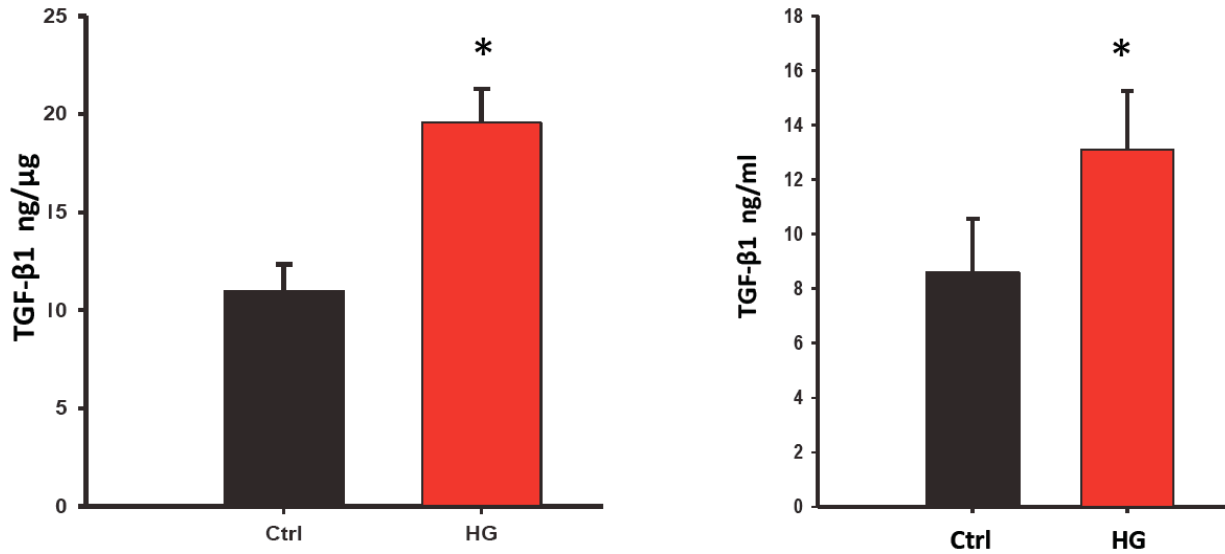


Figure 7. High glucose (HG) media effects on rat cardiac fibroblasts TGF-β1 protein levels as per ELISA. Results from n=5 experiments each, in triplicate.

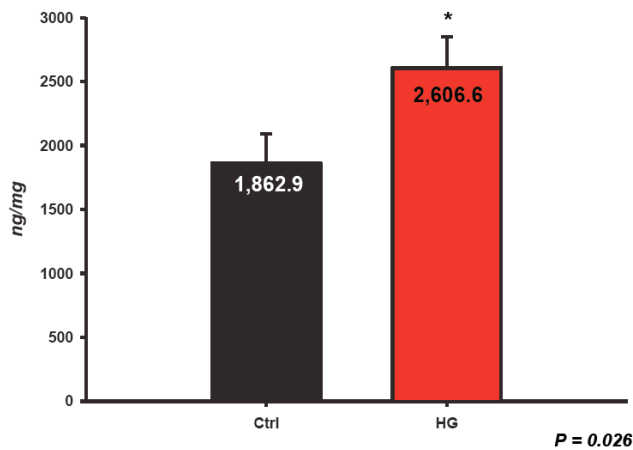


Figure 8. High glucose (HG) media effects on rat cardiac fibroblast collagen levels in cell lysate as per hydroxyproline assays. Results from n=5 experiments each, in triplicate.

III. Opportunities for training

As stated in our 2018 report, the pre-doctoral fellows (Moises Bustamante and Elva Garate) continue to be trained in techniques related to in vivo physiology and pharmacology. Both students are 100% committed to the project and they are now extensively trained on in vitro (cell culture), in vivo and ex vivo methods to assess for changes in cardiac fibroblast or heart structure and function and the impact that Epi treatment yields on relevant endpoints. Training activities also include one-on-one mentoring with senior staff so as to achieve technical proficiency in the methods they are being exposed to. Moises Bustamante is the 1st author listed on the published manuscript and Elva Garate as a middle author. Both students are also listed as authors in the listed abstracts and had the opportunity to present the study results at the 2018 and 2019 Experimental Biology meetings in San Diego, California and Orlando, Florida. Both students are

currently working on two additional manuscripts to be submitted in 2019 for publication purposes.

IV. Dissemination of results

As noted above, we have disseminated our initial results during the 2018 and 2019 Experimental Biology meetings. We also reported to the international heart failure community, the initial results of the effects of epicatechin in mitigating adverse changes driven by aging/estrogen and/or fructose induced metabolic syndrome at the European Society of Cardiology, Heart Failure meeting in May of 2018 in Vienna, Austria. We reported on further advances to the local academic community (presentation held October 12th, 2018). We will submit the most recent results of our studies to National and International meetings.

V. Plans

The project continues to progress well within the anticipated general plan as essentially all three large in vivo studies have been completed generating a highly detailed database of results. Over the course of the next 2-3 months, as the pending histology results emerge will be able to draw solid conclusions as to the impact that each of the examined factors have on cardiac structure/function and on the capacity of Epi to limit/reverse these. As noted above, all of the relevant data generated are being incorporated into computer based simulations to examine the effect that changing specific variables has on diastolic function. In vitro studies have quicken their pace significantly and are beginning to generate an ample body of evidence for the antifibrotic effects of epicatechin and associated mechanisms of action.

IMPACT

The work being generated by this project has begun to unmask an important role for estrogens in mitigating the risk of developing adverse changes in cardiac structure/function that are slowly compounded with aging and that can remain undetected in female subjects for years. This area of cardiology continues to be underappreciated, as the number of relevant publications that address these factors systematically is very limited. This study also lays the ground for the systematic analysis of differences in sex as it relates to the development of various types of cardiometabolic diseases. As our data begins to validate the potential of epicatechin to exert antifibrotic effects we may then design additional preclinical studies to support this concept and eventually evolve to the planning of clinical studies.

CHANGES/PROBLEMS

We repeatedly modified cell culture conditions and media to optimize the growth of female cells and have encountered a reticence of the cells to growth in a significant manner at passage 2. Thus, limiting greatly a capacity to have enough material to perform the planned experiments. We have thus, opted to use male cardiac fibroblasts from our frozen lots to perform the planned experiments. Cells are derived from young 3 month old healthy male rats. As documented above, we have implemented an initial round of cell culture experiments with encouraging results and will eventually culture cells from aged male rats to also examine the effects that aging has on

extracellular matrix production and explore the inhibitory effects of epicatechin as well as underlying mechanisms.

PRODUCTS

Journal Publications

1. Bustamante M, Garate-Carrillo A, Ito B, Garcia R, Carson N, Ceballos G, Ramirez-Sanchez I, Omens J, Villarreal F: Unmasking of Estrogen Dependent Left Ventricular Dysfunction in Aged Female Rats: A Potential Model of Early Stage HFpEF. *J Phys*, 597.7:1805-1817, 2019

2. Saucerman J, Tan P, Buchholz K, McCulloch A, Omens J. Mechanical regulation of gene expression in myocardium. *Nat Rev Cardiol*, 16:361-378, 2019

[Abstract: The intact heart undergoes complex and multiscale remodelling processes in response to altered mechanical cues. Remodelling of the myocardium is regulated by a combination of myocyte and non-myocyte responses to mechanosensitive pathways, which can alter gene expression and therefore function in these cells. Cellular mechanotransduction and its downstream effects on gene expression are initially compensatory mechanisms during adaptations to the altered mechanical environment, but under prolonged and abnormal loading conditions, they can become maladaptive, leading to impaired function and cardiac pathologies. In this Review, we summarize mechanoregulated pathways in cardiac myocytes and fibroblasts that lead to altered gene expression and cell remodelling under physiological and pathophysiological conditions. Developments in systems modelling of the networks that regulate gene expression in response to mechanical stimuli should improve integrative understanding of their roles in vivo and help to discover new combinations of drugs and device therapies targeting mechanosignalling in heart disease].

3. Carruth E, The I, Schneider J, McCulloch A, Omens J, Frank L. Regional Variations in Diffusion Tensor Anisotropy are Associated with Myocyte Remodeling in Left Ventricular Pressure Overload. Resubmitted, *Am J Phys*, 2019

[Abstract: In this study we hypothesized that regional (especially transmural) gradients in structural properties of myocardium would become more spatially uniform and would be reduced in pressure overload such as seen with hypertension to maintain uniformity of fiber strain. To test our hypothesis, we performed high-resolution, high-fidelity Diffusion Tensor-MRI (DTI) on rat hearts isolated/fixed from transverse aortic constricted and sham control animals and investigated the regional variations in DTI-derived parameters of orientation, diffusivity, and anisotropy in the LV. We found that there are indeed regional variations in myocyte geometry and structural organization, which become more uniform with pressure overload. Additionally, several structural features correlated significantly with DTI-derived parameters, regardless of phenotype. These results will be valuable in understanding the mechanisms by which cardiac myocytes in different regions of the LV respond to hypertension and may provide a tool for diagnosing the early stages of hypertrophy or other remodeling clinically and non-invasively, allowing for earlier lifestyle changes or interventions to reverse early stage remodeling before the progression to heart failure occurs].

Conference Papers

1. Bustamante M, Garate-Carrillo A, Loredó M, García R, Carson N, Ito B, Ceballos G, Omens J, Ramirez-Sanchez I, Villarreal F. Detrimental Effects of Aging, Ovariectomy and Weight Gain on Left Ventricular Structure and Function: A Potential Preclinical Model of Early Stage HFpEF. *FASEB J*, 32, S1, 2018
2. Bustamante M, Garate-Carrillo A, Ito B, Ceballos G, Omens J, Ramirez-Sanchez I, Villarreal F. Development of an aging female rat model of HFpEF and evaluation of the antifibrotic potential of (-)-epicatechin. *European Journal of Heart Failure*, 20, S1, 2018
3. Bustamante M, Garate-Carrillo A, Ito B, García R, Carson N, Ceballos G, Ramirez-Sanchez I, Omens J, Villarreal F. Antifibrotic Effect of (-)-Epicatechin in a Rodent Model of Early Stage HFpEF. *FASEB J*, 33, S1, 2019

Presentations

1. Presented Conference Paper listed as #1 above at the Experimental Biology meeting in April, 2018 in San Diego, CA
2. Presented Conference Paper listed as #2 above at the European Society of Cardiology, Heart Failure meeting in May, 2018 in Vienna, Austria
3. Presented in October 2018 at the UCSD Cardiology seminar series. Title: A female rodent model of early HFpEF: A potential critical role for estrogen depletion in the aged heart.
4. Presented Conference Paper listed as #3 above at the Experimental Biology meeting in April, 2019 in Orlando, FL

PARTICIPANTS & OTHER COLLABORATING ORGANIZATIONS

I. Individuals involved in the project

Francisco Villarreal (Principal Investigator)	no change
Jeffrey Omens (Co-Investigator)	no change
Israel Ramirez-Sanchez (Project Scientist)	no change
Diane Huang (SRA 2)	no change

Name	Moises Bustamante
Project role:	Graduate student
ID	114959
Cal months	12
Contribution to project	In vivo physiology and pharmacology
Funding support	CONACyT and DoD (this award)

Name	Elva Garate
Project role:	Graduate student
ID	000921750
Cal months	12
Contribution to project	In vitro biology and in vivo pharmacology
Funding support	CONACyT and DoD (this award)

II. Changes in other support

Nothing to report.

III. What other organizations were involved as partners?

Nothing to report.





SPECIAL REPORTING REQUIREMENTS

Not applicable

APPENDICES (Manuscripts)

1. Bustamante M, Garate-Carrillo A, Ito B, Garcia R, Carson N, Ceballos G, Ramirez-Sanchez I, Omens J, Villarreal F: Unmasking of Estrogen Dependent Left Ventricular Dysfunction in Aged Female Rats: A Potential Model of Early Stage HFpEF. *J Phys*, 597.7:1805-1817, 2019
2. Saucerman J, Tan P, Buchholz K, McCulloch A, Omens J. Mechanical regulation of gene expression in myocardium. *Nat Rev Cardiol*, 16:361-378, 2019

Unmasking of oestrogen-dependent changes in left ventricular structure and function in aged female rats: a potential model for pre-heart failure with preserved ejection fraction

Moises Bustamante^{1,2}, Alejandra Garate-Carrillo^{1,2}, Bruce R. Ito¹, Ricardo Garcia^{1,3}, Nancy Carson³ , Guillermo Ceballos² , Israel Ramirez-Sanchez^{1,2}, Jeffrey Omens¹  and Francisco Villarreal^{1,4} 

¹Department of Medicine, School of Medicine, University of California, San Diego, La Jolla, CA, USA

²Seccion de Estudios de Posgrado e Investigacion, Escuela Superior de Medicina, Instituto Politecnico Nacional, Mexico, DF

³Bristol-Myers Squibb, New York, NY, USA

⁴VA San Diego Health Care, San Diego, CA, USA

Edited by: Don Bers & Beth Habecker

Key points

- Heart failure with preserved ejection fraction (HFpEF) is seen more frequently in older women; risk factors include age, hypertension and excess weight.
- No female animal models of early stage remodelling (pre-HFpEF) have examined the effects that the convergence of such factors have on cardiac structure and function.
- In this study, we demonstrate that ageing can lead to the development of mild chamber remodelling, diffuse fibrosis and loss of diastolic function.
- The loss of oestrogens further aggravates such changes by leading to a notable drop in cardiac output (while preserving normal ejection fraction) in the presence of diffuse fibrosis that is more predominant in endocardium and is accompanied by papillary fibrosis.
- Excess weight did not markedly aggravate such findings.
- This animal model recapitulates many of the features recognized in older, female HFpEF patients and thus, may serve to examine the effects of candidate therapeutic agents.

Abstract Two-thirds of patients with heart failure with preserved ejection fraction (HFpEF) are older women, and risk factors include hypertension and excess weight/obesity. Pathophysiological factors that drive early disease development (before heart failure ensues) remain obscure and female animal models are lacking. The study evaluated the intersecting roles of ageing, oestrogen depletion and excess weight on altering cardiac structure/function. Female, 18-month-old, Fischer F344 rats were divided into an aged group, aged + ovariectomy (OVX) and aged + ovariectomy + 10% fructose (OVF) in drinking water ($n = 8-16/\text{group}$) to induce weight gain.

Moises Bustamante is a second year PhD student from the National Polytechnic Institute based in Mexico City. He obtained a BS in Chemistry and an MS in Clinical Microbiology at the Autonomous University of Baja in Tijuana, Mexico. He is working in Dr Francisco Villarreal's Laboratory at UCSD focusing on research in heart failure with preserved ejection fraction and how ageing, oestrogen depletion and metabolic syndrome impact cardiovascular structure and function in the female sex. He is also evaluating the beneficial potential of the flavanol (–)-epicatechin on skeletal and cardiac muscle, brain and other metabolic disorders.



Left ventricular (LV) structure/function was monitored by echocardiography. At 22 months of age, animals were anaesthetized and catheter-based haemodynamics evaluated, followed by histological measures of chamber morphometry and collagen density. All aged animals developed hypertension. OVX animals increased body weight. Echocardiography only detected mild chamber remodelling with ageing while intraventricular pressure–volume loop analysis showed significant ($P < 0.05$) decreases vs. ageing in stroke volume (13% OVX and 15% for OVF), stroke work (34% and 52%) and cardiac output (29% and 27%), and increases in relaxation time (10% OVX) with preserved ejection fraction. Histology indicated papillary and interstitial fibrosis with ageing, which was higher in the endocardium of OVX and OVF groups. With ageing, ovariectomy leads to the loss of diastolic and global LV function while preserving ejection fraction. This model recapitulates many cardiovascular features present in HFpEF patients and may help understand the roles that ageing and oestrogen depletion play in early (pre-HFpEF) disease development.

(Received 20 November 2018; accepted after revision 24 January 2019; first published online 25 January 2019)

Corresponding author F. Villarreal: UCSD School of Medicine, 9500 Gilman Drive BSB4028, La Jolla, CA 92093-0613J, USA. Email: fvillarr@ucsd.edu

Introduction

Heart failure (HF) is the most common cause for hospitalization in older patients and represents the greatest cost for Medicare (Owan *et al.* 2006; Lam *et al.* 2011). Currently, up to 50% of HF patients are now recognized to have what is termed HF with preserved ejection fraction (HFpEF). This is a poorly understood disease and there are no therapies identified as clearly effective in mitigating its pathology (Omar *et al.* 2016; Barandiarán Aizpurua *et al.* 2019). Certain features such as the preservation of left ventricular (LV) geometry and ejection fraction (while at rest) in the setting of diastolic dysfunction are recognized as ‘most common’ in HFpEF patients (Omar *et al.* 2016). To better understand its pathophysiological underpinnings and the effects of ‘preventive’ therapies, animal models of pre-HFpEF would be desirable. HFpEF is more predominant in elderly, post-menopausal female patients (2:1) vs. men (Pacher *et al.* 2008; Lam *et al.* 2011) and the causes for this unequal distribution remain unclear. In women, the disease is also closely associated with the presence of hypertension as well as excess weight/obesity (Eaton *et al.* 2016). The development of pre-HFpEF animal models would thus require the convergence of ‘risk’ factors known to be associated with the disease while recapitulating features commonly seen with the pathology (Borlaug, 2016; Omar *et al.* 2016).

Systemic processes suspected to play a prominent role in the development of diastolic dysfunction with HFpEF include endothelial and mitochondrial dysfunction as well as oxidative stress (Borlaug, 2014), all of which have been associated with the presence of menopause in women, as well as with ageing (Takahashi & Johnson, 2015). However, very few female animal models have examined the impact that the loss of oestrogens has in the evolution of LV function, in particular, as low oestrogen levels interact

with ageing, hypertension and/or excess weight before the onset of HF (Omar *et al.* 2016).

The Fischer F344 rat developed by NIH investigators has been extensively used as a model to study processes associated with ageing (Boluyt, 2004; Pacher *et al.* 2004). However, the great majority of published studies using rodent models of heart disease have used young, male animals with only an extremely limited number of studies focused on the female sex and the role of oestrogens (Conceição *et al.* 2016; Valero-Muñoz *et al.* 2017). While aged female rodents do not truly develop menopause, ovariectomy has been widely used and validated as a research tool to examine the role that oestrogen deprivation has on the control of multiple physiological systems (Sohrabji, 2005; Knowlton & Lee, 2012).

The main objective of this study was to develop and characterize a female rat model where ageing, oestrogen deprivation, hypertension and excess weight converge, with the intent to produce structural and functional changes that while not leading to HF, parallel those found in female HFpEF patients. To achieve this goal, older, female F344 rats undergoing ovariectomy and fructose supplementation were assessed for changes in LV structure and function, highlighting the changes associated with the presence of HFpEF in older, female patients.

Methods

Study design

Young (3-month-old) and aged (18-month-old) female Fischer F344 rats were used. Aged animals were obtained from the NIH/NIA ageing colony. Young animals were used as a reference control for all measurements. Animals were housed in pairs and maintained with a 12-h light–dark cycle with *ad libitum* intake of standard rat chow and sterilized tap water. Animal care and use

followed National Institutes of Health's *Guide for the Care and Use of Laboratory Animals* guidelines, and the Institutional Animal Care and Use Committee of the University of California San Diego School of Medicine approved the protocol for this study. Figure 1 summarizes the study design and protocol. Aged rats were acclimated to the environment for 1 week and then randomly assigned to three groups: aged ($n = 8$), ovariectomized (OVX, $n = 16$) and ovariectomy + 10% fructose in drinking water (OVF, $n = 16$). OVX animals underwent bilateral oophorectomy performed under isoflurane anaesthesia via a dorsal incision as previously described (Stout Steele & Bennett, 2011). OVF animals also had this surgery and were started on 10% fructose (w/v) in their drinking water 1 week after ovariectomy. Fructose intake was used to induce weight gain and replicate metabolic syndrome-like features known to be commonly present in female HFpEF patients. All aged animals were maintained under the same conditions for 3 months (to 21 months of age) with weekly measurement of body weight. At 21 months, all rats were subjected to a terminal study under isoflurane anaesthesia to measure *in vivo* LV haemodynamics, and *ex vivo* passive LV pressure–volume and epicardial strain–pressure curves. Young rats underwent the same terminal study after a 1 week period of acclimatization. Blood and select tissues including tibias were collected for further analysis.

Echocardiography

Closed-chest echocardiography was performed monthly for 3 months (between 18 and 21 months of age) in isoflurane-sedated animals using a GE Vivid 7 machine and an i12L probe (GE Healthcare, Milwaukee, WI, USA). Young rats were evaluated only once after the 1 week period of acclimatization. Measured parameters included anterior wall thickness in diastole and systole (AWThD/AWThS), posterior wall thickness in diastole and systole (PWThD/PWThS), LV internal diameter in

diastole and systole (LVIDD/LVIDS), heart rate (HR), ejection fraction (EF) and fractional shortening (FS).

In vivo haemodynamics

At the terminal time point, animals were anaesthetized using 2.5% isoflurane, intubated and mechanically ventilated. To measure haemodynamics, a 2 French pressure transducer/conductance catheter (SPR-838 Millar Instruments; Houston, TX, USA) was introduced via the carotid artery into the aorta and LV. LV pressure and volume data were acquired at baseline and during temporary occlusion of the inferior vena cava at the level of the diaphragm to change LV filling. At the end of each experiment, parallel conductance was determined using an intravenous saline injection (Pacher *et al.* 2008). Measurements were recorded at a sampling rate of 1000 Hz using ADInstruments Powerlab (Colorado Springs, CO, USA) hardware and LabChart software. Parameters recorded included stroke work (SW), cardiac output (CO, ml min^{-1}), stroke volume (SV, μl), end-diastolic and end-systolic volumes (μl) and indexes, ejection fraction (EF, %), LV first derivative of pressure (dP/dt maximum and minimum), isovolumic relaxation time constant (τ , ms) and systolic and diastolic aortic pressure (P_{ao}).

Ex vivo passive LV mechanics

After *in vivo* cardiac measurements were obtained, the heart was arrested with a slow infusion of 2 ml of a cardioplegia solution containing 0.03 M 2,3-butanedione monoxime and high potassium solution. The heart was rapidly excised and rinsed in sterile ice-cold saline, and remaining connective tissue was trimmed. The aorta was cannulated using a modified Langendorff system where it was perfused with the cold cardioplegia solution at 10–15 mmHg. A balloon was inserted into the LV from the left atrium and connected to a pressure transducer and an infusion pump as done previously (Omens *et al.* 1995).

To generate passive LV pressure–volume (PV) curves, the LV balloon was inflated at a constant rate of $200 \mu\text{l min}^{-1}$. Pressure and infused volume data were acquired using DATAQ Software and Data Acquisition Systems (Akron, OH, USA) at a sampling rate of 10 Hz. Just prior to initiation of the infusion–deflation cycles, discrete epicardial markers were placed on the anterior LV epicardial surface. During a PV inflation–deflation cycle, synchronized video images were acquired using a $\times 250$ digital USB microscope (Plugable Technologies, Redmond, WA, USA). The displacements of the epicardial markers were obtained during each infusion cycle to calculate two-dimensional circumferential (E_{11}) and longitudinal (E_{22}) strains relative to the long axis of the heart. Two to three preconditioning inflation runs

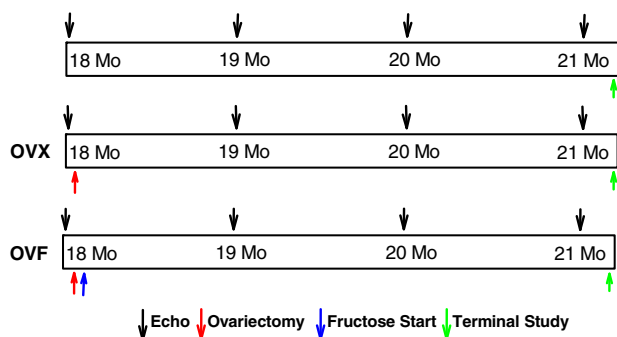


Figure 1. Scheme depicting the timeline of the study, measures and interventions used over the course of 3 months

were followed by two to three data acquisition runs with a maximal LV pressure of ~ 30 mmHg. Epicardial strains were calculated using customized strain software. Validation of these types of passive functional studies has been done previously (Omens *et al.* 1993).

Following these mechanical measures, hearts were perfusion fixed for 10 min using 10% formalin (EMD Millipore Corp., Billerica, MA, USA) introduced via the aortic cannula and with the LV balloon maintained at 10–15 mmHg. Fixed tissues were stored in conical tubes at a temperature of 4°C for 2 weeks until histological evaluation.

Histological analysis and collagen quantification

As shown in Fig. 2, formalin-fixed hearts were weighed and trimmed before sectioning at the midventricular region for subsequent embedding in paraffin. LV base and apical rings were then sectioned and mounted onto slides for Sirius Red staining and microscopic imaging. Using HALO[®] Digital Pathology Software (Indica Labs, Corrales, NM, USA) the analysis of the LV area and collagen positive area was performed by subdividing the LV ring into 18 discrete epicardial to endocardial wall sections. Of these regions, 12 were identified as free wall and six as septal. The ring sections of the LV were also digitally divided into inner half (subendocardium) and outer half (subepicardium) to allow comparison of endocardial *vs.* epicardial collagen distribution.

Statistical analysis

All data shown is presented as the mean \pm standard error of the mean (SEM). Statistical analyses used are one-way or two-way ANOVA and Holm–Sidak's *post hoc* test and Student's unpaired *t* test as appropriate using SigmaPlot (Systat Software, 2008, San Jose, CA, USA). Results were considered statistically significant at a value of $P < 0.05$.

Results

General parameters

Total body weight and percentage body weight gain over time of aged, OVX and OVF rats are shown in Fig. 3A and B. Aged and OVX animals showed a 6% and 10% increase in weight respectively while the OVF group gained 26% ($P < 0.05$, OVF *vs.* OVX and aged). As shown in Table 1, there were no differences in heart weights between aged groups, but there was a difference between OVF *vs.* young ($P < 0.05$ by unpaired *t* test). Calculated body surface area was higher in OVF and OVX *vs.* aged ($P < 0.001$).

Echocardiography

Echocardiographic results are summarized in Table 1. As shown in Fig. 4A–D, results reveal a time-dependent effect on cardiac morphometry in aged, OVX and OVF groups. AWThD significantly decreased as a function of time with no differences between aged, OVX and OVF groups (Fig. 4A). In AWThS, there was a significant difference between aged *vs.* OVX and OVF ($P < 0.05$). For PWThD and PWThS there was also a decrease in thickness over time without difference between aged, OVX and OVF groups (Fig. 4B). While LVIDD and LVIDS demonstrated no differences between aged, OVX and OVF groups, there was a significant time dependent increase in chamber diameters (Fig. 4C and D). HR, EF and FS were also not different between aged, OVX and OVF groups. BW, AWThD and AWThS of aged, OVX and OVF were different *vs.* young ($P < 0.001$). LVIDD, LVIDS and PWThD of aged, OVX and OVF were significantly different *vs.* young ($P = 0.003$, $P = 0.014$ and $P = 0.002$, respectively).

Haemodynamic measurements

Results from *in vivo* haemodynamic measurements are summarized in Table 2 and selected data are shown in Fig. 5A–C. For systolic P_{ao} , there was a significant increase in aged groups *vs.* young ($P = 0.009$). Cardiac index was decreased in aged, OVX and OVF *vs.* young animals ($P < 0.05$) while OVX and OVF were different *vs.* aged ($P < 0.001$). Stroke volume index was reduced in aged, OVX and OVF *vs.* young ($P < 0.05$), and differences between OVX and OVF were also present *vs.* aged ($P < 0.001$) indicating an effect of ovariectomy and fructose on cardiac function. EF was stable and not different between groups, being preserved at the normal range of $\geq 50\%$ (Fig. 5D). Figure 6A and B depicts isovolumic relaxation time constant (IVRT), also known as 'Tau', and arterial elastance (E_a), respectively, in the different groups. An increase in Tau was noted in aged, OVX and OVF groups *vs.* young ($P < 0.05$). Arterial elastance was significantly elevated in OVX and OVF *vs.* young ($P < 0.05$) with a trend from an increase in the aged group. The end-diastolic pressure–volume relationship (EDPVR) slope demonstrated differences between aged and OVX ($P < 0.05$).

Ex vivo LV mechanics

As shown in Fig. 7A, the analysis of LV PV curves did not demonstrate differences among the aged, OVX and OVF groups. However, all these groups were different *vs.* young ($P < 0.001$) demonstrating a global right-shift in aged, OVX and OVF animals. Epicardial circumferential strain analysis (Fig. 7B) revealed no differences in E_{11} between aged, OVX and OVF groups or when compared to young.

In longitudinal strain E_{22} , the maximal strain observed at 30 mmHg was ~ 0.04 (4%) and no differences were detected amongst all groups. Overall, E_{11} strains were higher than E_{22} for all groups, where the range for E_{11} was ~ 0.06 – 0.09 (i.e. 6–9%).

Histological analysis and collagen quantification

Representative Sirius Red-stained cross-sections of hearts from select animals of the different groups at low and high magnifications are shown in Fig. 8. Images similar to those shown in the panel were used to quantify collagen abundance in the LV by segments as outlined in Methods. Interestingly, a visual inspection of large areas of abnormal (patch like) fibrosis present in papillary muscles indicated that aged hearts showed such lesions in 1/4 aged animals (25%), 4/6 OVX (67%) and 5/7 OVF (71%) vs. none in young animals. Results from morphometry and histology are summarized in Fig. 9A–F. Aged rats demonstrated a

higher LV tissue area vs. young ($P < 0.05$). Aged, OVX and OVF groups exhibited increased LV collagen area, percentage free wall, septal and total LV collagen vs. young ($P < 0.05$). Whereas the endocardial/epicardial ratio did not demonstrate significant overall differences by ANOVA among the groups, there were differences between OVX and OVF vs. young ($P < 0.05$, by unpaired t test).

Discussion

Findings from this study indicate that with ageing in female rats, a modest degree of LV remodelling is observed which is accompanied by the prolongation of relaxation time. With ovariectomy, these changes are compounded by significant reductions in stroke volume and CO in the setting of preserved EF. Ageing in this animal model also showed the development of diffuse myocardial fibrosis, which becomes greater in the endocardium

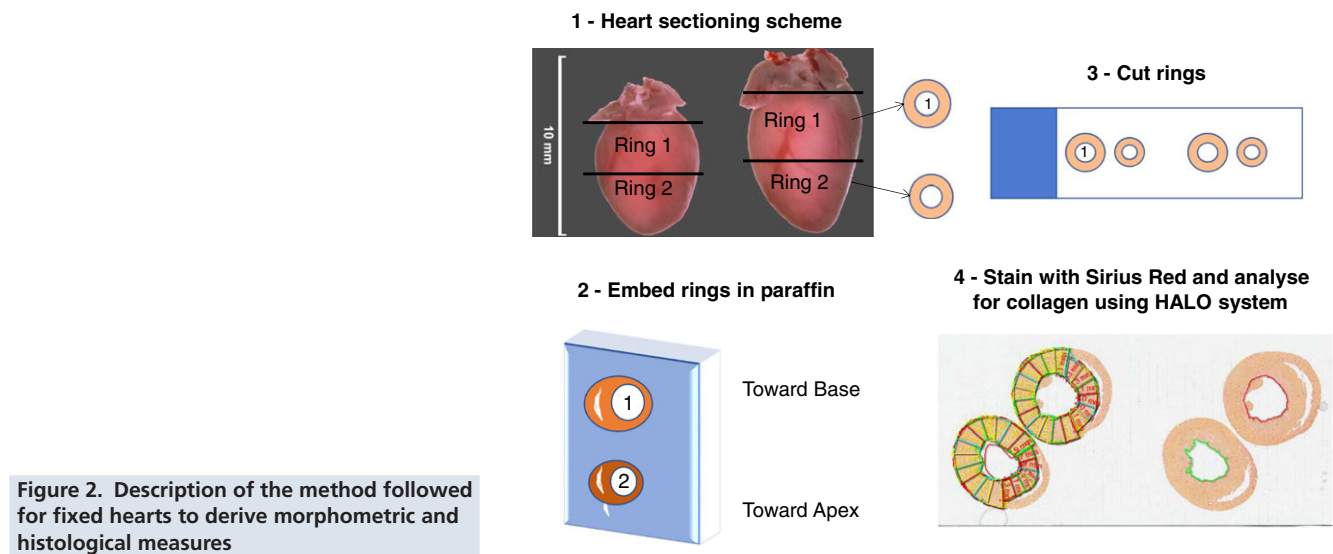


Figure 2. Description of the method followed for fixed hearts to derive morphometric and histological measures

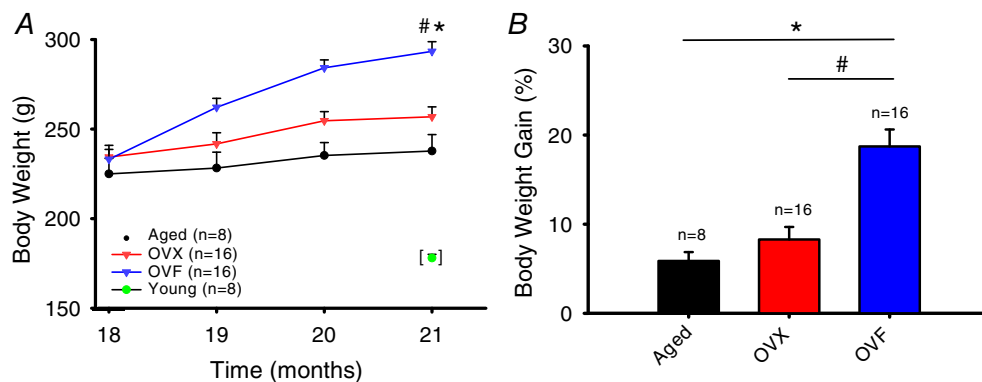


Figure 3. Changes in body weight observed in the different animal groups over 3 months. *A*, body weight gain in grams ($P < 0.001$, OVF vs. OVX and aged). *B*, body weight gain as a percentage of the initial weight ($P < 0.001$, OVF vs. OVX and aged). Young group single time-point data included as reference. Values are means \pm SEM. OVF, ovariectomized + fructose; OVX, ovariectomized.

Table 1. Body weight, heart weight and echocardiographic assessment of systolic and diastolic function of young and aged, ovariectomized (OVX) and ovariectomized + fructose (OVF) Fischer 344 female rats

Parameter	Group	3 months	18 months	19 months	20 months	21 months	P			All group
							Two-way ANOVA (aged, OVX and OVF)			
							Group	Interval	Interaction	
BW (g)	Young	178 ± 2.07								
	Aged		225.00 ± 8.58	228.25 ± 8.84	235.25 ± 7.23	237.75 ± 9.15	<0.001	<0.001	<0.001	<0.001
	OVX		234.38 ± 6.54	241.75 ± 6.21	254.53 ± 5.09	256.88 ± 5.53				
	OVF		233.13 ± 5.53	262.13 ± 5.03	284.19 ± 4.43	293.38 ± 5.42				
HW (g)	Young	0.730 ± 0.032								
	Aged					0.846 ± 0.054	0.300			
	OVX					0.896 ± 0.054				
	OVF					0.895 ± 0.037				
AWThD (mm)	Young	0.91 ± 0.006								
	Aged		1.09 ± 0.022	1.05 ± 0.023	1.03 ± 0.014	1.03 ± 0.020	0.809	<0.001	0.407	<0.001
	OVX		1.07 ± 0.013	1.07 ± 0.016	1.02 ± 0.009	1.01 ± 0.013				
	OVF		1.10 ± 0.017	1.08 ± 0.022	1.03 ± 0.014	1.01 ± 0.018				
AWThS (mm)	Young	1.20 ± 0.027								
	Aged		1.70 ± 0.074	1.55 ± 0.072	1.53 ± 0.030	1.51 ± 0.034	0.017	<0.001	0.044	<0.001
	OVX		1.51 ± 0.032	1.52 ± 0.043	1.43 ± 0.030	1.33 ± 0.021				
	OVF		1.47 ± 0.033	1.56 ± 0.047	1.44 ± 0.025	1.40 ± 0.031				
LVIDD (mm)	Young	6.74 ± 0.088								
	Aged		6.65 ± 0.089	6.76 ± 0.133	6.80 ± 0.124	6.99 ± 0.110	0.205	<0.001	0.142	0.003
	OVX		6.81 ± 0.110	6.87 ± 0.112	7.09 ± 0.084	7.32 ± 0.097				
	OVF		6.59 ± 0.091	6.85 ± 0.097	7.19 ± 0.109	7.20 ± 0.095				
LVIDS (mm)	Young	3.82 ± 0.065								
	Aged		3.64 ± 0.079	4.00 ± 0.113	4.04 ± 0.128	4.06 ± 0.141	0.388	<0.001	0.275	0.014
	OVX		3.74 ± 0.064	4.05 ± 0.123	4.25 ± 0.099	4.44 ± 0.154				
	OVF		3.61 ± 0.061	3.91 ± 0.114	4.25 ± 0.118	4.30 ± 0.108				
PWThD (mm)	Young	1.10 ± 0.028								
	Aged		1.49 ± 0.030	1.44 ± 0.045	1.38 ± 0.027	1.44 ± 0.065	0.729	<0.001	0.483	0.002
	OVX		1.46 ± 0.036	1.45 ± 0.038	1.35 ± 0.026	1.34 ± 0.047				
	OVF		1.52 ± 0.025	1.44 ± 0.042	1.35 ± 0.036	1.36 ± 0.051				
PWThS (mm)	Young	1.97 ± 0.280								
	Aged		2.44 ± 0.035	2.33 ± 0.056	2.35 ± 0.041	2.41 ± 0.084	0.298	0.003	0.951	0.216
	OVX		2.52 ± 0.044	2.37 ± 0.055	2.33 ± 0.038	2.36 ± 0.074				
	OVF		2.58 ± 0.041	2.43 ± 0.071	2.39 ± 0.057	2.45 ± 0.065				
HR (bpm)	Young	302.15 ± 10.972								
	Aged		292.75 ± 9.100	307.88 ± 11.038	291.13 ± 14.111	311.50 ± 8.113	0.225	0.006	0.275	0.199
	OVX		297.69 ± 5.702	335.38 ± 7.061	309.81 ± 8.930	302.38 ± 9.707				
	OVF		305.00 ± 7.484	323.13 ± 5.989	301.50 ± 11.431	326.56 ± 8.703				
EF (%)	Young	79.87 ± 0.429								
	Aged		81.75 ± 0.701	77.00 ± 1.239	77.00 ± 1.180	78.25 ± 1.449	0.597	<0.001	0.295	0.109
	OVX		81.56 ± 0.223	77.25 ± 1.039	76.44 ± 0.962	75.00 ± 1.497				
	OVF		81.75 ± 0.520	79.25 ± 1.135	77.00 ± 1.057	76.38 ± 1.197				
FS (%)	Young	43.33 ± 0.419								
	Aged		45.38 ± 0.596	40.75 ± 1.146	40.75 ± 1.098	42.13 ± 1.302	0.548	<0.001	0.333	0.146
	OVX		45.19 ± 0.277	41.00 ± 0.949	40.19 ± 0.823	39.38 ± 1.316				
	OVF		45.38 ± 0.523	42.94 ± 1.086	41.06 ± 0.994	40.50 ± 1.021				

Values are means ± SEM. AWThD, anterior wall thickness diastole; AWThS, anterior wall thickness systole; BW, body weight; EF, ejection fraction; FS, fractional shortening; HR, heart rate; HW, heart weight; LVIDD, left ventricle internal diameter diastole; LVIDS, left ventricle internal diameter systole; PWThD, posterior wall thickness diastole; PWThS, posterior wall thickness systole.

with ovariectomy, accompanied by a marked development of papillary fibrosis. The presence of modest chamber geometric remodelling, preservation of EF, prolongation of LV relaxation time, loss of CO and development of fibrosis recapitulates several of the features recognized in older, female HFpEF patients and suggests this model may be suitable to explore the role that risk factors play in early disease development and the effects of therapeutic interventions.

Multiple rodent models have been employed in an attempt to examine suspect pathophysiological events linked to the development of HFpEF (Conceição *et al.* 2016; Valero-Muñoz *et al.* 2017). While models commonly incorporate suspect aetiological factors such as pressure overload, obesity and diabetes, there is much less emphasis

on the use of female or aged animals, thus incompletely replicating the prototypical human female HFpEF patient (Omar *et al.* 2016). Common findings using young, male rodents with aortic banding/or hypertension include LV hypertrophy, inflammation, fibrosis, stiffer end-diastolic pressure–volume relationships (EDPVR), and prolongation of relaxation with minimal changes in EF (Conceição *et al.* 2016; Valero-Muñoz *et al.* 2017). Diabetic models also demonstrate hypertrophy and interstitial fibrosis, while obese animals show decreases in the E/A ratio (i.e. impaired LV relaxation) (Valero-Muñoz *et al.* 2017). There are certainly relevant applications for these animal models, but they do not replicate the convergence of ‘typical’ factors found in ageing female patients that subsequently develop HFpEF.

Ageing models have used various rat strains (mostly male) to characterize changes in cardiac structure/function (Boluyt, 2004; Pacher et al. 2004, 2008; Valero-Muñoz *et al.* 2017). When using ~2-year-old female Fischer 344 rats, ageing results in LV hypertrophy and diastolic dysfunction, while males from the same strain/age develop eccentric remodelling, mitral regurgitation, interstitial fibrosis and impaired systolic function (Forman *et al.* 1997). Hybrid Brown Norway–Fischer 344 rats (F344BN) have also been used to study the effects of ageing. Female rats of up to 30 months of age show development of LV hypertrophy, dilatation and diastolic dysfunction (Fannin *et al.* 2014), while decreases in collagen area fraction have been reported (Hacker, 2005). In our study, using echocardiography, we document the development of mild eccentric chamber remodelling from 18 to 21 months of age, with no apparent changes in diastolic or systolic function, including EF. However, direct catheter-based haemodynamics reveal with ageing hypertension, the prolongation of relaxation and a modest but significant reduction in CO while maintaining EF. Histology demonstrated an approximate doubling of collagen area fraction in the absence of chamber stiffening as revealed by *ex vivo* LV passive PV curves and epicardial strains. Therefore, the prolongation of relaxation is likely derived from impaired active LV

relaxation, and not the direct effect of excess collagen and tissue stiffening at the levels measured here (~5%). Thus, in aged female rats, there can be modest LV chamber remodelling, prolonged relaxation and interstitial fibrosis while maintaining normal EF.

The high prevalence of HFpEF in older women suggests a strong link between low oestrogen levels and the disease (Zhao *et al.* 2014). Interestingly, published studies suggest the development of greater levels of myocardial fibrosis in post-menopausal women *vs.* men (Barasch *et al.* 2009; Liu & Liu, 2014) with normal ageing or with HF. In rats, unlike menopausal women, oestradiol levels during ageing can be near their younger counterpart even past 20 months of age (Fannin *et al.* 2014). Thus, ovariectomy is commonly used to examine the role that low oestrogen levels play in altering cardiac structure/function (Knowlton & Lee, 2012). Unfortunately, only an extremely limited number of studies have used this approach. Using young male and female rats undergoing aortic banding (Douglas *et al.* 1998), a lesser degree of LV chamber remodelling, loss of function and fibrosis were noted in female animals. However, the protective role of oestrogens in rodent models of pressure overload is greatly diminished with ovariectomy (Bhuiyan *et al.* 2007). Stice *et al.* (2011) reported that ovariectomy in 20-month-old Norway Brown rats decreases LV fractional shortening from

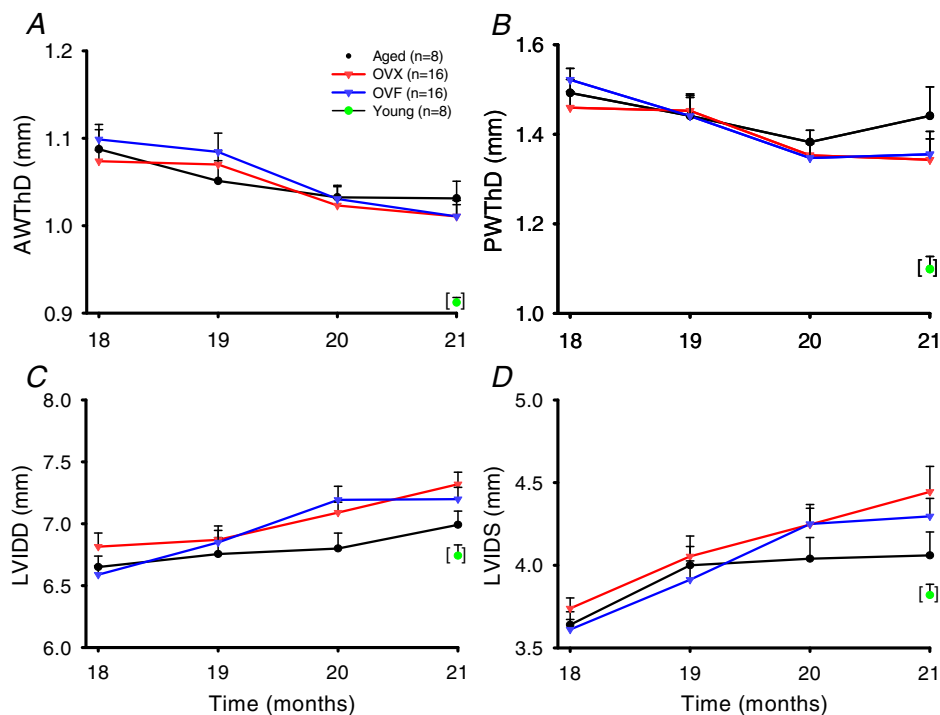


Figure 4. Left ventricular (LV) remodelling as serially tracked by echocardiography

Young group single time-point data included as reference. A, anterior wall thickness in diastole (AWThD). B, posterior wall thickness in diastole (PWThD). C, LV internal diameter diastole (LVIDD). D, LV internal diameter in systole (LVIDS). Values are mean \pm SEM. For panels A–D, $P < 0.001$ for time-dependent changes in all groups. OVf, ovariectomized + fructose; OVX, ovariectomized.

Table 2. Arterial and left ventricular (LV) haemodynamics by conductance catheter of young (Y), aged (A), ovariectomized (OVX) and ovariectomized + fructose (OVF) Fischer 344 female rats

Parameter	Group				P	Two-way ANOVA					
	Y (n = 8)	A (n = 8)	OVX (n = 16)	OVF (n = 16)		A vs. Y	OVX vs. Y	OVF vs. Y	OVX vs. A	OVF vs. A	OVF vs. OVX
SAC BW (g)	178.0 ± 2.1	238.3 ± 8.6	253.4 ± 5.4	290.8 ± 4.9	<0.001	<0.001	<0.001	<0.001	0.083	<0.001	<0.001
BSA (cm ²)	311.0 ± 2.4	377.4 ± 8.9	393.4 ± 5.7	431.3 ± 4.9	<0.001	<0.001	<0.001	<0.001	0.077	<0.001	<0.001
SW (mmHg ml)	157.2 ± 12.0	214.1 ± 18.6	143.4 ± 8.7	146.3 ± 10.8	0.001	0.031	0.824	0.789	0.001	0.002	0.842
CO (ml/min)	63.5 ± 6.3	63.5 ± 6.3	44.8 ± 2.4	46.3 ± 2.8	<0.001	0.899	<0.001	0.002	0.002	0.004	0.723
Cardiac index	0.212 ± 0.010	0.169 ± 0.017	0.114 ± 0.006	0.108 ± 0.007	<0.001	0.015	<0.001	<0.001	<0.001	<0.001	0.579
SV (μl)	194.8 ± 9.6	214.9 ± 29.3	167.2 ± 7.9	161.8 ± 8.8	0.031	0.605	0.404	0.323	0.051	0.049	0.730
SV index	0.627 ± 0.032	0.573 ± 0.080	0.427 ± 0.022	0.376 ± 0.022	<0.001	0.378	0.002	<0.001	0.024	0.002	0.426
V _{max} (μl)	386.6 ± 28.4	373.2 ± 29.1	339.0 ± 17.8	351.5 ± 31.9	0.667	NA	NA	NA	NA	NA	NA
V _{min} (μl)	191.8 ± 24.7	158.3 ± 27.8	171.8 ± 14.8	183.4 ± 30.3	0.870	NA	NA	NA	NA	NA	NA
V _{es} (μl)	208.1 ± 23.8	176.1 ± 27.4	198.5 ± 16.2	213.1 ± 32.5	0.830	NA	NA	NA	NA	NA	NA
V _{ed} (μl)	347.6 ± 31.9	350.6 ± 31.9	312.8 ± 17.1	318.9 ± 32.1	0.746	NA	NA	NA	NA	NA	NA
EDV index	1.121 ± 0.107	0.936 ± 0.093	0.800 ± 0.047	0.745 ± 0.078	0.013	0.434	0.040	0.013	0.432	0.361	0.563
P _{max}	114.1 ± 5.2	148.2 ± 11.6	138.0 ± 6.6	142.9 ± 6.1	0.042	0.050	0.133	0.049	0.740	0.636	0.831
P _{dev}	112.8 ± 5.3	146.3 ± 10.8	135.0 ± 6.0	140.8 ± 5.9	0.031	0.044	0.140	0.046	0.631	0.603	0.744
P _{es}	111.5 ± 5.0	144.1 ± 11.0	134.9 ± 6.2	139.6 ± 6.0	0.038	0.047	0.946	0.049	0.813	0.617	0.946
EF%	55.1 ± 4.1	61.4 ± 7.0	53.2 ± 2.6	56.3 ± 5.7	0.747	NA	NA	NA	NA	NA	NA
E _a	0.58 ± 0.03	0.759 ± 0.098	0.867 ± 0.094	0.913 ± 0.065	0.006	ns	<0.05	<0.05	ns	ns	ns
dP/dt _{max}	6645 ± 453	7902 ± 880	6459 ± 367	7001 ± 454	0.282	NA	NA	NA	NA	NA	NA
dP/dt _{min}	-9018 ± 621	-9377 ± 1158	-7746 ± 456	-8112 ± 638	0.192	NA	NA	NA	NA	NA	NA
dV/dt _{max}	8587 ± 516	7607 ± 734	6776 ± 734	6719 ± 438	0.077	NA	NA	NA	NA	NA	NA
dV/dt _{min}	-12937 ± 2451	-13087 ± 1762	-9511 ± 1525	-9189 ± 1192	0.228	NA	NA	NA	NA	NA	NA
Tau	10.0 ± 0.3	12.6 ± 0.9	13.8 ± 0.4	13.4 ± 0.5	<0.001	0.044	<0.001	<0.001	0.441	0.692	0.958
P _{ao,sys}	122.1 ± 6.9	180.5 ± 9.2	163.6 ± 7.4	166.7 ± 11.6	0.009	0.010	0.034	0.024	0.604	0.594	0.800
P _{ao,dia}	99.9 ± 3.3	115.3 ± 5.6	112.2 ± 3.8	111.6 ± 3.8	0.318	NA	NA	NA	NA	NA	NA
P _{ao,mean}	110.4 ± 4.1	142.7 ± 7.4	134.1 ± 5.0	134.1 ± 5.0	0.051	NA	NA	NA	NA	NA	NA
HR	339.0 ± 7.1	302.2 ± 11.3	271.4 ± 11.3	287.9 ± 9.9	0.002	0.220	0.001	0.017	0.193	0.391	0.404
PRSW	64.1 ± 4.5	73.8 ± 7.3	75.2 ± 4.5	74.3 ± 6.8	0.654	NA	NA	NA	NA	NA	NA
ESPVR slope	0.397 ± 0.03	0.617 ± 0.21	0.496 ± 0.101	0.675 ± 0.10	0.179	NA	NA	NA	NA	NA	NA
EDPVR slope	0.042 ± 0.006	0.0311 ± 0.005	0.0573 ± 0.007	0.0410 ± 0.004	0.022	0.484	0.285	0.896	0.030	0.610	0.111
EDVPR inter	-9.749 ± 3.55	-3.87 ± 2.01	-10.01 ± 2.22	-6.602 ± 1.87	0.329	NA	NA	NA	NA	NA	NA

Values are means ± SEM. NA, subgroup analysis not applicable. BSA, body surface area; CO, cardiac output; dP/dt_{max}, maximal rate of LV pressure rise over time; dP/dt_{min}, minimum rate of LV pressure decrease over time; E_a, arterial elastance; EDPVR, end-diastolic pressure–volume relationship slope; EDPVR inter, end-diastolic pressure volume relationship intercept; EDV, end-diastolic volume; EF, ejection fraction; ESPVR, end-systolic pressure–volume relationship slope; HR, heart rate; P_{ao,dia}, aortic diastolic pressure; P_{ao,mean}, mean aortic pressure; P_{ao,sys}, aortic systolic pressure; P_{dev}, LV developed pressure; P_{es}, end-systolic pressure; P_{max}, maximal LV pressure; PRSW, preload recruitable stroke work; SAC BW, terminal body weight; SV, stroke volume; SW, stroke work; Tau, isovolumic relaxation time constant; V_{max}, LV maximal volume; V_{ed}, end-diastolic volume; V_{es}, end-systolic volume; V_{min}, LV minimal volume.

50% (observed in control 4-month-old animals) to 40% and was restored by oestradiol supplementation. These changes were associated with the activation of regulators of inflammation in isolated myocytes, which were also suppressed by oestradiol. In a recent study by Alencar *et al.* (2017), the influence of ageing and oestrogen depletion on LV structure/function was examined in hybrid female F344BN rats. A subgroup of animals at 18 months of age underwent an ovariectomy for 2 months and relevant endpoints were examined. In their study, ovariectomy did not alter blood pressure, systolic function or lead to the development of hypertrophy or additional interstitial fibrosis beyond that noted for ageing. Significant alterations were only noted in LV relaxation and increases in filling pressure. Our echocardiography remodelling and systolic function data essentially replicate their results pertaining to the apparent lack of ‘added’

effects derived from ovariectomy. However, our use of a high-fidelity conductance catheter allowed us to provide evidence for a rather large (~30%) significant loss in stroke volume index, cardiac output index and increased arterial elastance in the presence of preserved EF in OVX rats that was not detected by echocardiography. *Ex vivo* LV passive PV curves did not demonstrate global changes in passive properties. However, OVX group EDPVR slopes were modestly higher *vs.* ageing. Conductance catheter results also replicated the increased in Tau noted in intact aged rats. Ovariectomy did not lead to further increases in collagen area fraction but did appear to uniquely influence the distribution of myocardial fibrosis towards the endocardium (*vs.* epicardium). Interestingly, papillary fibrosis was notably increased in OVX animals *vs.* ageing alone and may have important implications for disease development in the presence of mitral valve dysfunction.

In an attempt to incorporate excess body weight into our animal model, we utilized 10% fructose in water in OVX rats. As expected, ageing over 3 months led to a modest increase in body weight of ~6% while OVX yielded ~8% and OVF ~19%. However, none of the *in vivo*, *ex vivo* or histological endpoints showed greater differences between the OVF *vs.* the OVX groups. Thus, using this model, excess weight did not lead to greater, adverse changes in LV structure/function. A limitation of the approach used is that a blood-based metabolic profiling of these animal groups was not pursued.

As noted above, 'typical' female patients with HFpEF are older and suffer from hypertension and excess weight. Their hearts typically show minimal degrees of LV remodelling with fibrosis, and increases in active relaxation times while preserving EF. Reductions in CO typically become apparent upon physical exertion. The aged, female animal model implemented in this study recapitulates many of these features, and highlights an

important role for ovarian hormones in the maintenance of CO and possibly in the redistribution of excess interstitial cardiac collagens across the LV wall, and development of papillary fibrosis. These changes would likely be accentuated if animals were allowed to survive for a longer period of time and could lead to the development of a detectable HF phenotype. Furthermore, changes in the quality of collagen fibres would also need to be determined as, for example, the crosslinking of fibres can alter their mechanical properties. Surprisingly, the development of interstitial fibrosis as a function of ageing (about double *vs.* young) did not alter the mechanical properties of the LV in a uniform manner. However, an increase in Tau suggests impaired 'active' relaxation, likely related to alterations in calcium handling, which has been reported in other studies (Yang *et al.* 2017). The loss in stroke volume (and consequently in CO) in OVX does indicate that oestrogen depletion can contribute to impaired pump function. These data suggest that the use of invasive methods may

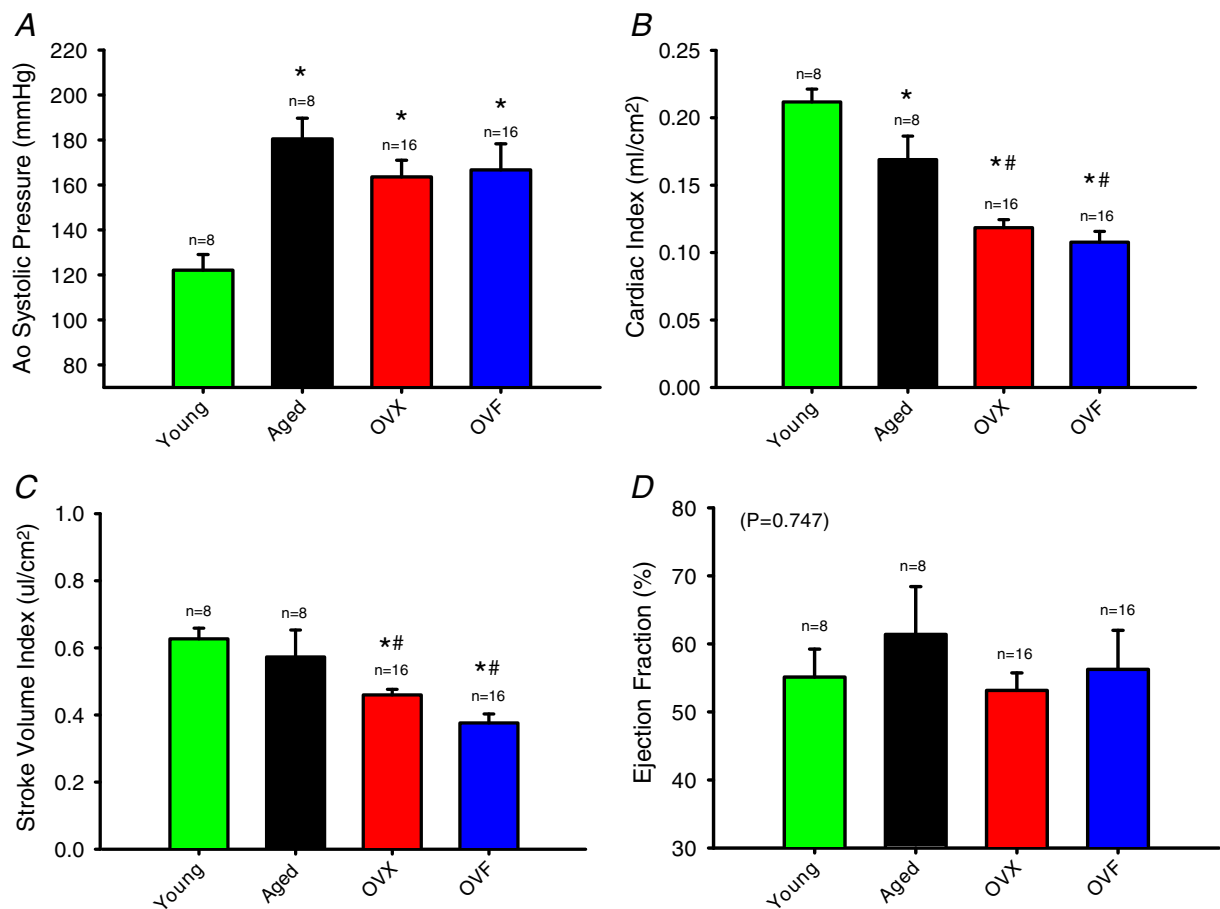


Figure 5. Haemodynamic values derived from arterial and left ventricular (LV) conductance catheter measurements during the terminal study

A, systolic aortic pressure ($P < 0.05$ aged, OVX and OVF *vs.* young). B, cardiac index ($*P < 0.05$, aged, OVX and OVF *vs.* young; and $\#P < 0.05$, OVX and OVF *vs.* aged). C, stroke volume index ($P < 0.05$ OVX and OVF *vs.* young, and $\#P < 0.05$, OVX and OVF *vs.* aged). D, ejection fraction. Values are means \pm SEM. OVF, ovariectomized + fructose; OVX, ovariectomized.

be required to accurately detect HFpEF in animal models. It is worth noting that all active functional measurements in the current studies were done with the animal in a 'resting' state. The true unmasking of the effect that specific interventions have in aged models may require the use of

'stress' interventions such as a dobutamine infusion during the acquisition of LV haemodynamics. This modality of testing would be equivalent to that done in HFpEF patients when stressed by exercise or heart rate stimulation to truly unmask the degree of LV dysfunction.

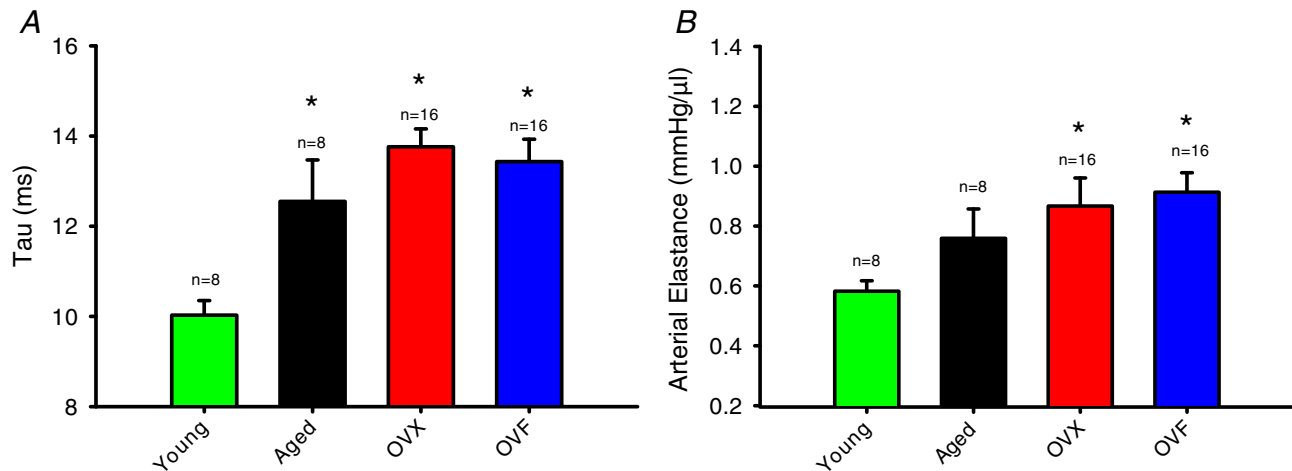


Figure 6. Hemodynamic values derived from arterial and left ventricular (LV) conductance catheter measurements during the terminal study

A, LV isovolumic relaxation time constant (τ) ($P < 0.05$ aged, OVX and OVF vs. young). B, arterial elastance ($P < 0.05$ OVX and OVF vs. young). Values are means \pm SEM. OVF, ovariectomized + fructose; OVX, ovariectomized.

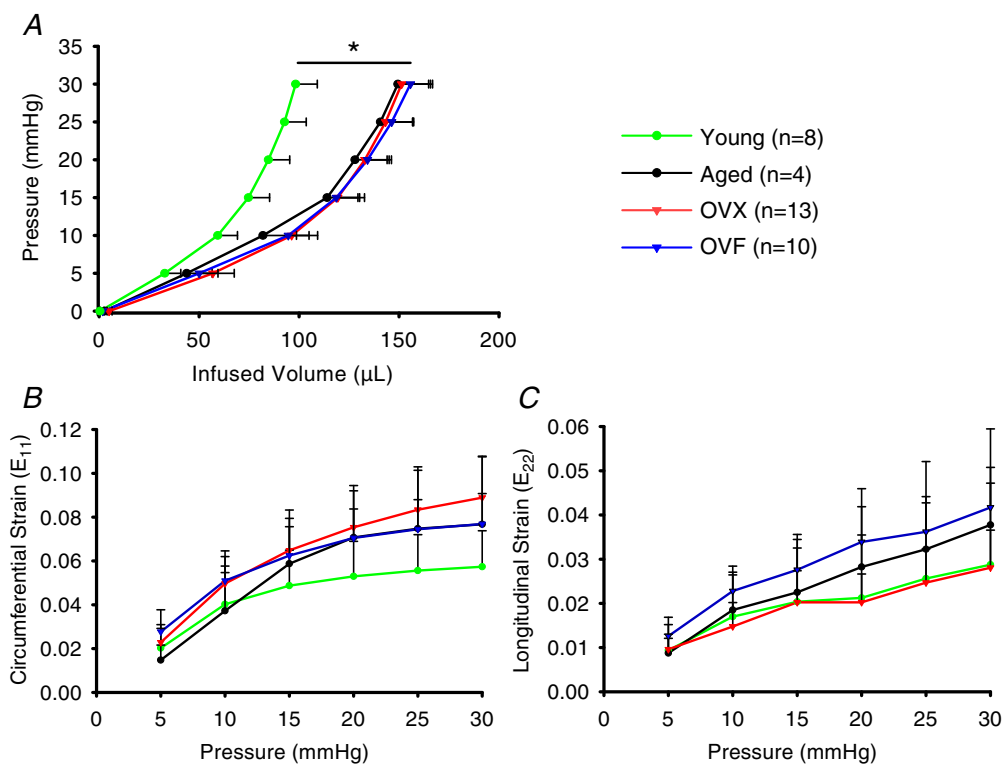


Figure 7. Ex vivo analysis of left ventricular (LV) mechanics

A, passive LV pressure–volume (PV) curves for all groups at 21 months of age ($P < 0.001$ aged, OVX and OVF vs. young). B and C, two-dimensional circumferential (E_{11}) and longitudinal (E_{22}) LV epicardial strains at incremental LV pressures. * $P < 0.001$, OVX vs. young. Values are means \pm SEM. OVF, ovariectomized + fructose; OVX, ovariectomized.

As the pathophysiology of HFpEF remains unclear, the identification and modelling of early stages of the disease is critical to its understanding. It is difficult to envision such measurements in a patient population at risk since the disease is likely to progress slowly over time. Thus, the need to develop and implement animal models

that incorporate recognized risk factors and ‘mimic’ early stages of the pathology allow for the evaluation of therapeutic strategies targeting those elements identified as critical to its evolution. Thus, the use of aged female rats undergoing ovariectomy may allow investigators to further examine the role that oestrogen depletion plays in

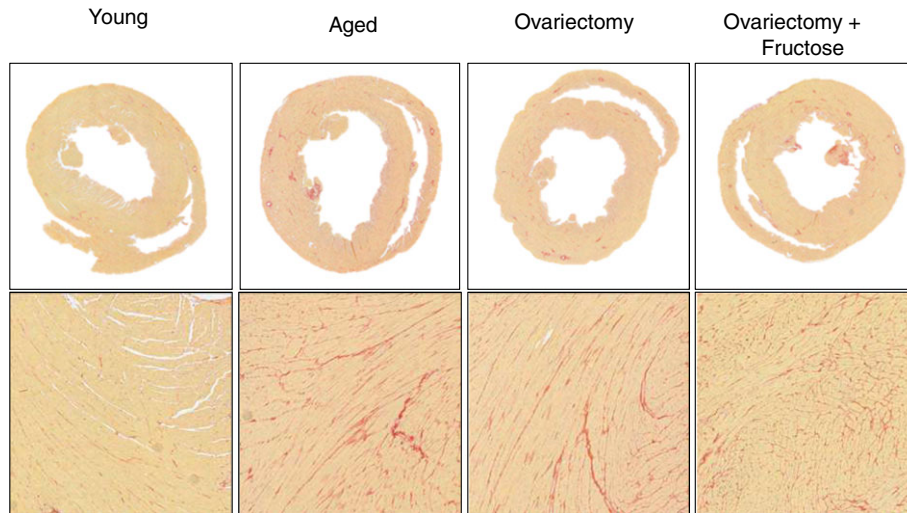


Figure 8. Composite of representative panels for left ventricular collagen as derived from Sirius Red staining

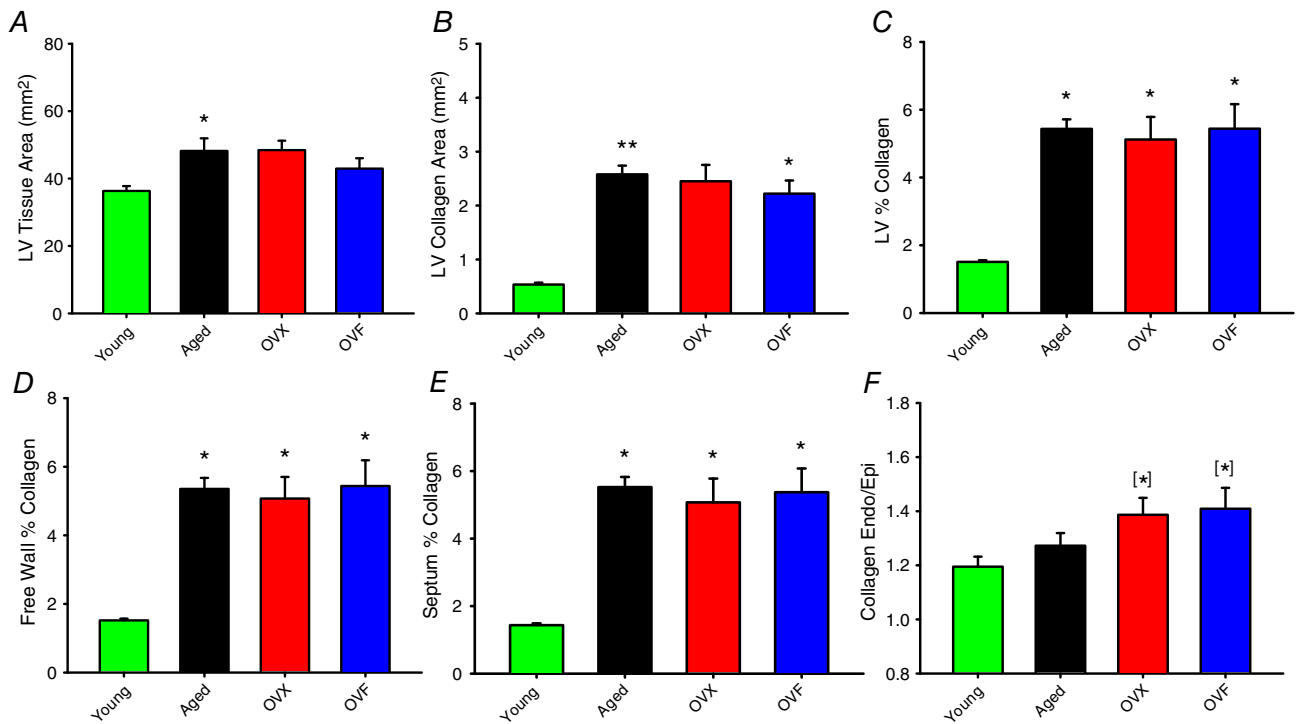


Figure 9. Morphometric and histological analysis of left ventricular (LV) tissue sections
 A, LV tissue area; B, LV collagen area; C, LV % collagen (collagen/LV area); D, free wall percentage collagen; E, septum percentage collagen; F, endocardium/epicardium collagen ratio. Values are means ± SEM. **P* < 0.05 vs. young, ANOVA. [*]*P* < 0.05 vs. young, unpaired *t* test. Endo: endocardium; Epi: epicardium; OVX, ovariectomized + fructose; OVX, ovariectomized.

the early stages of HFpEF development, as well as to test for pharmacological interventions that may modify this process.

References

- Alencar AK, da Silva JS, Lin M, Silva AM, Sun X, Ferrario CM, Cheng C, Sudo RT, Zapata-Sudo G, Wang H & Groban L (2017). Effect of age, estrogen status, and late-life GPER activation on cardiac structure and function in the Fischer344 × Brown Norway female rat. *J Gerontol A Biol Sci Med Sci* **72**, 152–162.
- Barandiarán Aizpurua A, Schroen B, van Bilsen M & van Empel VPM (2019). Targeted HFpEF therapy based on matchmaking of human and animal models. *Am J Physiol Circ Physiol* (**in press**; <https://doi.org/10.1152/ajpheart.00024.2018>).
- Barasch E, Gottdiener JS, Aurigemma G, Kitzman DW, Han J, Kop WJ & Tracy RP (2009). Association between elevated fibrosis markers and heart failure in the elderly: the cardiovascular health study. *Circ Heart Fail* **2**, 303–310.
- Bhuiyan MS, Shioda N & Fukunaga K (2007). Ovariectomy augments pressure overload-induced hypertrophy associated with changes in Akt and nitric oxide synthase signaling pathways in female rats. *Am J Physiol Endocrinol Metab* **293**, E1606–E1614.
- Boluyt MO (2004). Echocardiographic assessment of age-associated changes in systolic and diastolic function of the female F344 rat heart. *J Appl Physiol* **96**, 822–828.
- Borlaug BA (2014). The pathophysiology of heart failure with preserved ejection fraction. *Nat Rev Cardiol* **11**, 507–515.
- Borlaug BA (2016). Is HFpEF one disease or many? *J Am Coll Cardiol* **67**, 671–673.
- Conceição G, Heinonen I, Lourenço AP, Duncker DJ & Falcão-Pires I (2016). Animal models of heart failure with preserved ejection fraction. *Netherlands Heart J* **24**, 275–286.
- Douglas PS, Katz SE, Weinberg EO, Chen MH, Bishop SP & Lorell BH (1998). Hypertrophic remodeling: Gender differences in the early response to left ventricular pressure overload. *J Am Coll Cardiol* **32**, 1118–1125.
- Eaton CB, Pettinger M, Rossouw J, Martin LW, Foraker R, Quddus A, Liu S, Wampler NS, Hank Wu W-C, Manson JE, Margolis K, Johnson KC, Allison M, Corbie-Smith G, Rosamond W, Brethett K & Klein L (2016). Risk factors for incident hospitalized heart failure with preserved versus reduced ejection fraction in a multiracial cohort of postmenopausal women. *Circ Heart Fail* **9**, e002883.
- Fannin J, Rice KM, Thulluri S, Dornon L, Arvapalli RK, Wehner P & Blough ER (2014). Age-associated alterations of cardiac structure and function in the female F344 × BN rat heart. *Age (Omaha)* **36**, 9684.
- Forman DE, Cittadini A, Azhar G, Douglas PS & Wei JY (1997). Cardiac morphology and function in senescent rats: Gender-related differences. *J Am Coll Cardiol* **30**, 1872–1877.
- Hacker TA (2005). Age-related changes in cardiac structure and function in Fischer 344 × Brown Norway hybrid rats. *AJP Hear Circ Physiol* **290**, H304–H311.
- Knowlton AA & Lee AR (2012). Estrogen and the cardiovascular system. *Pharmacol Ther* **135**, 54–70.
- Lam CSP, Donal E, Kraigher-Krainer E & Vasan RS (2011). Epidemiology and clinical course of heart failure with preserved ejection fraction. *Eur J Heart Fail* **13**, 18–28.
- Liu CY, Liu YC, Wu C, Armstrong A, Volpe GJ, van der Geest RJ, Liu Y, Hundley WG, Gomes AS, Liu S, Nacif M, Bluemke DA & Lima JAC (2014). Evaluation of age-related interstitial myocardial fibrosis with cardiac magnetic resonance contrast-enhanced T1 mapping: MESA (Multi-Ethnic Study of Atherosclerosis). **62**, 1280–1287.
- Omar AMS, Bansal M & Sengupta PP (2016). Advances in echocardiographic imaging in heart failure with reduced and preserved ejection fraction. *Circ Res* **119**, 357–374.
- Omens JH, MacKenna DA & McCulloch AD (1993). Measurement of strain and analysis of stress in resting rat left ventricular myocardium. *J Biomech* **26**, 665–676.
- Omens JH, Milkes DE & Covell JW (1995). Effects of pressure overload on the passive mechanics of the rat left ventricle. *Ann Biomed Eng* **23**, 152–163.
- Owan TE, Hodge DO, Herges RM, Jacobsen SJ, Roger VL & Redfield MM (2006). Trends in prevalence and outcome of heart failure with preserved ejection fraction. *N Engl J Med* **355**, 251–259.
- Pacher P, Mabley JG, Liaudet L, Evgenov O V, Marton A, Haskó G, Kollai M & Szabó C (2004). Left ventricular pressure-volume relationship in a rat model of advanced aging-associated heart failure. *Am J Physiol Heart Circ Physiol* **287**, H2132–H2137.
- Pacher P, Nagayama T, Mukhopadhyay P, Bátkai S & Kass DA (2008). Measurement of cardiac function using pressure-volume conductance catheter technique in mice and rats. *Nat Protoc* **3**, 1422–1434.
- Sohrabji F (2005). Estrogen: A neuroprotective or proinflammatory hormone? Emerging evidence from reproductive aging models. *Ann N Y Acad Sci* **1052**, 75–90.
- Stice JP, Chen L, Kim SC, Jung JS, Tran AL, Liu TT & Knowlton AA (2011). 17 β -Estradiol, aging, inflammation, and the stress response in the female heart. *Endocrinology* **152**, 1589–1598.
- Stout Steele M & Bennett RA (2011). Clinical technique: Dorsal ovariectomy in rodents. *J Exot Pet Med* **20**, 222–226.
- Takahashi TA & Johnson KM (2015). Menopause. *Med Clin North Am* **99**, 521–534.
- Valero-Muñoz M, Backman W & Sam F (2017). Murine models of heart failure with preserved ejection fraction: A “fishing expedition.” *JACC Basic to Transl Sci* **2**, 770–789.
- Yang H-Y, Firth JM, Francis AJ, Alvarez-Laviada A & MacLeod KT (2017). The effect of ovariectomy on intracellular calcium (Ca²⁺) regulation in guinea pig cardiomyocytes. *Am J Physiol Hear Circ Physiol* **313**, H1031–H1043.
- Zhao Z, Wang H, Jessup JA, Lindsey SH, Chappell MC & Groban L (2014). Role of estrogen in diastolic dysfunction. *AJP Hear Circ Physiol* **306**, H628–H640.

Additional information

Competing interests

F.V. is a co-founder and he and G.C. are stockholders of Cardero Therapeutics, Inc.

Author contributions

MB, BI, RG, GC, JO and FV conceptualized and designed the work. All authors contributed to acquisition, analysis, interpretation, and drafting. Experiments were performed at UCSD. All authors have read and approved the final version of this manuscript and agree to be accountable for all aspects of the work in ensuring that questions related to the accuracy or integrity of any part of the work are appropriately investigated and resolved. All persons designated as authors qualify for authorship, and all those who qualify for authorship are listed.

Funding

Funding was provided by the Department of Defense PR150090 and National Institutes of Health DK98717, AG47326 to F.V. and Consejo Nacional De Ciencia y Tecnologia, Mexico to G.C.

Acknowledgements

We acknowledge the technical support of Diane Huang with animal and physiological studies.

Mechanical regulation of gene expression in cardiac myocytes and fibroblasts

Jeffrey J. Saucerman¹, Philip M. Tan¹, Kyle S. Buchholz², Andrew D. McCulloch²* and Jeffrey H. Omens²

Abstract | The intact heart undergoes complex and multiscale remodelling processes in response to altered mechanical cues. Remodelling of the myocardium is regulated by a combination of myocyte and non-myocyte responses to mechanosensitive pathways, which can alter gene expression and therefore function in these cells. Cellular mechanotransduction and its downstream effects on gene expression are initially compensatory mechanisms during adaptations to the altered mechanical environment, but under prolonged and abnormal loading conditions, they can become maladaptive, leading to impaired function and cardiac pathologies. In this Review, we summarize mechanoregulated pathways in cardiac myocytes and fibroblasts that lead to altered gene expression and cell remodelling under physiological and pathophysiological conditions. Developments in systems modelling of the networks that regulate gene expression in response to mechanical stimuli should improve integrative understanding of their roles in vivo and help to discover new combinations of drugs and device therapies targeting mechanosignalling in heart disease.

Physiological and pathological cardiac structural remodelling are commonly associated with chronic alterations in haemodynamics, chamber shape and myocardial mechanics that can initially compensate for, but ultimately exacerbate, the physical triggers of cardiac remodelling^{1,2}. Cell-mediated mechanotransduction responses are important regulators of adaptive and maladaptive myocyte and matrix remodelling³. Mechanical loading also induces the release of factors such as angiotensin II, endothelin 1 and transforming growth factor- β (TGF β), which are potent activators of myocyte hypertrophy and matrix remodelling^{4–6}.

At the organ and tissue scales, concentric hypertrophy during pressure overload and exercise-induced physiological hypertrophy can be homeostatic or compensatory by normalizing wall stress or increasing cardiac output. These hypertrophic responses can also be accompanied by adaptive remodelling of the extracellular matrix (ECM) and coronary vasculature. In vitro studies suggest that these responses can be derived from fundamental regulatory mechanisms that drive normal sarcomerogenesis and match ventricular structure to mechanical workload demands⁷. However, under pathological conditions, myocardial mechanoregulated remodelling responses frequently become maladaptive, leading to decompensation and failure associated with

elevated wall stresses, insufficient or inappropriate cardiomyocyte hypertrophy, apoptosis, pathological fibrosis or energetic mismatches between supply and demand^{8–10}. Haemodynamic loading itself is an important therapeutic target, and mechanical unloading with left ventricular assist devices (LVADs) or other device strategies can, under some conditions, reverse changes in gene expression and structural remodelling and partially restore ventricular function^{11–13}.

Cardiac tissue remodelling is regulated by multiple cell types, including cardiomyocytes, fibroblasts, endothelial cells, smooth muscle cells and haematopoietic-derived cells. Endothelial cells constitute the majority of non-cardiomyocytes in the heart¹⁴ and are involved in multiple regulatory and disease responses in the myocardium. Because of the central roles of cardiomyocytes and fibroblasts in cardiac structural remodelling, in this Review, we focus on these cell types and their responses to multiple biomechanical signals^{15–17}, although other cell types are clearly also mechanoregulated. The cellular mechanosensors, signalling pathways, timescales and functional responses share similarities between these two cell types. Fibroblast–cardiomyocyte crosstalk during mechanical stimulation is clearly present and important, although still not fully understood^{18,19}. All whole-tissue and many in vitro studies reflect the

¹Department of Biomedical Engineering, University of Virginia, Charlottesville, VA, USA.

²Departments of Bioengineering and Medicine, University of California San Diego, La Jolla, CA, USA.

*e-mail: amcculloch@ucsd.edu

<https://doi.org/10.1038/s41569-019-0155-8>

Key points

- The complex remodelling processes in the myocardium are regulated by mechanical signals that are sensed and transduced into transcriptional responses by cardiac myocytes and fibroblasts.
- Mechanosensitive pathways regulate expression of genes that encode proteins mediating cardiac myocyte hypertrophy, myofibroblast differentiation and remodelling of the extracellular matrix.
- Mathematical systems models are beginning to address outstanding challenges regarding how cardiac cells integrate complex mechanical and biochemical signals to coordinate gene expression and cell remodelling.
- Integrative experimental and computational mechanotransduction studies should provide further insights into mechanisms and potential therapies for mechano-based diseases, including chronic tissue and chamber pathological remodelling.

combined gene-expression response in myocytes and non-myocytes.

Cardiac myocytes and fibroblasts have been shown to respond to a variety of mechanical stimuli, including static and dynamic, isotropic and anisotropic, compressive and tensile stresses and strains, as well as fluid flow shear stresses and alterations in substrate stiffness. The features of the mechanical stimulus can induce distinct signalling mechanisms and gene-expression profiles. A variety of molecular mediators and pathways have been identified. Regardless of the specific experimental system or stimulus, there seem to be common mechano-regulated gene programmes, such as the re-expression of fetal gene programmes³⁰ and the induction of genes encoding ECM²¹ and cytoskeletal proteins²², suggesting that these genes might be critical in the remodelling responses of the heart to altered mechanical conditions. We review the major pathways shown to be mechano-regulated and the major downstream transcriptional responses in cardiac myocytes and fibroblasts (FIG. 1).

Nevertheless, how these numerous mechanical signals and pathways are integrated *in vivo*, and how they determine hypertrophic versus fibrotic responses, eccentric versus concentric hypertrophy, hypertrophic versus dilated cardiomyopathy^{23,24}, compensated versus decompensated adaptation, or heart failure with reduced ejection fraction versus heart failure with preserved ejection fraction remains poorly understood^{25,26}. Therefore, we also emphasize the need for more integrative analyses of mechanoregulatory mechanisms in cardiac cells and discuss new, integrative approaches to analysing cardiac cell mechanosignalling that promise to advance this synthesis. Given that these approaches need to account for the wide variety of mechanical stimuli, mechanosensors, signalling pathways, and transcriptional and phenotypic responses, we conclude by surveying new systems biology approaches, such as multiscale computational models that promise to advance our understanding of the relationships between altered cardiac wall mechanics, changes in gene expression, and chronic tissue and chamber remodelling.

Cardiac mechanosensitive pathways

The myocardium in adult mammals is a structurally complex tissue composed of many cell types, including myocytes, fibroblasts, endothelial cells and perivascular smooth muscle cells. Myocytes make up >70%

of the myocardial volume, but only 25–40% of the cells by number^{14,27}. In this section, we review cardiac cell structural and functional pathways that mediate mechanosensitive responses in two predominant and well-characterized cell types in the heart: myocytes and fibroblasts. These pathways are especially active during cardiac growth and development and are downregulated under normal homeostatic conditions in adults. Many pathways are also altered or reactivated by abnormal or pathological conditions in the mature heart. Mechanosensing and the subsequent signalling processes and gene expression are associated with structures and protein complexes on the surface of, inside and between these cells (FIG. 1).

Cell membrane and downstream pathways

The integrin complex in cardiac myocytes. Transmission of forces between the interior and exterior of cardiac myocytes is facilitated by transmembrane proteins such as integrins and their associated intercellular complexes. Forces generated by the contractile filaments are transmitted outside the cell through this complex and, likewise, cells sense external mechanical cues via these connections. Integrins are receptors that form dimers with α and β subunits, which can bind to ECM proteins, including fibronectin, laminin and collagen²⁸. In response to pressure-overload-induced hypertrophy, the expression of $\alpha1$, $\alpha5$, $\alpha7$ and $\beta1D$ integrin subunits increases²⁹. Hearts deficient in $\beta1$ integrin have a blunted hypertrophic response to transverse aortic constriction (TAC)³⁰. Integrins are connected to intracellular signalling proteins, such as integrin-linked protein kinase (ILK), an important regulator of sarcoplasmic/endoplasmic reticulum calcium ATPase (SERCA) and phospholamban, which both regulate cardiomyocyte contractility³¹.

The costamere is an organized membrane complex localized at the Z-disc in muscle cells that incorporates integrins and other proteins such as vinculin and talin, mechanically linking cytoskeletal structures and the sarcomeres to the sarcolemma and ECM³². Forces at the costamere not only cause cell deformations³³ but also induce activation of vinculin, focal adhesion kinase (FAK), proto-oncogene tyrosine-protein kinase SRC and the small GTPase RhoA^{34,35}. Vinculin also localizes to the intercalated disc, which has made it harder to isolate the specific function of vinculin in mechanotransduction³⁶. Vinculin heterozygous-null mice have decreased cardiac function after 6 weeks of TAC³⁷. Mice deficient in talin 1 have a blunted hypertrophic response to TAC³⁸. Talin can recruit FAK to the costamere³⁹. FAK is an important regulator of cytoskeletal organization and hypertrophic gene expression⁴⁰, has been shown to mediate integrin signalling leading to hypertrophy and is activated by α_1 -adrenergic stimulation⁴¹. In addition to its function at the costameres, FAK and its carboxy-terminal-binding partners p130 CRK-associated substrate (p130Cas) and paxillin also translocate to the Z-disc with hypertrophy. Therefore, the assembly of signalling complexes that include the costameric proteins as well as p130Cas, FAK and paxillin at Z-discs might regulate, either directly or indirectly, both cytoskeletal

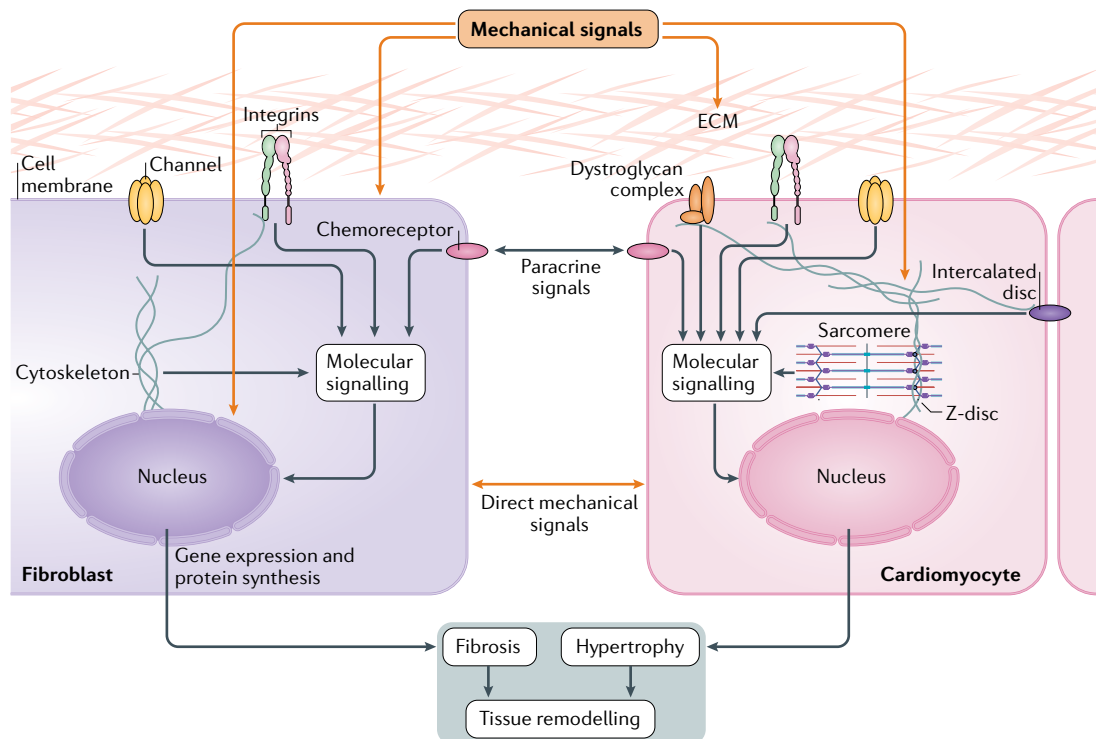


Fig. 1 | **Major mechanosensitive mechanisms and pathways in cardiac fibroblasts and myocytes.** Mechanical signals that act on the extracellular matrix (ECM) and cell membranes and internally on the cytoskeleton and nucleus initiate complex molecular signalling cascades, leading to changes in gene expression and protein synthesis in both cell types. Direct and indirect interactions between cells also mediate these responses. The net result of the changes in the mechanical cues is tissue remodelling and, in many cases, pathophysiological outcomes.

organization and gene expression associated with the cardiac myocyte hypertrophic stretch response⁴⁰.

The integrin complex in fibroblasts. Cardiac fibrosis and the accumulation of ECM is found in almost all forms of cardiac disease⁴², and the transformation of cardiac fibroblasts to myofibroblasts and their regulation of tissue fibrosis and ECM is mediated by a variety of chemical and physical stimuli⁴³. The ECM is an important mediator in the regulation of cell surface growth factor receptors and adhesion molecules in fibroblasts, such as integrins⁴³. When cardiac fibroblasts bind to ECM ligands, these cells can sense and respond to mechanical signals via membrane receptors, including integrins, which cluster to form focal adhesions. In fibroblasts, the focal adhesion–integrin complex is a primary mechanosensing organelle⁴⁴. Integrins interact with >150 known partners, making the focal adhesion complex the initiator of many downstream signalling pathways⁴⁵. These pathways include crosstalk with other membrane receptors, including G-protein-coupled receptors and tyrosine kinase receptors^{46,47}.

Activation of fibrotic signalling depends on specific integrins⁴⁸ and ECM ligands^{43,49}. Multiple components of the focal adhesion complex and their interactions result in fibrosis-related signalling cascades in response to mechanical stimuli. Integrins also directly activate non-receptor tyrosine-protein kinases, such as FAK, SRC and FYN in response to mechanical cues^{49,50}, and pathways such as mitogen-activated protein kinases (MAPKs) and

p38 (REF.⁵¹), leading to ECM production and fibrosis^{52,53}. Therefore, strong feedback exists between integrin-mediated responses to the stretched ECM and the fibroblast-mediated remodelling of ECM synthesis, degradation and crosslinking⁴⁹, as discussed further below.

The dystroglycan complex in cardiac myocytes. The dystroglycan complex is another mechanical link between the cardiomyocyte cytoskeleton and the ECM⁵⁴. Proteins associated with this transmembrane complex include dystrophin, sarcoglycans, dystroglycan, dystrobrevins, syntrophins, sarcospan, caveolin 3 and neuronal nitric oxide synthase⁵⁴. Dystroglycan attaches to the actin cytoskeleton via dystrophin⁵⁵ and connects externally to the ECM protein laminin⁵⁶. Dystrophin mutations lead to Duchene muscular dystrophy^{57,58}, and force production and power output are substantially reduced in the skeletal muscle of dystrophin-deficient mice⁵⁹. Disruption of the dystrophin–dystroglycan complex impairs the capacity of cardiomyocytes to produce nitric oxide and might increase cell slippage and chamber dilatation in response to stretch^{60,61}.

Changes in gene expression in models with dystroglycan complex defects are consistent with an inflammatory response⁶² and involve genes encoding both cellular (actins, cardiac ankyrin repeat protein (CARP; also known as ANKRD1) and cathepsins) and ECM (procollagens, biglycan, matrix metalloproteinases and tenascin C) proteins⁵⁴. Genes in metabolic and energetic pathways tend to be downregulated⁶³.

Mechanosensitive channels in cardiac myocytes. Many mechanoregulated responses, such as mechanoelectric feedback, in cardiac myocytes have been attributed to stretch-activated ion currents. Mechanosensitive channels are important mediators of sarcolemmal stretch sensing and have been implicated in arrhythmias induced by acute and chronic changes in cardiac mechanical loading⁶⁴. Mechanosensitive ion channels have been reported in the sarcolemma and transverse-tubule system in cardiac myocytes and regulate transmembrane fluxes of sodium, potassium, calcium and chloride ions⁶⁴.

Intracellular calcium release was reported in some of the earliest studies of myocyte responses to acute stretch^{65–67}, but it has taken many years to identify the origins of this calcium. Among the calcium channels claimed to be stretch-sensitive, the L-type calcium channel (LTCC)^{68–70} and members of the transient receptor potential (TRP) channel family^{71–73} have the most evidence. As is the case with angiotensin II receptor activation, calcium release triggers the upregulation of a wide range of hypertrophic factors⁷⁴. Many of these calcium-dependent effects are mediated by the calcineurin–nuclear factor of activated T cells (NFAT) pathway^{75,76}. Importantly, the mechanosensing capacity of cardiac calcium and other ion channels has relevance for electrophysiology as well as cellular hypertrophy⁷⁷. As further studies clarify the role of LTCCs and TRP channels in the heart, their pharmacological relevance will continue to increase⁷⁸.

Mechanosensitive channels in fibroblasts. Although well documented in cardiac myocytes, mechanosensitive channels in cardiac fibroblasts and their role in regulating cell function are not as clear. Cardiac fibroblasts express several ion channels that are not necessarily mechanically sensitive ($\text{Na}_v1.5$, K_{ATP} and BK_{Ca})⁷⁹, but fibroblasts might have stretch-activated ion currents through channels such as TRPs⁶⁴ and other nonselective cation conductance channels⁸⁰ that might affect mechanoelectric feedback⁸¹. Other functions in cardiac fibroblasts, such as myofibroblast differentiation in response to $\text{TGF}\beta$ and matrix stiffness, are regulated by mechanosensitive ion channels, such as TRPs generally⁸² and TRPV4 specifically⁸³, and involve downstream signalling of AKT, SMAD and myocardin-related transcription factor A (MRTF-A) pathways. Studies in mouse pressure-overloaded hearts have shown that inhibition of TRPC3 activity reduces fibrosis, suggesting a role for these types of stretch-sensitive ion channels in fibrosis signalling⁸². Studies have also suggested that mechanosensitive TRPV4 channels are involved in the integration of mechanical and $\text{TGF}\beta$ signals into myofibroblast differentiation⁸⁴ and thereby the cardiac fibrosis response.

Calcium-related signalling in cardiac myocytes. In addition to its well-described function in excitation–contraction coupling, calcium is an important second messenger in the regulation of metabolism, apoptosis and transcription⁸⁵. A variety of external and internal mechanical loads affect intracellular calcium signalling⁸⁶. Stretch induces transient increases in intracellular calcium^{87,88} and sarcoplasmic reticulum calcium spark rate⁸⁹ via multiple mechanisms, including the influx of calcium

via membrane channels (as described above), triggering sarcoplasmic reticulum calcium release via ryanodine receptors⁸⁷. Studies suggest that stretch induces an increase in reactive oxygen species (ROS) in a process dependent on membrane-bound NADPH oxidase 2 (NOX2) and microtubules (termed X-ROS signalling), which increases the calcium sensitivity of ryanodine receptors and the frequency of calcium sparks⁹⁰. This stretch-induced X-ROS signalling has been associated with arrhythmia and diseases such as muscular dystrophy⁹¹. Myofilaments can also supply the increase in intracellular calcium via load-dependent changes in myofilament calcium sensitivity⁹² or by crossbridge detachment leading to calcium dissociation from troponin C⁹³. Elevated intracellular calcium can increase protein kinase C (PKC), calcineurin and calcium–calmodulin-dependent protein kinase II (CaMKII) signalling and thereby lead to downstream gene-expression changes⁸⁵. Calcium dynamics in atrial myocytes are also sensitive to mechanical stimuli, possibly mediated by a surface-membrane-associated compartment⁹⁴.

Several calcium-related pathways are associated with regulation of cellular hypertrophy and might be one mechanism by which cardiac myocytes sense external loads and respond with long-term gene regulation and cell growth. The calcium–calmodulin pathway regulates hypertrophic signalling and myocyte growth⁹⁵. Related to calcium signalling and cardiac hypertrophy are the CaMKII–histone deacetylase (HDAC) and calcineurin–NFAT pathways. HDACs can be regulated by hypertrophic stress signals⁹⁶ and have been associated with transcription factors including activator protein 1 (AP-1), activating transcription factor 1 (ATF1), serum response factor (SRF), cAMP-response element binding protein (CREB) and myocyte enhancer factor 2 (MEF2)⁹⁷. NFAT signalling is downstream of calcineurin and low-frequency calcium changes⁹⁸. Several hypertrophic pathways are related to NFAT signals via transcription factors such as GATA4 (REF.⁹⁹), and calcium-dependent calcineurin–NFAT pathway activation by stretch in myocytes is implicated in cellular hypertrophy¹⁰⁰.

Calcium-related signalling in fibroblasts. Stretch-activated ion channels in cardiac fibroblasts create an early signal within the cell that is responsive to stretch of the membrane¹⁰¹. Deformation of the fibroblast membrane is associated with fluxes of calcium and other ions, and the calcium influx is seen in various cell-stretch studies and is associated with fibrosis in the tissue²¹. Increases in calcium signals activate multiple signalling pathways in fibroblasts including MAPK signalling¹⁰² and CaMKII pathways, which activate transcription factors, such as CREB¹⁰³. The TRPC6 calcium channel in fibroblasts has been shown to be critical for myofibroblast differentiation via angiotensin-II-stimulated and $\text{TGF}\beta$ -stimulated calcineurin pathways¹⁰⁴.

Angiotensin II signalling in cardiac myocytes. Angiotensin II has multiple effects in the myocardium, and specific signalling pathways have been discovered in cardiac myocytes. Angiotensin II, via specific angiotensin II membrane receptors, mediates cardiac

contractility, coupling between myocytes and electrical propagation, and long-term regulation of growth and remodelling¹⁰⁵. Angiotensin II is likely to be produced and released by cardiac myocytes, in particular under pathological conditions¹⁰⁶. The angiotensin II type 1 receptors (AT1Rs) start the signalling cascades associated with angiotensin II in the heart and are associated with short-term blood-pressure control and long-term cardiomyocyte growth. AT1R was one of the first molecules implicated in cardiac mechanosignalling^{107,108}. In cardiac myocytes, angiotensin II directly leads to cell growth, but this effect is mostly seen in neonatal cells rather than in adult myocytes¹⁰⁹. In response to stretch, AT1R signalling increases MAPK phosphorylation^{110,111}, JAK–STAT signalling^{112,113} and expression of several hypertrophic markers^{107,114}. Studies have also shown that matrix metalloproteinase (MMP) expression by cardiac myocytes is angiotensin-II-dependent¹¹⁵. AT1R has also proved to be directly stretch-sensitive, independent of the binding of ligands such as angiotensin II¹¹⁶. AT1R signalling via G-protein-coupled pathways is biased to β -arrestin-mediated pathways during mechanoactivation, suggesting that myocyte stretch can mediate AT1R signalling with or without ligand binding^{14,117–119}. Interestingly, β -arrestin activity in coordination with AT1R was shown to mediate the Frank–Starling mechanism of cardiac contractility¹²⁰. Although cardiomyocytes do release angiotensin II in response to stretch^{107,108,110,121,122}, both the mechanism underlying angiotensin II release and its specific effect on cardiomyocyte remodelling remain unclear¹²³. Nonetheless, the importance of angiotensin II and AT1R in cardiomyocyte mechanosensing is firmly established, especially given the prevalence and efficacy of AT1R blockers for treating cardiovascular disease¹²⁴.

Angiotensin II signalling in fibroblasts. Angiotensin II has well-documented profibrotic effects in cardiac fibroblasts¹²⁵. Angiotensin II can regulate cardiac ECM via an increase in collagen expression through activation of AT1Rs^{126,127}. This type of fibrotic response is likely to be mediated through TGF β synthesis and related pathways^{128,129}. Evidence exists for both direct downstream activation of TGF β by angiotensin II and via paracrine mechanisms^{130,131}. Angiotensin II also exerts its profibrotic effects by decreasing MMP activity¹³² and increasing tissue inhibitor of metalloproteinases (TIMP) activity¹³³. Pathways that have been associated with angiotensin II signalling in the heart include syndecan¹⁷, IL-6 and ERK–p38 MAPK–JNK¹³⁴. Stretch and angiotensin II can mediate cytokine release from fibroblasts¹³⁵ that might further regulate fibrosis. In addition to the profibrotic effects of angiotensin II on cardiac fibroblasts, effects have also been documented on myofibroblast differentiation¹³⁶ and possibly proliferation of adult fibroblasts, probably via autocrine or paracrine mechanisms¹³⁷; these pathways involved growth factors such as vascular endothelial growth factor¹³⁸ and endothelin 1 (REF. 139).

TGF β signalling in cardiac myocytes. TGF β is well described as a contributor to fibrosis in many different tissues, including the myocardium¹⁰⁹, although TGF β signalling in cardiac myocytes is not as well defined as

in fibroblasts. The expression of TGF β in cardiomyocytes increases in both dilated and hypertrophic cardiomyopathies^{140,141}. In cultured cardiomyocytes, TGF β mRNA and protein are upregulated by angiotensin II¹⁴², and TGF β itself promotes expression of the fetal gene programme associated with cell hypertrophy^{143,144}. TGF β expression in cardiomyocytes is regulated by several molecular signals including PKC, p38 MAPK and the AP-1 complex¹⁴². TGF β signalling in myocytes might also be involved in maladaptive hypertrophy and cardiac dysfunction¹⁴⁵. Stretch might directly regulate TGF β –SMAD signalling in neonatal cardiomyocytes, modulating gene expression and inhibiting cardiomyocyte proliferation during development¹⁴⁶.

TGF β signalling in fibroblasts. In cardiac fibroblasts, TGF β is centrally involved in many aspects of fibrosis, including myofibroblast differentiation, inflammation, gene expression and ECM synthesis^{147–149}. TGF β receptors signal via SMAD proteins, which translocate to the nucleus and regulate gene transcription¹⁵⁰. SMADs interact with a large number of DNA-binding transcription factors and therefore trigger a diverse set of gene transcription responses¹⁵¹. TGF β also initiates transcription through noncanonical pathways including p38 MAPK, ERK, JNK, TAK1 and RhoA GTPase¹⁴⁷.

In addition to the many molecular signals that activate fibroblasts during injury response¹⁵², mechanical stress stimulates TGF β signalling in cardiac fibroblasts via regulation of ECM organization and TGF β bioavailability. Stretched fibroblasts increase expression of TGF β mRNA and protein¹⁵³. TGF β is secreted in latent form and then activated through contraction-mediated conformational changes in the integrin-latent TGF β –ECM¹⁵⁴ complex¹⁵⁵ and by numerous other mechanisms including MMP2 and/or MMP9 proteolytic cleavage¹⁵⁶. This system can involve complex feedbacks, because mechanical stretch of cardiac fibroblasts can modulate gene expression of *MMP2* and *TIMP2* (REF. 157) as well as MMP activity¹⁵⁸, probably through the PKC and tyrosine kinase pathways¹⁵⁷. Furthermore, mechanical loading of some ECM components, such as collagen, causes conformational changes that can shield them from MMP-mediated proteolysis^{159,160}. Crosslinking enzymes, such as lysyl oxidase-like 2 (LOXL2), are upregulated in the heart in response to mechanical stress and are associated with cardiac fibrosis and increased stiffness¹⁶¹. In addition to increasing collagen organization and therefore TGF β bioavailability, LOXL2 was found to stimulate cardiac fibroblasts to produce TGF β , mediating TGF β signalling. Inhibition of LOXL2 reduced cardiac fibrosis in response to left ventricular pressure overload and improved overall cardiac function¹⁶¹.

Cytoskeletal complexes

The cytoskeleton has a complex structural arrangement in most cell types, and specific components have been associated with transduction of mechanical signals in cardiac myocytes and fibroblasts. Most cytoskeletal mechano-transduction processes in myocytes are associated with the sarcomere and Z-disc, whereas in fibroblasts, the actin cytoskeleton is central to these pathways (FIG. 1).

MLP, titin and associated complexes in cardiac myocytes. Myofilament perturbations can affect mechanotransduction by altering either sarcomere contraction or calcium buffering^{162,163}. The Z-disc of the sarcomere is directly connected to the cytoskeleton, but in addition to mediating force transmission¹⁶⁴, Z-disc-associated proteins are now well recognized to have important functions in mechanosensing and mechanotransduction.

Titin is a giant protein that connects the Z-disc to the M-line and is responsible for the passive stiffness of cardiac muscle¹⁶⁵. Titin has been proposed to be an important mechanosensor and interacts with many proteins that have been implicated in mechanosensitive signalling pathways¹⁶⁶. These cytoskeletal proteins that can bind to titin include muscle LIM protein (MLP), telethonin (also known as titin cap protein; TCAP), four-and-a-half LIM domains protein 1 (FHL1) and muscle ankyrin-repeat protein (MARPs) family members¹⁶⁷.

MLP has been widely investigated as a prime mechanosensing element in the Z-disc, with direct binding to α -actinin^{168,169}. In MLP-deficient mice, a lack of upregulation of fetal gene markers, such as *Nppa* (encoding atrial natriuretic peptide) and *Nppb* (encoding B-type natriuretic peptide), in response to mechanical stress suggests that MLP has a specific role in mechanotransduction and cardiomyocyte hypertrophy¹⁷⁰. Mice deficient in MLP eventually develop heart failure and die prematurely¹⁶⁸, possibly owing to abnormal mechanotransduction at the Z-disc. The loss of MLP and its interactions with TCAP have also been suggested to alter the elastic properties of titin, leading to the inability of cardiac muscle cells to sense mechanical stress properly¹⁷⁰. As shown in smooth muscle cells, MLP mediates gene expression via binding to GATA and SRF transcription factors¹⁷¹ and possibly modulates gene expression through similar pathways in cardiac myocytes. Additionally, MLP has also been implicated in anchoring calcineurin at the Z-disc¹⁶⁹, which might be part of the calcineurin–NFAT hypertrophic pathway. PKC-interacting cousin of thioredoxin (PICOT; also known as glutaredoxin 3) is a protein found at the Z-disc and has also been implicated in hypertrophic signalling via the calcineurin–NFAT pathway⁷⁵. PICOT interacts with MLP, which in turn mediates the binding of calcineurin to MLP, leading to its displacement from the Z-disc.

The Z-disc giant protein titin has been shown to be an important contributor to passive stiffness of the myocardium¹⁷². FHL1 binds to titin at its elastic region¹⁷³ and is upregulated in animal models of hypertrophy^{174,175}, implicating FHL1 in the biomechanical stress responses in cardiac hypertrophy. This stress response is likely to be related to the signalosome that encompasses components of the MAPK signalling pathway RAF1–MEK2–ERK2 at the stretch sensor domain of titin¹⁷³. Further studies have suggested a direct link between FHL1-mediated mechanotransduction and G_q pathways, with FHL1 deficiency preventing ERK2 phosphorylation caused by constitutively active G_q overexpression in a mouse model¹⁷³. FHL1 might also act as a scaffold for MAPK-mediated hypertrophic signalling¹⁷⁶.

Similar to FHL1, all three MARP members, including CARP, ankyrin repeat domain-containing protein 2

(ANKRD2) and diabetes-related ankyrin repeat protein (DARP; also known as ANKRD23), bind to titin. However, MARP members bind to the N2A region instead of the N2B region. In response to stretch of neonatal rat cardiac myocytes, CARP and DARP translocate to the nucleus¹⁷⁷. Additionally, eccentric contractions of skeletal muscle cause upregulation of CARP and ANKRD2 gene expression¹⁷⁸. MARP members have been linked to protein kinase A and PKC¹⁷⁹.

Actin and associated complexes in fibroblasts. As in other cell types, the cytoskeleton in cardiac fibroblasts is a structural network responsible for maintaining cell shape and stability and is the mechanical structure that can transmit mechanosignals both outside-in and inside-out. The ECM is a regulator of cytoskeletal stress¹⁸⁰, and fibroblasts have been shown to use mechanotransduction signalling pathways from surface molecules (such as integrins) to control and maintain their actin cytoskeleton. RhoA, a member of the family of small Rho GTPases¹⁸¹, activates Rho kinase (ROCK), which phosphorylates downstream targets associated with actin stress fibre regulation, including LIM kinases and myosin light chain¹⁷. RhoA-dependent signalling affects nuclear translocation of transcription factors in part through these changes in the actin cytoskeleton¹⁷.

An important example of cytoskeleton-mediated control of transcription is via MRTF-A and MRTF-B. When fibroblasts undergo changes in their external mechanical environment, G-actin assembles into F-actin polymers, liberating MRTF-A and allowing it to enter the nucleus¹⁸². Deficiency of MRTF-A reduces fibrosis after myocardial infarction¹⁸³, implicating MRTF-A as an important component of the fibrosis pathway in response to mechanical signals. Another pathway associated with cytoskeletal dynamics and sensing of ECM mechanical signals is the Hippo signalling pathway^{184,185}. Inhibition of Rho and disruption of F-actin results in pathway inactivation¹⁸⁶ and can lead to alterations in translocation of the transcription co-activators yes-associated protein (YAP) and transcriptional co-activator with PDZ-binding motif (TAZ) between the cytoplasm and the nucleus¹⁸⁷. These transcriptional co-activators, possibly interacting with SMAD3 from the TGF β signalling pathway, might regulate fibroblast myofibroblast differentiation¹⁸⁸.

Nuclear mechanosensing

Cardiac myocytes. Evidence suggests that myocyte stretch can have direct effects on the nucleus via force transmission through the sarcolemma and cytoskeleton and that mechanosensing might occur inside the nucleus of myocytes via modulation of protein activity in the nucleus¹⁸⁹. The nucleus has been shown to be mechanically connected to the cytoskeleton inside the cytoplasm by linker of nucleoskeleton and cytoskeleton (LINC) complexes¹⁹⁰, probably mediated by nuclear lamins^{191,192}. Lamins are specialized structural proteins that provide structural stability to the nucleus. Other integral nuclear membrane proteins include emerin, inner nuclear membrane protein Man1, LEM domain-containing protein 2, spindle-associated membrane protein 1, barrier-to-autointegration factor and certain transcription

factors^{193,194}. The LINC complex has been shown to be a direct nuclear mechanotransducer¹⁹⁵ and can regulate transcription factors and chromatin structure in the nucleus and, therefore, gene transcription¹⁸⁹. Mutations in the proteins of the nuclear envelope can disrupt this type of force transmission and directly influence mechanotransduction and transcriptional regulation¹⁹⁶. Without the intact cytoskeleton, in particular actin filament connections to the nuclear membrane, deformation of the nucleus can occur with defective mechanotransduction¹⁹⁷. Force distributions within nuclear lamina are altered with varying nuclear properties¹⁹². Laminopathies, caused by mutations in the *LMNA* gene, are associated with muscular dystrophies, lipodystrophies and premature ageing syndromes¹⁹⁸, with an inflammatory component linked to some of these diseases¹⁹⁹. Evidence also exists that stresses transmitted to the nucleus can affect chromatin structure, possibly regulating transcription factors directly²⁰⁰. In mice overexpressing high mobility group nucleosome-binding domain-containing protein 5 (HMGN5)²⁰¹, the mutation of the protein alters the interaction between H1 histone and chromatin, reducing chromatin compaction²⁰², which suggests a link between forces transmitted through the nuclear membrane and chromatin structure.

Fibroblasts. Direct cytoskeletal force transmission to the nucleus might also mediate mechanically regulated gene expression in fibroblasts¹⁹⁰. This mechanism is likely to be a ubiquitous and efficient way for cells to respond rapidly to external mechanical forces¹⁷. Studies in fibroblasts with defective lamins have shown alterations in proliferation, suggesting this nuclear structural protein has a role in fibroblast activation and probably differentiation into myofibroblasts²⁰³. The lamins and emerin can regulate actin function in mouse embryonic fibroblasts, regulating MRTF-A and SRF activity²⁰⁴ and cardiac myofibroblast differentiation¹⁸³. Mechanosensing in the nucleus is suggested by changes in nuclear shape, and these shape changes have been associated with alterations in gene expression. For example, fibroblast collagen synthesis has been reported to depend on the shape of the nucleus²⁰⁵. The LINC complex is involved in nuclear mechanosensing and gene transcriptional changes in response to the altered mechanical environment of the cell²⁰⁶. Nuclear shape is associated with fibroblast cell spreading and migration speed, and this mechanosensing is defective when the LINC complex is disrupted²⁰⁷.

As the heart develops and matures, the nuclei of cardiac fibroblasts and myocytes are exposed to varying degrees of mechanical forces. Therefore, in cells with a defective or fragile nuclear membrane and associated interconnections to the cytoskeleton, the nucleus can show decompacted chromatin and nuclear blebbing, as seen in cell death. These observations indicate the mechanosensitivity of nuclei and that its structural integrity is important for cardiac cell adaptation to physical loads¹⁷.

Cell–cell interactions

Intercalated discs in cardiac myocytes. The intercalated disc is the cell–cell junction that longitudinally connects neighbouring cardiac myocytes. The intercalated

disc has multiple functions related to maintenance of mechanical and electrical coupling between cardiomyocytes^{208,209}. In response to cyclic cardiac volume overload, the intercalated disc undergoes ultrastructural changes that might be associated with sarcomere restructuring, implicating the cell–cell junction as part of the mechanotransduction pathway associated with myocyte hypertrophic growth²¹⁰. The three types of cell junctions that make up an intercalated disc are fascia adherens, desmosomes and gap junctions. Fascia adherens are anchoring sites for cytoskeletal actin and connect to the closest sarcomere. Intermediate filaments bind to desmosomes²⁰⁹. Ions can pass through gap junctions, which allows action potentials to propagate along muscle fibres.

The fascia adherens junctional complex is composed of proteins such as cadherins, catenins and catenin-binding proteins²¹¹. N-Cadherin (also known as cadherin 2) can form attachment sites with neighbouring cardiac myocytes and transmit forces between cells²¹². N-Cadherin has also been shown to be upregulated in response to stretch²¹³. Hearts from N-cadherin-deficient mice have altered cell–cell mechanosensing that affects their sarcomere structure and causes dilated cardiomyopathy²¹⁴. Cardiac myocytes from these mice do not have identifiable fascia adherens junctions, and their sarcomeres are shorter in length. β 1 Integrin levels are increased in hearts from N-cadherin-knockout mice, which indicates a compensatory response in which other mechanotransductive proteins increase in expression owing to the deficit of N-cadherin²¹⁴. Catenins are also part of the fascia adherens junctional complex and regulate cadherin-based and binding proteins, such as muscle-specific mouse mXina, vinculin–metavinculin and α -actinin, which link the fascia adherens to the cytoskeleton and modulate catenin activity^{211,212}. α -Catenin recruits vinculin to the fascia adherens junction through force-dependent changes in α -catenin²¹⁵. α -Catenins have also been shown to modulate cytoskeletal mechanotransmission, which can regulate YAP-mediated cell proliferation during development²¹⁶. As with deficiency of N-cadherin, α -catenin deficiency alters the structure of the intercalated disc and leads to dilated cardiomyopathy. Vinculin localization is lost at the fascia adherens junction; however, vinculin also localizes to the costamere and remains there after α -catenin inactivation²¹⁷. Experimental evidence also exists for a role of the striated muscle-specific protein, nebulin-related-anchoring protein (N-RAP), in myocyte mechanotransduction between the fascia adherens junction and the sarcomere^{218,219}.

Desmosomes connect intermediate filament cytoskeletal networks between cells and contain cadherins, desmocollin 2 and desmoglein 2. Mutations in these proteins are associated with arrhythmogenic right ventricular cardiomyopathy (ARVC)²⁰⁹. Desmoplakin connects desmosomes to the intermediate desmin filaments²⁰⁹ in conjunction with desmosomal proteins junction plakoglobin (JUP) and plakophilin 2 (PKP2)²¹¹. A potential direct link between JUP and PKP2 in the cardiac muscle shear stress response has been shown²²⁰. Desmoplakin has been shown to be a critical component of the desmosome and cell–cell junctional integrity²²¹;

knocking out *Dsp* (encoding desmoplakin) causes sarcomeric defects and loss of desmosomal but not N-cadherin-based proteins and has been associated with ARVC²²². Studies have suggested a role for desmosomes in transducing mechanical forces into multiple cellular responses related to tissue mechanics. Mutations in the desmosomal cadherins, desmocollin 2 and desmoglein 2 are linked to human ARVC²²³.

Gap junctions are cell–cell connections that allow ions to pass between neighbouring cells, thereby electrically and metabolically connecting adjacent cells. Connexin 43 (also known as gap junction- α 1 protein) is a gap junctional protein that is upregulated in response to mechanical stretch²²⁴. Upregulation of connexin 43 is accompanied by an increased number and size of gap junctions as well as by an accelerated conduction velocity²²⁵. Gap junctions are sensitive to mechanical stress²⁰⁸ and remodel in several cardiac diseases. Crosstalk between adherens junctions, desmosomes and gap junction proteins, including α -catenin, tight junction protein ZO1, connexin 43 and PKP2, at the intercalated disc might account for the mechanisms of gap junction remodelling in cardiac disease²²⁶.

Fibroblast–myocyte interactions. Interactions between cardiac myocytes and fibroblasts can be via paracrine cell–cell signalling or via direct physical coupling between the different cell types, possibly mediated by the ECM. Fibroblasts can mediate myocardial electrophysiology via electrical coupling to myocytes and alterations in myocyte membrane potential and therefore electrical conduction^{18,227–229}. Many fibroblast–myocyte interactions have been implicated in cardiac arrhythmogenesis^{230–232}. Coupling between myocytes and fibroblasts can occur in vivo and represents electrotonic coupling between these different cell types^{233,234}. Ongstad and colleagues suggest several ways in which cardiac myocytes and fibroblasts can couple to each other, including fibroblasts acting as insulators between myocytes or with small numbers of gap junctional channels that could serve as short-range or long-range conduction of electrical excitation²³⁴. Modifying heterotypic cell–cell interactions and coupling might be useful in reducing arrhythmias after myocardial infarction²³⁵. Secreted factors such as angiotensin II, cardiotrophin 1, fibroblast growth factor, IL-6, insulin-like growth factor I, TGF β and tumour necrosis factor have been shown to mediate cell–cell communication via indirect autocrine or paracrine mechanisms^{236–238}. These factors regulate a host of physiological functions in the cells and tissue of the heart, most of which are described in the preceding sections involving signalling pathways related to development, electrical activity, contractile function and pathological tissue remodelling.

Systems-level cardiac mechanosignalling

As described in the previous section, a wide range of pathways have been implicated in mechanosensing. Appropriately, these studies have focused largely on gaining a more detailed understanding of particular mechanosensing mechanisms. However, as indicated in FIG. 1, how these mechanisms work in concert to

mediate cardiac mechanoresponses is less understood. Global measurement and modelling approaches are complementing more mechanistically focused studies to progress towards a systems-level understanding of cardiac mechanosignalling.

Mechanosensitive gene expression

Heart. Studies of gene expression downstream of individual mechanosensitive pathways have most often focused on the fetal gene programme or a small number of candidate genes in that particular pathway. By contrast, gene expression profiling using cDNA microarrays or RNA sequencing have allowed for a more comprehensive view of the transcriptome and discovery of mechanosensitive gene programmes. Although the most prevalent causes of heart failure, including myocardial infarction and hypertension, have highly complex biochemical and mechanical perturbations that evolve slowly over time, studies of direct perturbations to myocardial mechanics have helped to inform which aspects are more closely associated with mechanosensing. Animal models of pressure overload by TAC, which induces concentric hypertrophy and interstitial fibrosis, have consistently demonstrated increased expression of natriuretic peptide genes, ECM-related genes (notably connective tissue growth factor and periostin) and cytoskeleton-related genes^{239,240}. Knockout of *Nppa* further exacerbates the hypertrophic and fibrotic gene expression profiles caused by pressure overload²⁴⁰. Cardiac transcriptomes from rats subjected to pressure or volume overload identified consistent expression of *Nppa*, *Nppb*, *Mt1* (encoding metallothionein 1) and genes encoding proteins involved in mitochondrial metabolism or the cytoskeleton. Volume overload induced more distinct upregulation of genes encoding actin-binding proteins (such as tropomyosin 4 and thymosin- β 4) and some ECM proteins (such as osteopontin)²⁴¹. Volume overload and eccentric remodelling caused by mitral valve regurgitation is associated with increased expression of metalloproteinases and decreases in the expression of genes encoding non-collagen ECM proteins²⁴².

Several studies have characterized gene expression profiles from human failing hearts before and after mechanical unloading with an LVAD. Initial reports demonstrated that LVAD-induced reverse remodelling coincided with a decrease in the expression of genes associated with natriuretic peptides, ECM, sarcomeres, cytoskeleton and metabolism^{243,244}. Subsequent studies, including comparisons with non-failing heart samples, demonstrated that LVAD-induced reverse structural remodelling does not similarly induce widespread reversal of gene expression but instead induces a distinct state^{245–247}. In terms of functional responses related to gene expression, LVAD therapy has been shown, for example, to correlate with changes in calcium dynamics in cardiomyocytes²⁴⁸. Even in experiments and treatments involving direct mechanical intervention, the parallel effects on vascular remodelling, neurohormonal feedback and multiple cell types hinder the identification of genes whose expression is regulated directly by the mechanosensitivity of cardiac myocytes or fibroblasts.

Cardiac myocytes. In the first transcriptomic measurements of stretched cardiac myocytes, Weinberg and colleagues found strongly mechanosensitive expression of *Il1rl1*, which encodes suppression of tumorigenicity 2 (ST2; also known as IL-1 receptor-like 1)²⁴⁹. After confirming mechanoregulated expression by traditional methods, they demonstrated increased levels of soluble ST2 protein after myocardial infarction in the serum of mice and humans²⁴⁹. Subsequently, ST2 has been developed substantially as a clinical biomarker and is approved by the FDA to predict outcomes from myocardial infarction and heart failure^{250,251}. Frank and colleagues used microarrays to identify highly mechanoresponsive genes in rat stretched cultured cardiomyocytes, identifying *Gdf15* and *Hmox1* in addition to strong induction of the fetal gene programme and other previously reported stretch-responsive genes²⁵². The investigators further demonstrated that stretch-responsive transcription of several genes could be blocked by angiotensin II receptor antagonists or mimicked by angiotensin II²⁵², thereby linking transcription to a known mechanotransduction pathway. McCain and colleagues used a novel stretching device with micropatterned membranes to control cardiac myocyte alignment, characterizing how the direction and duration of stretch affects the transcriptome²⁵³. Clustering of genes by expression pattern across conditions elucidated coordinated expression of genes associated with ECM and cytoskeletal remodelling as well as those previously associated with pathological hypertrophy or heart failure in vivo²⁵³. This study nicely illustrated how clustering of transcriptomic data from multiple treatment conditions and time points aids in the identification of coordinated gene expression programmes. A subsequent study in rat isolated ventricular myocytes subjected to cyclic stretch investigated gene expression at even more time points between 1 h and 48 h (REF²⁵⁴). Detailed data on signalling and expression time courses remain limited; however, as more studies on the sequences of signalling events become available, the data will provide new insight into which mechanisms are acting in parallel, which are dependent on upstream processes and which components of the network are sensors, transducers or effectors.

Fibroblasts. As an early application of cDNA microarrays, in 2001 Kessler and colleagues profiled the response of fibroblasts cultured in 3D collagen gels that were either mechanically restrained or unrestrained from cell-induced contraction²⁵⁵. Mechanical stress induced expression of many genes encoding proteins known to be related to focal adhesions, cytoskeletal remodelling and ECM, including those encoding collagen type I, MMP1 and connective tissue growth factor²⁵⁵. Driesen and colleagues demonstrated that spontaneous differentiation of cardiac fibroblasts on a rigid substrate could be prevented or even reversed by inhibition of TGF β receptor type 1 (TGF β R1)²⁵⁶. Transcriptome profiling showed that compared with stiffness-induced myofibroblasts, TGF β R1-inhibited cells had lower expression of genes encoding proteins associated with fibrosis, adhesion and TGF β signalling. By contrast, TGF β -treated myofibroblasts had reduced expression of genes

encoding proteins related to the cell cycle²⁵⁶. Alam and colleagues used RNA sequencing to identify how fibroblast mechanosensitive gene expression and microRNAs are regulated by the LINC complex²⁰⁶. Disruption of the LINC complex by expressing a dominant-negative SUN domain-containing protein 1 (SUN1) caused increased expression of genes encoding proteins associated with ion transport, adhesion, motility and ECM organization on stiff but not soft substrates²⁰⁶.

Studies of gene expression from cultured papillary muscles and engineered heart tissues have helped to bridge cellular and in vivo studies because these tissues are well suited for precise mechanical perturbations and contain multiple cardiac cell types. To elucidate transcriptomic responses to particular mechanical signals, Haggart and colleagues measured transcriptomic responses of contracting papillary muscles under combinations of physiological versus reduced myocyte shortening (as occurs with pressure overload) and mean stretch (as occurs with an LVAD)²⁵⁷. Reduced muscle shortening strongly regulated genes encoding proteins associated with the ECM and cardiomyocyte hypertrophy, partially overlapping with the gene expression seen with pressure overload in vivo. Hirt and colleagues found that engineered heart tissues with increased afterload developed hypertrophy and fibrosis consistent with that seen in pressure overload in vivo²⁵⁸. Transcriptome measurements demonstrated that increased afterload was associated with strong induction of genes associated with the fetal gene programme, ECM and glycolytic metabolism in a manner consistent with that seen with biochemically induced hypertrophy and in partial overlap with that seen with pressure overload in vivo²⁵⁸. Of note, in both papillary muscles²⁵⁷ and engineered heart tissues²⁵⁸, although only 10–15% of genes overlapped with in vivo reports, the most highly responsive overlapping genes were associated with the fetal gene programme and the ECM.

TABLE 1 compares mechanoresponsive gene sets across animal models, human studies and cardiac cells. Individual genes that were noteworthy in each study are also listed. Nearly all studies showed significant expression of genes encoding protein related to the ECM, with the gene encoding connective tissue growth factor often being among the most mechanoresponsive. Cardiac tissue or cardiac myocyte studies typically show increased expression of natriuretic peptides, consistent with their use as clinical biomarkers. Genes encoding focal adhesion proteins are also consistently responsive to stretch in cardiac myocytes and fibroblasts, whereas fibroblasts show additional expression of proliferation-related genes. Gene expression has been profiled with varying measurement technologies and analyses, which contributes to variation between studies in the consistency of reported gene sets. Cardiac myocyte cultures also contain non-myocytes, which might contribute to measured responses.

Regulation by microRNAs. Gene expression is also substantially regulated at the post-transcriptional level by microRNAs, and some studies have begun to focus specifically on their role in response to mechanical

stretch. MicroRNAs are short (~22-nucleotide), non-coding RNAs that bind complementary mRNAs to regulate mRNA degradation or protein translation. A large number of microRNAs are differentially expressed and control cardiac remodelling in vivo, as reviewed previously²⁵⁹. Microarrays were used to discover differentially expressed microRNAs in mice subjected to TAC-induced pressure overload or calcineurin overexpression, leading to identification of miR-195 as a regulator of cardiac hypertrophy²⁶⁰. To find microRNAs specifically responsive to cardiac myocyte stretch, Frey and colleagues used microarrays to identify eight stretch-responsive microRNAs²⁶¹. Follow-up experiments identified miR-20a as being responsive to both stretch and simulated ischaemia–reperfusion, that overexpression of miR-20a was sufficient to protect cardiomyocytes from apoptosis and that expression of miR-20a was inversely correlated with pro-apoptotic miR-20a targets Egl nine homologue 3 and E2F family transcription factors²⁶¹. Motivated by studies showing miR-208a regulation of cardiac hypertrophy^{262,263}, studies of cultured cardiac myocytes and myoblasts showed stretch-responsive TGFβ signalling that controlled miR-208a expression and either β-myosin heavy chain (also known as myosin 7) or collagen in the respective cell types^{264,265}. Dynamics of mRNA and microRNA expression of stretched cardiac myocytes has also been examined by Rysa and colleagues, who predicted involvement of nuclear factor-like 2 and interferon regulatory transcription factors and let-7 family microRNAs²⁵⁴.

Long (>200-nucleotide) intergenic non-coding RNAs²⁶⁶ have also been shown to regulate cardiac remodelling²⁶⁷ and more strongly correlate with reverse remodelling of human hearts after LVAD support²⁴⁷. Long non-coding RNAs have been shown to regulate the stretch response of vascular smooth muscle cells²⁶⁸, but corresponding studies in stretched cardiac myocytes have not yet been reported.

Challenges of complexity

Despite a wealth of characterized mechanosensitive proteins, pathways and global transcriptional profiles, considerable knowledge gaps must be overcome to obtain a molecular systems-level understanding of how mechanical signals regulate gene expression and cardiac remodelling (BOX 1). Addressing these challenges of mechanosignalling complexity requires quantitative comparisons between combinations of mechanobiochemical perturbations, measurements and experimental contexts. However, testing of all combinations is clearly not feasible and would overwhelm rather than provide new conceptual insights. When closely integrated with experimental studies, mathematical systems models can provide rigorous frameworks for data integration, hypothesis generation, prioritization of experiments and understanding of complex systems²⁶⁹. In the following section, we provide an overview of how systems models have been applied to address complexity challenges for cardiac signalling networks, focusing on the latest work extending into mechanosignalling of cardiac myocytes and fibroblasts.

Table 1 | **Mechanoresponsive gene programmes in the heart and specific cardiac cells**

Experimental system	Gene sets	Example genes	Refs
Cardiac pressure overload	NP, ECM and metabolism	CTGF and FHL1	239
	NP and ECM	POSTN and SPP1	240
	NP and ECM	LOXL1, MT1 and PDK1	241
Cardiac volume overload	NP, ECM and cytoskeleton	MT1 and TAGLN	241
	Decreased ECM	MMP1, MMP9 and decreased CTGF	242
Patients after LVAD implantation	NP, ECM and metabolism	HSPB6 and MT1	243
	Sarcomere, cytoskeleton, ECM and FA	ITGB1 and VCL	244
	Limited	PDK1 and SOCS3	245
	Limited	CRYM, TNNT3 and multiple microRNAs	246
	Limited	Multiple lncRNAs	247
Engineered heart tissue	NP, ECM, sarcomere and metabolism	ACTA1 and COL1A1	258
Papillary muscle	NP, ECM and sarcomere	CTGF and HSP90AB1	257
Cardiac myocytes	Not reported	IL1RL1	249
	NP, sarcomere and cell adhesion	FHL1, GDF15 and HMOX1	252
	ECM, FA and sarcomere	TRPC1 and ITGA6	253
	ECM, cytoskeleton and metabolism	–	322
	NP and proliferation	SERPINB2 and let-7 family	254
Fibroblasts	ECM, FA, cytoskeleton and proliferation	CTGF and SERPINB2	255
	FA, proliferation and TGFβ signalling	–	256
	ECM, FA, cytoskeleton and proliferation	–	206

Gene expression measured by cDNA microarrays or RNA sequencing. ECM, extracellular matrix; FA, focal adhesions; lncRNA, long non-coding RNA; LVAD, left ventricular assist device; NP, natriuretic peptides; TGFβ, transforming growth factor-β.

Box 1 | Challenges in understanding complex mechanoregulation of cardiac cells**What are the specific mechanical signals that are transduced by particular mechanosensitive proteins?**

Some studies have shown distinct remodelling or transcriptional responses of cardiac myocytes to the timing²¹⁹ or direction of stretch^{253,320} and to externally applied versus cell-generated stresses or strains²⁵⁷. These factors cannot be independently controlled in most experimental systems; therefore, studies on particular mechanosensitive proteins have largely used a single mechanical stimulus.

Are downstream mechanosensitive pathways and gene expression sensitive to signals propagating from specific mechanosensors?

The majority of studies examining mechano-responsive changes in global gene expression have not directly perturbed putative mechanosensors²⁰⁶. Such experiments are complicated because putative mechanosensor proteins have pleiotropic signalling or structural roles that cannot easily be dissociated from mechanosensing mechanisms.

How do downstream mechanosensitive pathways integrate combined inputs from multiple mechanosensors and biochemical stimuli?

Cardiac stresses are multifactorial. Many mechanosensors are likely to respond to a given mechanical stimulus, but combinatorial perturbations to mechanosensors have rarely been performed. Feedback between mechanosensory pathways (such as mutually reinforcing focal adhesions and stress fibres) and with autocrine or paracrine factors (such as angiotensin II, endothelin 1 or transforming growth factor- β) complicates interpretation.

To what extent does mechanosignalling generalize across experimental contexts?

As in other areas of science³²¹, integration of data between laboratories and experimental systems is challenged by the unknown extent to which mechanosignalling mechanisms and responses depend on experimental variables, such as genetic background, surgical technique or cell culture conditions.

Systems models of mechanosignalling

Computational models of signalling and gene regulation in cardiac myocytes. Mathematical models have long provided crucial insights into how complex molecular systems regulate cardiac myocyte physiology²⁷⁰. Classic mathematical models provided insights into the molecular mechanisms of actin–myosin cross-bridge cycling²⁷¹ and feedback between ionic currents that drive cardiac pacemaking²⁷². Over several decades, mathematical models have provided a wide range of systems-level insights into the molecular regulation of excitation–contraction coupling²⁷³, arrhythmia²⁷⁴, metabolism^{275,276} and signalling pathways^{277,278} in normal and pathological²⁷⁹ conditions.

In contrast to the larger number of models of short-term (milliseconds to minutes) cardiac myocyte physiology, fewer models have examined the molecular networks that control longer-term gene expression and remodelling (hours to days)^{269,280}. Tavi and colleagues used a model of calcium–calmodulin–calcineurin kinetics to show that calcineurin might act as a frequency-sensitive integrator of cytosolic calcium signals^{281,282}, which correlates with experimental measurements of NFAT activity, mRNA expression²⁸¹ and myocyte hypertrophy²⁸³. Other models coupled these systems to more detailed systems of upstream subcellular calcium dynamics²⁸⁴ or mechanisms of NFAT nuclear transport²⁸⁵. Cooling and colleagues developed models of receptor-stimulated inositol 1,4,5-trisphosphate (IP₃) transients that regulate calcium–calcineurin, showing that the distinct kinetics of transients could be explained by differences in the kinetics of endothelin and angiotensin II receptors²⁸⁶. Combining simulations

and perturbation experiments, Shin and colleagues characterized crosstalk between calcineurin, PI3K and ERK pathways that produce a biphasic switching mechanism by which calcipressin 1 regulates calcineurin–NFAT activity²⁸⁷. Ryall and colleagues developed a systems model of the overall cardiac myocyte hypertrophy signalling network, predicting RAS as an integrating network hub for many biochemical stimuli²⁸⁸. Their model also included a simplified integrin pathway that was sufficient to accurately predict stretch-responsive activation of three transcription factors and six hypertrophic genes²⁸⁸. This and other systems models were developed using data from cultured cardiac myocytes, whose relevance to *in vivo* hypertrophy has been debated^{289,290}. To test the generalizability of this network model²⁸⁸, overexpression of 34 genes was simulated and compared with *in vivo* data from cardiac-specific transgenic mice²⁹¹. The model accurately predicted 72% of 168 *in vivo* measurements, as well as the hypertrophic phenotypes of four double-transgenic mice, with mispredictions guiding subsequent model revision on the basis of *in vivo* data²⁹¹.

Models linking mechanosignalling to cytoskeletal remodelling and gene expression. A number of mathematical models have provided insights into the biophysical mechanisms that guide cytoskeletal remodelling, as reviewed previously²⁹². Biophysical models have demonstrated how long stress fibres and heterogeneous distributions of focal adhesions in fibroblasts arise from positive feedback between adhesion and stress fibre contractility²⁹³, how further incorporation of cytoskeletal mechanics can predict regional orientation and density of stress fibres²⁹⁴ and how cells re-orient in response to the direction of stretch²⁹⁵. Coupled biochemical–mechanical models have also been used to understand cardiac myocyte myofibre formation, accounting for differences from fibroblast stress fibres. Grosberg and colleagues accurately predicted myofibrillar patterning of geometrically constrained cardiac myocytes²⁹⁶, which was driven by both fibre length–force dependence²⁹³ and mutual alignment of myofibres due to parallel coupling²⁹⁷. Simulations by Yuan and colleagues predicted that cell–cell adhesion forces reduce local focal adhesion formation²⁹⁸, helping cardiac myocytes to form a syncytium with aligned myofibrils, as found experimentally²⁹⁹.

Systems-level models are further needed to provide insight into how mechanical cues are transduced and integrated into downstream signalling pathways and gene expression^{269,292,300}. For example, discriminating the regulation by specific mechanical stimuli of particular signalling pathways is confounded by crosstalk and overlap between these different stimuli and downstream pathways. Several studies have illustrated the promise of such models to address challenges in mechanosignalling network integration.

Although studies of mechanosignalling have focused primarily on linear pathways from sensor to response, mechano-responsiveness can also emerge from the interplay of more subtle relationships. Dingal and colleagues used a series of simplified models to illustrate

how tension-inhibited protein degradation³⁰¹ (such as is seen with many cardiac sarcomeric, cytoskeletal and matrix proteins^{152,302}) coupled with positive regulation from protein to transcription can lead to tension-enhanced gene expression. Proteins such as lamin A with long protein half-lives but short mRNA half-lives were predicted to show steady, tension-enhanced mRNA and protein abundance, whereas proteins such as collagen with short protein half-lives were predicted to generate transient increases with stretch as seen experimentally. Coupling of mRNA–protein modules illustrated how tension-inhibited degradation of one protein might indirectly drive mechanoresponsive expression of other genes in a cytoskeletal network (for example, the effects of myosin 2 on lamin A) or coordinated gene expression in fibroblasts and cardiac myocytes³⁰¹.

Myofibroblast differentiation is highly responsive to mechanical signals as well as multiple growth factors, but the mechanisms underlying crosstalk between these signals are not well characterized. Schroer and colleagues developed a dynamic computational model of how integrin, TGF β and fibroblast growth factor signals converge on p38 and ERK to coordinately regulate α -smooth muscle actin (α SMA) expression, a key marker of myofibroblasts³⁰³. Rather than using a single model, uncertainty regarding mechanisms involving SRC, ERK and p38 was addressed by comparing eight candidate models, each representing alternative hypotheses of the signalling network. Candidate networks incorporating SRC-dependent α SMA expression and SRC feedback provided the most parsimonious explanations for their experimentally observed responses to matrix stiffness, growth factors and genetic perturbations³⁰³.

Mechanoresponsiveness of the transcriptional effectors YAP–TAZ has been shown to rely on cytoskeletal tension, non-muscle myosin and RhoA activity downstream of integrins and cell adhesion³⁰⁴. Sun and colleagues developed a systems model integrating these mechanisms and crosstalk with cell–cell adhesion-sensitive Hippo pathway members, such as serine/threonine-protein kinase LATS³⁰⁵. A strength of this model is that the equations were largely based on biophysical mechanisms of cytoskeletal proteins and their biochemical regulation by signalling, effectively linking cytoskeletal regulation to signalling pathways. The model recapitulated a range of previously reported effects of perturbations on YAP–TAZ nuclear translocation³⁰⁴, including inhibitors for myosin, RhoA, ROCK, F-actin and altered matrix stiffness³⁰⁵. The model was then used to make new predictions regarding increased mechanosensitivity of YAP–TAZ compared with SRF as well as synergistic regulation of YAP–TAZ by LATS³⁰⁶ and RhoA pathways³⁰⁵.

Large-scale systems models can integrate heterogeneous data from many sources to identify network control principles. Zeigler and colleagues developed a systems model of the cardiac fibroblast signalling network, which integrated 11 biochemical or mechanical cues to regulate myofibroblast genes and ECM components in agreement with a wealth of independent literature³⁰⁷. Computational screening of network perturbations in multiple cell contexts predicted mechanoresponsive

α SMA expression to require an autocrine loop with AP-1-dependent TGF β expression and TGF β R1–SMAD3 signalling. Further simulations and validation experiments of fibroblasts in mechanically restrained collagen gels confirmed that TGF β R1 inhibition prevented α SMA expression³⁰⁷. These predictions were consistent with subsequent *in vivo* experiments by Khalil and colleagues showing that fibroblast-specific deletion of *Tgfb1* and *Tgfb2* or *Smad2* and *Smad3* suppressed cardiac fibrosis in response to pressure overload³⁰⁸.

Despite the wide range of mechanosensitive pathways that have been identified, the systems models described above examined crosstalk between biochemical signals and only a single mechanosensor. To assess how cardiomyocytes integrate mechanical signals from multiple mechanosensitive proteins, Tan and colleagues reconstructed a cardiomyocyte mechanosignalling network model linking nine mechanoresponsive proteins (five shown to be directly responsive to stretch in reconstituted assays) to cardiomyocyte size, protein synthesis and eight mechanosensitive genes³⁰⁹ (FIG. 2). Comparison of model predictions to independent published experiments yielded a validation rate of 78% (134 out of 172). Although the 11 transcription factors showed selective sensitivity to particular mechanosensors, functional cooperativity between transcription factors was predicted to make downstream genes more broadly sensitive. Computational perturbation screens predicted combinatorial ‘mechanotherapies’ that might suppress hypertrophic gene expression, including combined stimulation of cGMP and inhibition of AT1R as might occur with the drug Entresto (Novartis; previous known as LCZ696, combining valsartan and sacubitril). The direct effects of Entresto on cardiomyocyte mechanosignalling have not yet been tested experimentally; however, in rats subjected to aortic constriction, Entresto suppressed cardiac expression of *Myh7* and *Nppa* and cardiomyocyte hypertrophy and increased expression of *Myh6* (REF.³¹⁰) — all consistent with the previous model’s predictions³⁰⁹. Entresto has also been shown to attenuate cardiac hypertrophy after myocardial infarction³¹¹, in chronic kidney disease³¹² and in angiotensin-II-stimulated cardiomyocytes³¹¹.

Multiscale models of mechanoregulated ventricular growth and remodelling. Ultimately, mathematical models will need to link predicted mechanotransduction mechanisms, signalling networks and gene expression to cardiac hypertrophy and myocardial tissue remodelling in response to haemodynamic changes and other alterations that affect myocardial mechanics. To date, progress has been made in organ-scale modelling of biomechanically stimulated growth and remodelling using empirical growth and remodelling laws³¹³. Witzenburg and Holmes examined the capacity of several proposed hypertrophic growth laws to predict remodelling in response to pressure or volume overload³¹⁴. Kerckhoffs and colleagues assumed that cardiomyocytes grow by adding sarcomeres in series when maximum fibre lengthening (that is, normally during filling) exceeds a homeostatic threshold and by adding sarcomeres in parallel when maximum cross-fibre strain (that is, typically during systole) exceeds a homeostatic threshold³¹⁵.

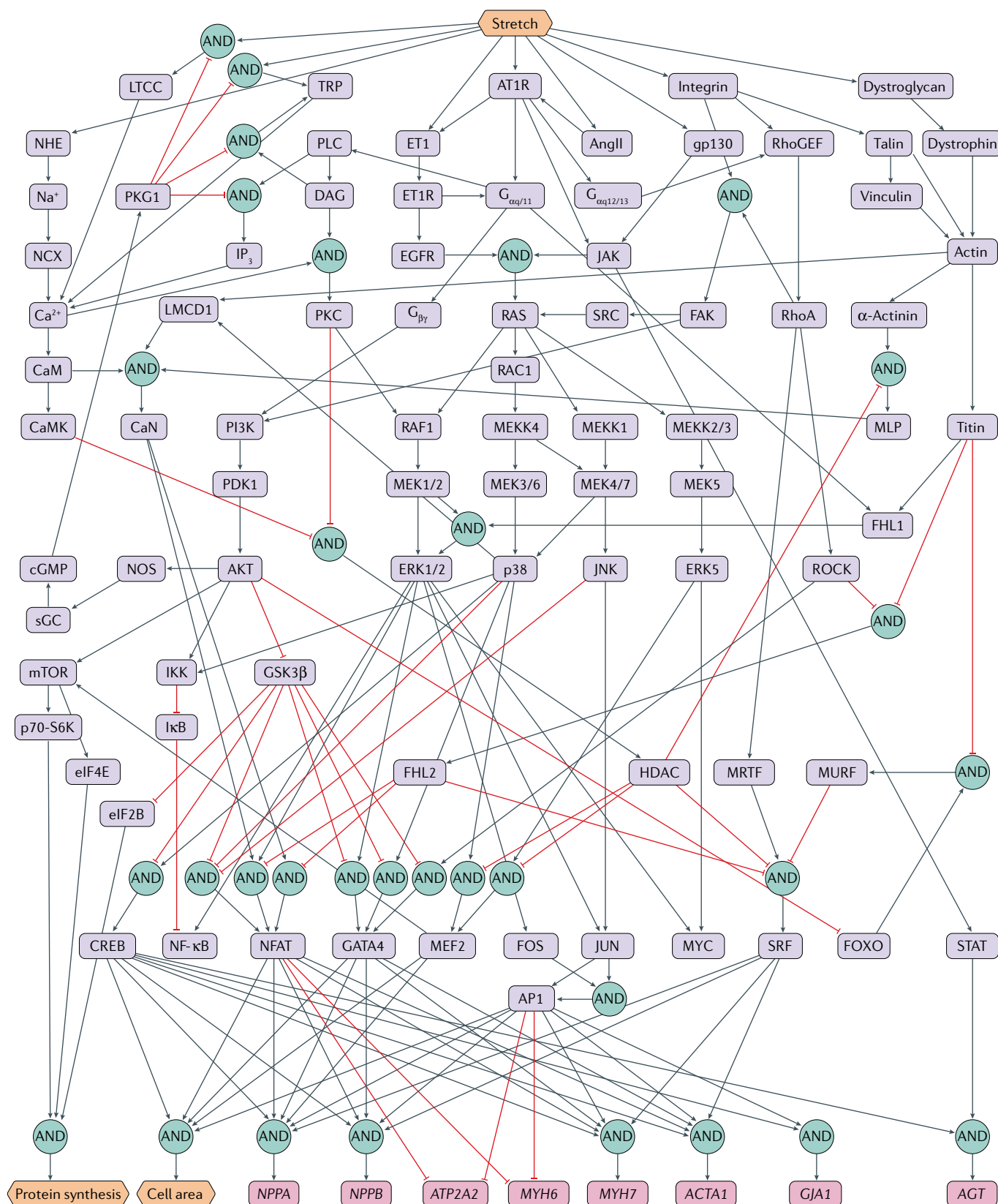


Fig. 2 | **Systems model of the cardiac myocyte signalling network.** The model predicts how mechanical stretch is sensed by nine proteins to regulate transcription factors, protein synthesis, cell size and gene expression of *NPPA* (encoding atrial natriuretic peptide), *NPPB* (encoding B-type natriuretic peptide), *ATP2A2* (encoding sarcoplasmic/endoplasmic reticulum calcium ATPase), *MYH6* (encoding α-myosin heavy chain), *MYH7*

(encoding β-myosin heavy chain), *ACTA1* (encoding skeletal α-actin), *GJA1* (encoding connexin 43) and *AGT* (encoding angiotensinogen). AND logic gates indicate multiplicative activation or inhibition of the downstream node. Adapted from REF.³⁰⁹, CC-BY-4.0 (<https://creativecommons.org/licenses/by/4.0/>), and details of the model logic can be found in this publication.

When the investigators implemented these rules in a 3D biomechanical model of the canine left and right ventricles coupled to haemodynamic models of the circulation, they found that the mechanical changes induced by simulated mitral valve regurgitation indeed predicted a pattern of eccentric ventricular hypertrophy consistent with experimental observations³¹⁶. Similarly, the same growth rules under conditions of simulated aortic stenosis gave rise to a pattern of concentric hypertrophy similar to observations in canine experiments³¹⁷. Multiscale models of extracellular remodelling by mechanically stimulated fibroblast activity have also been created. Rouillard and Holmes used a technique known as agent-based modelling to simulate collagen matrix synthesis and remodelling by fibroblasts in response to physicochemical stimuli and incorporated the multicellular model into a 3D model of post-infarction scar formation in the ventricular wall³¹⁸. Taken together, these different modelling approaches provide the foundations for future, more mechanistic and integrated multiscale models that represent the biophysical mechanisms of cellular mechanotransduction of specific mechanical stimuli, the cell signalling pathways that integrate these responses, their downstream regulation of gene expression and phenotypic responses, the multicellular and tissue-scale changes in tissue structure and mechanical properties, and the feedback effects of these changes on the driving mechanical stimuli. Multiscale models could

be particularly valuable for assessing potential therapies that combine pharmacological and device-based interventions.

Conclusions

A wide range of signalling pathways have been identified that mediate mechanosensing by cardiac myocytes and fibroblasts. The molecular responses to mechanical stimuli have also been profiled with increasing scope. However, the complexity of molecular networks has challenged attempts to understand more fully how particular mechanical signals are processed and integrated to control gene expression and cardiac remodelling. Systems models of mechanosignalling have begun to provide insights into how mechanical signals are integrated from multiple mechanosensors and crosstalk with biochemical stimuli to regulate fibroblast and cardiac myocyte gene expression. These models will need to be closely integrated with extensive quantitative experiments that compare distinct mechanosignals and combinations of perturbations to mechanosensors and biochemical pathways. Such integrative systems analyses promise to integrate data across diverse experimental contexts, improve understanding of multiscale relationships and accelerate the development of therapeutics that control how mechanical stimuli remodel the heart.

Published online 25 January 2019

1. Azevedo, P. S., Polegato, B. F., Minicucci, M. F., Paiva, S. A. R. & Zornoff, L. A. M. Cardiac remodeling: concepts, clinical impact, pathophysiological mechanisms and pharmacologic treatment. *Arq. Bras. Cardiol.* **106**, 62–69 (2016).
2. Mann, D. L. Left ventricular size and shape: determinants of mechanical signal transduction pathways. *Heart Fail. Rev.* **10**, 95–100 (2005).
3. Swynghedauw, B. Darwinian evolution and cardiovascular remodeling. *Heart Fail. Rev.* **21**, 795–802 (2016).
4. Chiquet, M., Gelman, L., Lutz, R. & Maier, S. From mechanotransduction to extracellular matrix gene expression in fibroblasts. *Biochim. Biophys. Acta* **1793**, 911–920 (2009).
5. Barry, S. P., Davidson, S. M. & Townsend, P. A. Molecular regulation of cardiac hypertrophy. *Int. J. Biochem. Cell Biol.* **40**, 2023–2039 (2008).
6. Ruwhof, C. & van der Laarse, A. Mechanical stress-induced cardiac hypertrophy: mechanisms and signal transduction pathways. *Cardiovasc. Res.* **47**, 23–37 (2000).
7. Russell, B., Motlagh, D. & Ashley, W. W. Form follows function: how muscle shape is regulated by work. *J. Appl. Physiol.* **88**, 1127–1132 (2000).
8. Braunwald, E. Heart failure. *JACC Heart Fail.* **1**, 1–20 (2013).
9. Rohini, A., Agrawal, N., Koyani, C. N. & Singh, R. Molecular targets and regulators of cardiac hypertrophy. *Pharmacol. Res.* **61**, 269–280 (2010).
10. Douglas, P. S., Morrow, R., Ioli, A. & Reichel, N. Left ventricular shape, afterload and survival in idiopathic dilated cardiomyopathy. *J. Am. Coll. Cardiol.* **13**, 311–315 (1989).
11. Gupta, S., Das, B. & Sen, S. Cardiac hypertrophy: mechanisms and therapeutic opportunities. *Antioxid. Redox Signal.* **9**, 623–652 (2007).
12. Topkara, V. K. et al. Myocardial recovery in patients receiving contemporary left ventricular assist devices: results from the interagency registry for mechanically assisted circulatory support (INTERMACS). *Circ. Heart Fail.* **9**, e003157 (2016).
13. Heerdt, P. M. et al. Chronic unloading by left ventricular assist device reverses contractile dysfunction and alters gene expression in end-stage heart failure. *Circulation* **102**, 2713–2719 (2000).
14. Pinto, A. R. et al. Revisiting cardiac cellular composition. *Circ. Res.* **118**, 400–409 (2016).
15. Humphrey, J. D., Dufresne, E. R. & Schwartz, M. A. Mechanotransduction and extracellular matrix homeostasis. *Nat. Rev. Mol. Cell Biol.* **15**, 802–812 (2014).
16. Lyon, R. C., Zanella, F., Omens, J. H. & Sheikh, F. Mechanotransduction in cardiac hypertrophy and failure. *Circ. Res.* **116**, 1462–1476 (2015).
17. Herum, K. M., Lunde, I. G., McCulloch, A. D. & Christensen, G. The soft- and hard-heartedness of cardiac fibroblasts: mechanotransduction signaling pathways in fibrosis of the heart. *J. Clin. Med.* **6**, E53 (2017).
18. Zeigler, A. C., Richardson, W. J., Holmes, J. W. & Saucerman, J. J. Computational modeling of cardiac fibroblasts and fibrosis. *J. Mol. Cell. Cardiol.* **93**, 73–83 (2016).
19. Civitarese, R. A., Kapus, A., McCulloch, C. A. & Connelly, K. A. Role of integrins in mediating cardiac fibroblast-cardiomyocyte cross talk: a dynamic relationship in cardiac biology and pathophysiology. *Bas. Res. Cardiol.* **112**, 6 (2017).
20. Park, J. Y. et al. Comparative analysis of mRNA isoform expression in cardiac hypertrophy and development reveals multiple post-transcriptional regulatory modules. *PLOS ONE* **6**, e22391 (2011).
21. Wang, J. H., Thampatty, B. P., Lin, J. S. & Im, H. J. Mechanoregulation of gene expression in fibroblasts. *Gene* **391**, 1–15 (2007).
22. Lichter, J. G. et al. Remodeling of the sarcomeric cytoskeleton in cardiac ventricular myocytes during heart failure and after cardiac resynchronization therapy. *J. Mol. Cell. Cardiol.* **72**, 186–195 (2014).
23. Haque, Z. K. & Wang, D. Z. How cardiomyocytes sense pathophysiological stresses for cardiac remodeling. *Cell. Mol. Life Sci.* **74**, 983–1000 (2017).
24. Davis, J. et al. A tension-based model distinguishes hypertrophic versus dilated cardiomyopathy. *Cell* **165**, 1147–1159 (2016).
25. Pliitt, G. D., Spring, J. T., Moulton, M. J. & Agrawal, D. K. Mechanisms, diagnosis, and treatment of heart failure with preserved ejection fraction and diastolic dysfunction. *Expert Rev. Cardiovasc. Ther.* **16**, 579–589 (2018).
26. Kassi, M., Hannawi, B. & Trachtenberg, B. Recent advances in heart failure. *Curr. Opin. Cardiol.* **33**, 249–256 (2018).
27. Zhou, P. & Pu, W. T. Recounting cardiac cellular composition. *Circ. Res.* **118**, 368–370 (2016).
28. Carter, W. G., Wayner, E. A., Bouchard, T. S. & Kaur, P. The role of integrins alpha 2 beta 1 and alpha 3 beta 1 in cell-cell and cell-substrate adhesion of human epidermal cells. *J. Cell Biol.* **110**, 1387–1404 (1990).
29. Babbitt, C. J., Shai, S. Y., Harpf, A. E., Pham, C. G. & Ross, R. S. Modulation of integrins and integrin signaling molecules in the pressure-loaded murine ventricle. *Histochem. Cell Biol.* **118**, 431–439 (2002).
30. Li, R. et al. beta 1 integrin gene excision in the adult murine cardiac myocyte causes defective mechanical and signaling responses. *Am. J. Pathol.* **180**, 952–962 (2012).
31. Traister, A. et al. Integrin-linked kinase mediates force transduction in cardiomyocytes by modulating SERCA2a/PLN function. *Nat. Commun.* **5**, 4533 (2014).
32. Kostin, S. et al. The internal and external protein scaffold of the T-tubular system in cardiomyocytes. *Cell Tissue Res.* **294**, 449–460 (1998).
33. Wang, N., Butler, J. P. & Ingber, D. E. Mechanotransduction across the cell surface and through the cytoskeleton. *Science* **260**, 1124–1127 (1993).
34. Kuppaswamy, D. et al. Association of tyrosine-phosphorylated c-Src with the cytoskeleton of hypertrophying myocardium. *J. Biol. Chem.* **272**, 4500–4508 (1997).
35. Zhang, S. J., Truskey, G. A. & Kraus, W. E. Effect of cyclic stretch on beta1-D-integrin expression and activation of FAK and RhoA. *Am. J. Physiol. Cell Physiol.* **292**, C2057–C2069 (2007).
36. Israeli-Rosenberg, S., Manso, A. M., Okada, H. & Ross, R. S. Integrins and integrin-associated proteins in the cardiac myocyte. *Circ. Res.* **114**, 572–586 (2014).
37. Zemljic-Harpf, A. E. et al. Heterozygous inactivation of the vinculin gene predisposes to stress-induced cardiomyopathy. *Am. J. Pathol.* **165**, 1033–1044 (2004).
38. Manso, A. M. et al. Talin1 has unique expression versus talin 2 in the heart and modifies the hypertrophic response to pressure overload. *J. Biol. Chem.* **288**, 4252–4264 (2013).
39. Critchley, D. R. Biochemical and structural properties of the integrin-associated cytoskeletal protein talin. *Annu. Rev. Biophys.* **38**, 235–254 (2009).
40. Kovacic-Milivojevic, B. et al. Focal adhesion kinase and p130Cas mediate both sarcomeric organization and activation of genes associated with cardiac myocyte hypertrophy. *Mol. Biol. Cell* **12**, 2290–2307 (2001).

41. Pham, C. G. et al. Striated muscle-specific beta(1D)-integrin and FAK are involved in cardiac myocyte hypertrophic response pathway. *Am. J. Physiol. Heart Circ. Physiol.* **279**, H2916–H2926 (2000).
42. Travers, J. G., Kamal, F. A., Robbins, J., Yutzy, K. E. & Blaxall, B. C. Cardiac fibrosis: the fibroblast awakens. *Circ. Res.* **118**, 1021–1040 (2016).
43. Kim, S. H., Turnbull, J. & Guimond, S. Extracellular matrix and cell signalling: the dynamic cooperation of integrin, proteoglycan and growth factor receptor. *J. Endocrinol.* **209**, 139–151 (2011).
44. MacKenna, D., Summerour, S. R. & Villarreal, F. J. Role of mechanical factors in modulating cardiac fibroblast function and extracellular matrix synthesis. *Cardiovasc. Res.* **46**, 257–263 (2000).
45. Zaidel-Bar, R., Itzkovitz, S., Maayan, A., Lyengar, R. & Geiger, B. Functional atlas of the integrin adhesome. *Nat. Cell Biol.* **9**, 858–867 (2007).
46. Teoh, C. M., Tam, J. K. & Tran, T. Integrin and GPCR crosstalk in the regulation of ASM contraction signaling in asthma. *J. Allergy* **2012**, 341282 (2012).
47. Margadant, C. & Sonnenberg, A. Integrin-TGF-beta crosstalk in fibrosis, cancer and wound healing. *EMBO Rep.* **11**, 97–105 (2010).
48. MacKenna, D. A., Dolfi, F., Vuori, K. & Ruoslahti, E. Extracellular signal-regulated kinase and c-Jun NH2-terminal kinase activation by mechanical stretch is integrin-dependent and matrix-specific in rat cardiac fibroblasts. *J. Clin. Invest.* **101**, 301–310 (1998).
49. Herum, K. M., Choppe, J., Kumar, A., Engler, A. J. & McCulloch, A. D. Mechanical regulation of cardiac fibroblast profibrotic phenotypes. *Mol. Biol. Cell* **28**, 1871–1882 (2017).
50. Seong, J. et al. Distinct biophysical mechanisms of focal adhesion kinase mechanoactivation by different extracellular matrix proteins. *Proc. Natl Acad. Sci. USA* **110**, 19372–19377 (2013).
51. Hynes, R. O. Integrins: bidirectional, allosteric signaling machines. *Cell* **110**, 673–687 (2002).
52. Davis, J. & Molkenin, J. D. Myofibroblasts: trust your heart and let fate decide. *J. Mol. Cell. Cardiol.* **70**, 9–18 (2014).
53. Molkenin, J. D. et al. Fibroblast-specific genetic manipulation of p38 mitogen-activated protein kinase in vivo reveals its central regulatory role in fibrosis. *Circulation* **136**, 549–561 (2017).
54. Lapidos, K. A., Kakkar, R. & McNally, E. M. The dystrophin glycoprotein complex: signaling strength and integrity for the sarcolemma. *Circ. Res.* **94**, 1023–1031 (2004).
55. Jung, D., Yang, B., Meyer, J., Chamberlain, J. S. & Campbell, K. P. Identification and characterization of the dystrophin anchoring site on beta-dystroglycan. *J. Biol. Chem.* **270**, 27305–27310 (1995).
56. Ervasti, J. M. & Campbell, K. P. Dystrophin-associated glycoproteins: their possible roles in the pathogenesis of Duchenne muscular dystrophy. *Mol. Cell Biol. Hum. Dis. Ser.* **3**, 139–166 (1993).
57. Emery, A. E. Duchenne muscular dystrophy—Meryon's disease. *Neuromuscul. Disord.* **3**, 263–266 (1993).
58. Towbin, J. A. et al. X-Linked dilated cardiomyopathy. Molecular genetic evidence of linkage to the Duchenne muscular dystrophy (dystrophin) gene at the Xp21 locus. *Circulation* **87**, 1854–1865 (1993).
59. Lynch, G. S., Hinkle, R. T., Chamberlain, J. S., Brooks, S. V. & Faulkner, J. A. Force and power output of fast and slow skeletal muscles from mdx mice 6–28 months old. *J. Physiol.* **535**, 591–600 (2001).
60. Barnabei, M. S. & Metzger, J. M. Ex vivo stretch reveals altered mechanical properties of isolated dystrophin-deficient hearts. *PLOS ONE* **7**, e32880 (2012).
61. Garbincius, J. F. & Michele, D. E. Dystrophin-glycoprotein complex regulates muscle nitric oxide production through mechanoregulation of AMPK signaling. *Proc. Natl Acad. Sci. USA* **112**, 13663–13668 (2015).
62. Porter, J. D. et al. A chronic inflammatory response dominates the skeletal muscle molecular signature in dystrophin-deficient mdx mice. *Hum. Mol. Genet.* **11**, 263–272 (2002).
63. Chen, Y. W., Zhao, P., Borup, R. & Hoffman, E. P. Expression profiling in the muscular dystrophies: identification of novel aspects of molecular pathophysiology. *J. Cell Biol.* **151**, 1321–1336 (2000).
64. Reed, A., Kohl, P. & Peyronnet, R. Molecular candidates for cardiac stretch-activated ion channels. *Glob. Cardiol. Sci. Pract.* **2014**, 9–25 (2014).
65. Komuro, I. et al. Mechanical stretch activates the stress-activated protein kinases in cardiac myocytes. *FASEB J.* **10**, 631–636 (1996).
66. Sadoshima, J. & Izumo, S. Mechanical stretch rapidly activates multiple signal transduction pathways in cardiac myocytes: potential involvement of an autocrine/paracrine mechanism. *EMBO J.* **12**, 1681–1692 (1993).
67. Sigurdson, W., Ruknudin, A. & Sachs, F. Calcium imaging of mechanically induced fluxes in tissue-cultured chick heart: role of stretch-activated ion channels. *Am. J. Physiol.* **262**, H1110–H1115 (1992).
68. Lyford, G. L. et al. alpha(1C) (CaV1.2) L-type calcium channel mediates mechanosensitive calcium regulation. *Am. J. Physiol. Cell Physiol.* **283**, C1001–1008 (2002).
69. Peng, S.-Q., Hajela, R. K. & Atchison, W. D. Fluid flow-induced increase in inward Ba²⁺ current expressed in HEK293 cells transiently transfected with human neuronal L-type Ca²⁺ channels. *Brain Res.* **1045**, 116–125 (2005).
70. Rosa, A. O., Yamaguchi, N. & Morad, M. Mechanical regulation of native and the recombinant calcium channel. *Cell Calcium* **53**, 264–274 (2013).
71. Katanosaka, Y. et al. TRPV2 is critical for the maintenance of cardiac structure and function in mice. *Nat. Commun.* **5**, 3932 (2014).
72. Teng, J., Loukin, S., Zhou, X. & Kung, C. Yeast luminescent and Xenopus oocyte electrophysiological examinations of the molecular mechanosensitivity of TRPV4. *J. Vis. Exp.* **82**, 50816 (2013).
73. Qi, Y. et al. Uniaxial cyclic stretch stimulates TRPV4 to induce realignment of human embryonic stem cell-derived cardiomyocytes. *J. Mol. Cell. Cardiol.* **87**, 65–73 (2015).
74. Cadre, B. M. et al. Cyclic stretch down-regulates calcium transporter gene expression in neonatal rat ventricular myocytes. *J. Mol. Cell. Cardiol.* **30**, 2247–2259 (1998).
75. Jeong, D. et al. PICOT attenuates cardiac hypertrophy by disrupting calcineurin-NFAT signaling. *Circ. Res.* **102**, 711–719 (2008).
76. Finsen, A. V. et al. Syndecan-4 is essential for development of concentric myocardial hypertrophy via stretch-induced activation of the calcineurin-NFAT pathway. *PLoS ONE* **6**, e28302 (2011).
77. Peyronnet, R., Nerbonne, J. M. & Kohl, P. Cardiac mechano-gated ion channels and arrhythmias. *Circ. Res.* **118**, 311–329 (2016).
78. Striessnig, J., Ortner, N. J. & Pinggera, A. Pharmacology of L-type calcium channels: novel drugs for old targets? *Curr. Mol. Pharmacol.* **8**, 110–122 (2015).
79. Rog-Zielinska, E. A., Norris, R. A., Kohl, P. & Markwald, R. The living scar — cardiac fibroblasts and the injured heart. *Trends Mol. Med.* **22**, 99–114 (2016).
80. Kamkin, A., Kiseleva, I. & Isenberg, G. Activation and inactivation of a non-selective cation conductance by local mechanical deformation of acutely isolated cardiac fibroblasts. *Cardiovasc. Res.* **57**, 793–803 (2003).
81. Kamkin, A. et al. Cardiac fibroblasts and the mechano-electric feedback mechanism in healthy and diseased hearts. *Prog. Biophys. Mol. Biol.* **82**, 111–120 (2003).
82. Numaga-Tomita, T. et al. TRPC3-GEF-H1 axis mediates pressure overload-induced cardiac fibrosis. *Sci. Rep.* **6**, 39383 (2016).
83. Sharma, S. et al. TRPV4 ion channel is a novel regulator of dermal myofibroblast differentiation. *Am. J. Physiol. Cell Physiol.* **312**, C562–C572 (2017).
84. Adapala, R. K. et al. TRPV4 channels mediate cardiac fibroblast differentiation by integrating mechanical and soluble signals. *J. Mol. Cell. Cardiol.* **54**, 45–52 (2013).
85. Bers, D. M. Calcium cycling and signaling in cardiac myocytes. *Annu. Rev. Physiol.* **70**, 23–49 (2008).
86. Chen-Lzu, Y. & Lzu, L. T. Mechano-chemo-transduction in cardiac myocytes. *J. Physiol.* **595**, 3949–3958 (2017).
87. Ruwhof, C. et al. Mechanical stress stimulates phospholipase C activity and intracellular calcium ion levels in neonatal rat cardiomyocytes. *Cell Calcium* **29**, 73–83 (2001).
88. Gerdes, A. M. & Capasso, J. M. Structural remodeling and mechanical dysfunction of cardiac myocytes in heart failure. *J. Mol. Cell. Cardiol.* **27**, 849–856 (1995).
89. Iribe, G. et al. Axial stretch of rat single ventricular cardiomyocytes causes an acute and transient increase in Ca²⁺ spark rate. *Circ. Res.* **104**, 787–795 (2009).
90. Limbu, S., Hoang-Trong, T. M., Prosser, B. L., Lederer, W. J. & Jafri, M. S. Modeling local X-ROS and calcium signaling in the heart. *Biophys. J.* **109**, 2037–2050 (2015).
91. Prosser, B. L., Ward, C. W. & Lederer, W. J. X-ROS signaling: rapid mechano-chemo transduction in heart. *Science* **333**, 1440–1445 (2011).
92. Allen, D. G. & Kentish, J. C. The cellular basis of the length-tension relation in cardiac muscle. *J. Mol. Cell. Cardiol.* **17**, 821–840 (1985).
93. Kurihara, S. & Komukai, K. Tension-dependent changes of the intracellular Ca²⁺ transients in ferret ventricular muscles. *J. Physiol.* **489**, 617–625 (1995).
94. Morad, M., Javaheri, A., Risius, T. & Belmonte, S. Multimodality of Ca²⁺ signaling in rat atrial myocytes. *Ann. NY Acad. Sci.* **1047**, 112–121 (2005).
95. Gruver, C. L., DeMayo, F., Goldstein, M. A. & Means, A. R. Targeted developmental overexpression of calmodulin induces proliferative and hypertrophic growth of cardiomyocytes in transgenic mice. *Endocrinology* **133**, 376–388 (1993).
96. Zhang, C. L. et al. Class II histone deacetylases act as signal-responsive repressors of cardiac hypertrophy. *Cell* **110**, 479–488 (2002).
97. Linseman, D. A. et al. Inactivation of the myocyte enhancer factor-2 repressor histone deacetylase-5 by endogenous Ca(2+)//calmodulin-dependent kinase II promotes depolarization-mediated cerebellar granule neuron survival. *J. Biol. Chem.* **278**, 41472–41481 (2003).
98. Dolmetsch, R. E., Lewis, R. S., Goodnow, C. C. & Healy, J. I. Differential activation of transcription factors induced by Ca²⁺ response amplitude and duration. *Nature* **386**, 855–858 (1997).
99. Molkenin, J. D. Calcineurin-NFAT signaling regulates the cardiac hypertrophic response in coordination with the MAPKs. *Cardiovasc. Res.* **63**, 467–475 (2004).
100. Zobel, C. et al. Mechanisms of Ca²⁺-dependent calcineurin activation in mechanical stretch-induced hypertrophy. *Cardiology* **107**, 281–290 (2007).
101. Wu, Z., Wong, K., Glogauer, M., Ellen, R. P. & McCulloch, C. A. Regulation of stretch-activated intracellular calcium transients by actin filaments. *Biochem. Biophys. Res. Commun.* **261**, 419–425 (1999).
102. Rosen, L. B. & Greenberg, M. E. Stimulation of growth factor receptor signal transduction by activation of voltage-sensitive calcium channels. *Proc. Natl Acad. Sci. USA* **93**, 1113–1118 (1996).
103. Iqbal, J. & Zaidi, M. Molecular regulation of mechanotransduction. *Biochem. Biophys. Res. Commun.* **328**, 751–755 (2005).
104. Davis, J., Burr, A. R., Davis, G. F., Birnbaumer, L. & Molkenin, J. D. A TRPC6-dependent pathway for myofibroblast transdifferentiation and wound healing in vivo. *Dev. Cell* **23**, 705–715 (2012).
105. De Mello, W. C. & Danser, A. H. Angiotensin II and the heart: on the intracrine renin-angiotensin system. *Hypertension* **35**, 1183–1188 (2000).
106. Leenen, F. H., Skarda, V., Yuan, B. & White, R. Changes in cardiac ANG II postmyocardial infarction in rats: effects of nephrectomy and ACE inhibitors. *Am. J. Physiol.* **276**, H317–H325 (1999).
107. Sadoshima, J., Xu, Y., Slayter, H. S. & Izumo, S. Autocrine release of angiotensin II mediates stretch-induced hypertrophy of cardiac myocytes in vitro. *Cell* **75**, 977–984 (1993).
108. Miyata, S., Haneda, T., Osaki, J. & Kikuchi, K. Renin-angiotensin system in stretch-induced hypertrophy of cultured neonatal rat heart cells. *Eur. J. Pharmacol.* **307**, 81–88 (1996).
109. Rosenkranz, S. TGF-beta1 and angiotensin networking in cardiac remodeling. *Cardiovasc. Res.* **63**, 423–432 (2004).
110. Yamazaki, T., Komuro, I. & Yazaki, Y. Molecular aspects of mechanical stress-induced cardiac hypertrophy. *Mol. Cell. Biochem.* **163**, 197–201 (1996).
111. Aikawa, R. et al. Rho family small G proteins play critical roles in mechanical stress-induced hypertrophic responses in cardiac myocytes. *Circ. Res.* **84**, 458–466 (1999).
112. McWhinney, C. D., Hunt, R. A., Conrad, K. M., Dostal, D. E. & Baker, K. M. The type I angiotensin II receptor couples to Stat1 and Stat3 activation through Jak2 kinase in neonatal rat cardiac myocytes. *J. Mol. Cell. Cardiol.* **29**, 2513–2524 (1997).
113. Pan, J. et al. Mechanical stretch activates the JAK/STAT pathway in rat cardiomyocytes. *Circ. Res.* **84**, 1127–1136 (1999).
114. van Wamel, A. J., Ruwhof, C., van der Valk-Kokshoorn, L. E., Schrier, P. I. & van der Laarse, A. The role of angiotensin II, endothelin-1 and transforming growth factor-beta as autocrine/paracrine mediators of stretch-induced cardiomyocyte hypertrophy. *Mol. Cell. Biochem.* **218**, 113–124 (2001).
115. Wang, T. L., Yang, Y. H., Chang, H. & Hung, C. R. Angiotensin II signals mechanical stretch-induced cardiac matrix metalloproteinase expression via

- JAK-STAT pathway. *J. Mol. Cell. Cardiol.* **37**, 785–794 (2004).
116. Zou, Y. et al. Mechanical stress activates angiotensin II type 1 receptor without the involvement of angiotensin II. *Nat. Cell Biol.* **6**, 499–506 (2004).
 117. Rakesh, K. et al. beta-Arrestin-biased agonism of the angiotensin receptor induced by mechanical stress. *Sci. Signal.* **3**, ra46 (2010).
 118. Tang, W., Strachan, R. T., Lefkowitz, R. J. & Rockman, H. A. Allosteric modulation of beta-arrestin-biased angiotensin II type 1 receptor signaling by membrane stretch. *J. Biol. Chem.* **289**, 28271–28283 (2014).
 119. Jiang, G. et al. Identification of amino acid residues in angiotensin II type 1 receptor sensing mechanical stretch and function in cardiomyocyte hypertrophy. *Cell. Physiol. Biochem.* **37**, 105–116 (2015).
 120. Abraham, D. M. et al. beta-arrestin mediates the Frank-Starling mechanism of cardiac contractility. *Proc. Natl Acad. Sci. USA* **113**, 14426–14431 (2016).
 121. Leri, A. et al. Stretch-mediated release of angiotensin II induces myocyte apoptosis by activating p53 that enhances the local renin-angiotensin system and decreases the Bcl-2-to-Bax protein ratio in the cell. *J. Clin. Invest.* **101**, 1326–1342 (1998).
 122. Shyu, K. G., Chen, C. C., Wang, B. W. & Kuan, P. Angiotensin II receptor antagonist blocks the expression of connexin43 induced by cyclical mechanical stretch in cultured neonatal rat cardiac myocytes. *J. Mol. Cell. Cardiol.* **33**, 691–698 (2001).
 123. Zablocki, D. & Sadoshima, J. Solving the cardiac hypertrophy riddle: The angiotensin II-mechanical stress connection. *Circ. Res.* **113**, 1192–1195 (2013).
 124. von Lueder, T. G. & Krum, H. RAAS inhibitors and cardiovascular protection in large scale trials. *Cardiovasc. Drugs Ther.* **27**, 171–179 (2013).
 125. Porter, K. E. & Turner, N. A. Cardiac fibroblasts: at the heart of myocardial remodeling. *Pharmacol. Ther.* **123**, 255–278 (2009).
 126. Weber, K. T. Fibrosis in hypertensive heart disease: focus on cardiac fibroblasts. *J. Hypertens.* **22**, 47–50 (2004).
 127. Staufenberger, S. et al. Angiotensin II type 1 receptor regulation and differential trophic effects on rat cardiac myofibroblasts after acute myocardial infarction. *J. Cell. Physiol.* **187**, 326–335 (2001).
 128. Sun, Y., Zhang, J. Q., Zhang, J. & Ramires, F. J. Angiotensin II, transforming growth factor-beta1 and repair in the infarcted heart. *J. Mol. Cell. Cardiol.* **30**, 1559–1569 (1998).
 129. Lee, A. A., Dillmann, W. H., McCulloch, A. D. & Villarreal, F. J. Angiotensin II stimulates the autocrine production of transforming growth factor-beta 1 in adult rat cardiac fibroblasts. *J. Mol. Cell. Cardiol.* **27**, 2347–2357 (1995).
 130. Gray, M. O., Long, C. S., Kalinyak, J. E., Li, H. T. & Karliner, J. S. Angiotensin II stimulates cardiac myocyte hypertrophy via paracrine release of TGF-beta 1 and endothelin-1 from fibroblasts. *Cardiovasc. Res.* **40**, 352–363 (1998).
 131. Campbell, S. E. & Katwa, L. C. Angiotensin II stimulated expression of transforming growth factor-beta 1 in cardiac fibroblasts and myofibroblasts. *J. Mol. Cell. Cardiol.* **29**, 1947–1958 (1997).
 132. Pan, C. H., Wen, C. H. & Lin, C. S. Interplay of angiotensin II and angiotensin(1–7) in the regulation of matrix metalloproteinases of human cardiocytes. *Exp. Physiol.* **93**, 599–612 (2008).
 133. Lijnen, P., Petrov, V., van Pelt, J. & Fagard, R. Inhibition of superoxide dismutase induces collagen production in cardiac fibroblasts. *Am. J. Hypertens.* **21**, 1129–1136 (2008).
 134. Sano, M. et al. ERK and p38 MAPK, but not NF-kappaB, are critically involved in reactive oxygen species-mediated induction of IL-6 by angiotensin II in cardiac fibroblasts. *Circ. Res.* **89**, 661–669 (2001).
 135. Yokoyama, T. et al. Angiotensin II and mechanical stretch induce production of tumor necrosis factor in cardiac fibroblasts. *Am. J. Physiol.* **276**, H1968–H1976 (1999).
 136. Olson, E. R., Naugle, J. E., Zhang, X., Bomser, J. A. & Meszaros, J. G. Inhibition of cardiac fibroblast proliferation and myofibroblast differentiation by resveratrol. *Am. J. Physiol. Heart Circ. Physiol.* **288**, H1131–H1138 (2005).
 137. Bouzeghrane, F. & Thibault, G. Is angiotensin II a proliferative factor of cardiac fibroblasts? *Cardiovasc. Res.* **53**, 304–312 (2002).
 138. Chintalgattu, V., Harris, G. S., Akula, S. M. & Katwa, L. C. PPAR-gamma agonists induce the expression of VEGF and its receptors in cultured cardiac myofibroblasts. *Cardiovasc. Res.* **74**, 140–150 (2007).
 139. Chao, H. H. et al. Inhibition of angiotensin II induced endothelin-1 gene expression by 17-beta-oestradiol in rat cardiac fibroblasts. *Heart* **91**, 664–669 (2005).
 140. Pauschinger, M. et al. Dilated cardiomyopathy is associated with significant changes in collagen type I/III ratio. *Circulation* **99**, 2750–2756 (1999).
 141. Li, R. K. et al. Overexpression of transforming growth factor-beta 1 and insulin-like growth factor-1 in patients with idiopathic hypertrophic cardiomyopathy. *Circulation* **96**, 874–881 (1997).
 142. Wenzel, S., Taimor, G., Piper, H. M. & Schluter, K. D. Redox-sensitive intermediates mediate angiotensin II-induced p38 MAP kinase activation, AP-1 binding activity, and TGF-beta expression in adult ventricular cardiomyocytes. *FASEB J.* **15**, 2291–2293 (2001).
 143. Brand, T. & Schneider, M. D. The TGF beta superfamily in myocardium: ligands, receptors, transduction, and function. *J. Mol. Cell. Cardiol.* **27**, 5–18 (1995).
 144. Parker, T. G., Packer, S. E. & Schneider, M. D. Peptide growth factors can provoke “fetal” contractile protein gene expression in rat cardiac myocytes. *J. Clin. Invest.* **85**, 507–514 (1990).
 145. Koitabashi, N. et al. Pivotal role of cardiomyocyte TGF-beta signaling in the murine pathological response to sustained pressure overload. *J. Clin. Invest.* **121**, 2301–2312 (2011).
 146. Banerjee, I. et al. Cyclic stretch of embryonic cardiomyocytes increases proliferation, growth, and expression while repressing TGF-beta signaling. *J. Mol. Cell. Cardiol.* **79**, 133–144 (2015).
 147. Frangogiannis, N. G. The role of transforming growth factor (TGF)-beta in the infarcted myocardium. *J. Thorac. Dis.* **9**, S52–S63 (2017).
 148. Biernacka, A., Dobaczewski, M. & Frangogiannis, N. G. TGF-beta signaling in fibrosis. *Growth Factors* **29**, 196–202 (2011).
 149. Eghbali, M., Tomek, R., Sukhatme, V. P., Woods, C. & Bhambi, B. Differential effects of transforming growth factor-beta 1 and phorbol myristate acetate on cardiac fibroblasts. Regulation of fibrillar collagen mRNAs and expression of early transcription factors. *Circ. Res.* **69**, 483–490 (1991).
 150. Shi, Y. & Massague, J. Mechanisms of TGF-beta signaling from cell membrane to the nucleus. *Cell* **113**, 685–700 (2003).
 151. Feng, X. H. & Derynck, R. Specificity and versatility in tgf-beta signaling through Smads. *Annu. Rev. Cell Dev. Biol.* **21**, 659–693 (2005).
 152. Chen, W. & Frangogiannis, N. G. Fibroblasts in post-infarction inflammation and cardiac repair. *Biochim. Biophys. Acta* **1833**, 945–953 (2013).
 153. Lee, A. A., Delhaas, T., McCulloch, A. D. & Villarreal, F. J. Differential responses of adult cardiac fibroblasts to in vitro biaxial strain patterns. *J. Mol. Cell. Cardiol.* **31**, 1833–1843 (1999).
 154. Wipff, P. J., Rifkin, D. B., Meister, J. J. & Hinz, B. Myofibroblast contraction activates latent TGF-beta 1 from the extracellular matrix. *J. Cell Biol.* **179**, 1311–1323 (2007).
 155. van Putten, S., Shafiqyan, Y. & Hinz, B. Mechanical control of cardiac myofibroblasts. *J. Mol. Cell. Cardiol.* **93**, 133–142 (2016).
 156. Jenkins, G. The role of proteases in transforming growth factor-beta activation. *Int. J. Biochem. Cell Biol.* **40**, 1068–1078 (2008).
 157. Husse, B., Briest, W., Homagk, L., Isenberg, G. & Gekle, M. Cyclical mechanical stretch modulates expression of collagen I and collagen III by PKC and tyrosine kinase in cardiac fibroblasts. *Am. J. Physiol. Regul. Integr. Comp. Physiol.* **293**, R1898–R1907 (2007).
 158. Tyagi, S. C. et al. Stretch-induced membrane type matrix metalloproteinase and tissue plasminogen activator in cardiac fibroblast cells. *J. Cell. Physiol.* **176**, 374–382 (1998).
 159. Flynn, B. P. et al. Mechanical strain stabilizes reconstituted collagen fibrils against enzymatic degradation by mammalian collagenase matrix metalloproteinase 8 (MMP-8). *PLOS ONE* **5**, e12337 (2010).
 160. Chang, S. W., Flynn, B. P., Ruberti, J. W. & Buehler, M. J. Molecular mechanism of force induced stabilization of collagen against enzymatic breakdown. *Biomaterials* **33**, 3852–3859 (2012).
 161. Yang, J. et al. Targeting LOXL2 for cardiac interstitial fibrosis and heart failure treatment. *Nat. Commun.* **7**, 13710 (2016).
 162. Gautel, M. The sarcomeric cytoskeleton: who picks up the strain? *Curr. Opin. Cell Biol.* **23**, 39–46 (2011).
 163. Spudich, J. A. The myosin swinging cross-bridge model. *Nat. Rev. Mol. Cell Biol.* **2**, 387–392 (2001).
 164. Frank, D. & Frey, N. Cardiac Z-disc signaling network. *J. Biol. Chem.* **286**, 9897–9904 (2011).
 165. Granzier, H. L. & Labellet, S. The giant protein titin: a major player in myocardial mechanics, signaling, and disease. *Circ. Res.* **94**, 284–295 (2004).
 166. Anderson, B. R. & Granzier, H. L. Titin-based tension in the cardiac sarcomere: molecular origin and physiological adaptations. *Prog. Biophys. Mol. Biol.* **110**, 204–217 (2012).
 167. Hoshijima, M. Mechanical stress-strain sensors embedded in cardiac cytoskeleton: Z disk, titin, and associated structures. *Am. J. Physiol. Heart Circ. Physiol.* **290**, H1313–H1325 (2006).
 168. Arber, S., Halder, G. & Caroni, P. Muscle LIM protein, a novel essential regulator of myogenesis, promotes myogenic differentiation. *Cell* **79**, 221–231 (1994).
 169. Heineke, J. et al. Attenuation of cardiac remodeling after myocardial infarction by muscle LIM protein-calcineurin signaling at the sarcomeric Z-disc. *Proc. Natl Acad. Sci. USA* **102**, 1655–1660 (2005).
 170. Knoll, R. et al. The cardiac mechanical stretch sensor machinery involves a Z disc complex that is defective in a subset of human dilated cardiomyopathy. *Cell* **111**, 945–955 (2002).
 171. Chang, D. F. et al. Cysteine-rich LIM-only proteins CRP1 and CRP2 are potent smooth muscle differentiation cofactors. *Dev. Cell* **4**, 107–118 (2003).
 172. Linke, W. A. & Kruger, M. The giant protein titin as an integrator of myocyte signaling pathways. *Physiology* **25**, 186–198 (2010).
 173. Sheikh, F. et al. An FHLL1-containing complex within the cardiomyocyte sarcomere mediates hypertrophic biomechanical stress responses in mice. *J. Clin. Invest.* **118**, 3870–3880 (2008).
 174. Chu, P. H., Ruiz-Lozano, P., Zhou, Q., Cai, C. & Chen, J. Expression patterns of FHU/LIM family members suggest important functional roles in skeletal muscle and cardiovascular system. *Mech. Dev.* **95**, 259–265 (2000).
 175. Gausson, V. et al. Common genomic response in different mouse models of beta-adrenergic-induced cardiomyopathy. *Circulation* **108**, 2926–2933 (2003).
 176. Raskin, A. et al. A novel mechanism involving four-and-a-half LIM domain protein-1 and extracellular signal-regulated kinase-2 regulates titin phosphorylation and mechanics. *J. Biol. Chem.* **287**, 29273–29284 (2012).
 177. Miller, M. K. et al. The muscle ankyrin repeat proteins: CARP, ankrd2/Arpp and DARP as a family of titin filament-based stress response molecules. *J. Mol. Biol.* **333**, 951–964 (2003).
 178. Barash, I. A., Mathew, L., Ryan, A. F., Chen, J. & Lieber, R. L. Rapid muscle-specific gene expression changes after a single bout of eccentric contractions in the mouse. *Am. J. Physiol. Cell Physiol.* **286**, C355–C364 (2004).
 179. Lun, A. S., Chen, J. & Lange, S. Probing muscle ankyrin-repeat protein (MARP) structure and function. *Anat. Rec.* **297**, 1615–1629 (2014).
 180. Ingber, D. E., Wang, N. & Stamenovic, D. Tensegrity, cellular biophysics, and the mechanics of living systems. *Rep. Prog. Phys.* **77**, 046603 (2014).
 181. Amano, M., Nakayama, M. & Kaibuchi, K. Rho-kinase/ROCK: a key regulator of the cytoskeleton and cell polarity. *Cytoskeleton* **67**, 545–554 (2010).
 182. Moulleron, S., Langer, C. A., Guettler, S., McDonald, N. O. & Treisman, R. Structure of a pentavalent G-actin*MRTF-A complex reveals how G-actin controls nucleocytoplasmic shuttling of a transcriptional coactivator. *Sci. Signal.* **4**, ra40 (2011).
 183. Small, E. M. et al. Myocardin-related transcription factor-a controls myofibroblast activation and fibrosis in response to myocardial infarction. *Circ. Res.* **107**, 294–304 (2010).
 184. Codellia, V. A., Sun, G. & Irvine, K. D. Regulation of YAP by mechanical strain through Jnk and Hippo signaling. *Curr. Biol.* **24**, 2012–2017 (2014).
 185. Aragona, M. et al. A mechanical checkpoint controls multicellular growth through YAP/TAZ regulation by actin-processing factors. *Cell* **154**, 1047–1059 (2013).
 186. Muehlich, S., Rehm, M., Ebenau, A. & Goppelt-Strube, M. Synergistic induction of CTGF by cytochalasin D and TGFbeta-1 in primary human renal epithelial cells: role of transcriptional regulators MKL1, YAP/TAZ and Smad2/3. *Cell. Signal.* **29**, 31–40 (2017).
 187. Liu, F. et al. Mechanosignaling through YAP and TAZ drives fibroblast activation and fibrosis. *Am. J. Physiol. Lung Cell. Mol. Physiol.* **308**, L344–L357 (2015).
 188. Chan, M. W., Hinz, B. & McCulloch, C. A. Mechanical induction of gene expression in connective tissue cells. *Methods Cell Biol.* **98**, 178–205 (2010).

189. Fedorchak, G. R., Kaminski, A. & Lammerding, J. Cellular mechanosensing: getting to the nucleus of it all. *Prog. Biophys. Mol. Biol.* **115**, 76–92 (2014).
190. Crisp, M. et al. Coupling of the nucleus and cytoplasm: role of the LINC complex. *J. Cell Biol.* **172**, 41–53 (2006).
191. Lammerding, J., Kamm, R. D. & Lee, R. T. Mechanotransduction in cardiac myocytes. *Ann. NY Acad. Sci.* **1015**, 53–70 (2004).
192. Eryedi, B. & Niethammer, P. Nuclear membrane stretch and its role in mechanotransduction. *Nucleus* **8**, 156–161 (2017).
193. Caputo, S. et al. The carboxyl-terminal nucleoplasmic region of MAN1 exhibits a DNA binding winged helix domain. *J. Biol. Chem.* **281**, 18208–18215 (2006).
194. Chang, W., Worman, H. J. & Gundersen, G. G. Accessorizing and anchoring the LINC complex for multifunctionality. *J. Cell Biol.* **208**, 11–22 (2015).
195. Guilluy, C. et al. Isolated nuclei adapt to force and reveal a mechanotransduction pathway in the nucleus. *Nat. Cell Biol.* **16**, 376–381 (2014).
196. Cupesi, M. et al. Attenuated hypertrophic response to pressure overload in a lamin A/C haploinsufficiency mouse. *J. Mol. Cell. Cardiol.* **48**, 1290–1297 (2010).
197. Eryedi, B., Jelcic, M. & Niethammer, P. The cell nucleus serves as a mechanotransducer of tissue damage-induced inflammation. *Cell* **165**, 1160–1170 (2016).
198. Schreiber, K. H. & Kennedy, B. K. When lamins go bad: nuclear structure and disease. *Cell* **152**, 1365–1375 (2013).
199. Komaki, H. et al. Inflammatory changes in infantile-onset LMNA-associated myopathy. *Neuromuscul. Disord.* **21**, 563–568 (2011).
200. Iyer, K. V., Pulford, S., Mogilner, A. & Shivashankar, G. V. Mechanical activation of cells induces chromatin remodeling preceding MKL nuclear transport. *Biophys. J.* **103**, 1416–1428 (2012).
201. Furusawa, T. et al. Chromatin decompaction by the nucleosomal binding protein HMG5 impairs nuclear sturdiness. *Nat. Commun.* **6**, 6138 (2015).
202. Rochman, M. et al. The interaction of NSBP1/HMG5 with nucleosomes in euchromatin counteracts linker histone-mediated chromatin compaction and modulates transcription. *Mol. Cell* **35**, 642–656 (2009).
203. Nikolova, V. et al. Defects in nuclear structure and function promote dilated cardiomyopathy in lamin A/C-deficient mice. *J. Clin. Invest.* **113**, 357–369 (2004).
204. Ho, C. Y., Jaalouk, D. E., Vartiainen, M. K. & Lammerding, J. Lamin A/C and emerin regulate MKL1-SRF activity by modulating actin dynamics. *Nature* **497**, 507–511 (2013).
205. Thomas, C. H., Collier, J. H., Sfeir, C. S. & Healy, K. E. Engineering gene expression and protein synthesis by modulation of nuclear shape. *Proc. Natl Acad. Sci. USA* **99**, 1972–1977 (2002).
206. Alam, S. G. et al. The mammalian LINC complex regulates genome transcriptional responses to substrate rigidity. *Sci. Rep.* **6**, 38063 (2016).
207. Lovett, D. B., Shekhar, N., Nickerson, J. A., Roux, K. J. & Lele, T. P. Modulation of nuclear shape by substrate rigidity. *Cell. Mol. Bioeng.* **6**, 230–238 (2013).
208. Vermij, S. H., Abriel, H. & van Veen, T. A. Refining the molecular organization of the cardiac intercalated disc. *Cardiovasc. Res.* **113**, 259–275 (2017).
209. Sheikh, F., Ross, R. S. & Chen, J. Cell-cell connection to cardiac disease. *Trends Cardiovasc. Med.* **19**, 182–190 (2009).
210. Yoshida, M. et al. Weaving hypothesis of cardiomyocyte sarcomeres: discovery of periodic broadening and narrowing of intercalated disk during volume-load change. *Am. J. Pathol.* **176**, 660–678 (2010).
211. Mezzano, V. & Sheikh, F. Cell-cell junction remodeling in the heart: possible role in cardiac conduction system function and arrhythmias? *Life Sci.* **90**, 313–321 (2012).
212. Michaelson, J. E. & Huang, H. Cell-cell junctional proteins in cardiovascular mechanotransduction. *Ann. Biomed. Engineer.* **40**, 568–577 (2012).
213. Chopra, A., Tabdanov, E., Patel, H., Janmey, P. A. & Kresh, J. Y. Cardiac myocyte remodeling mediated by N-cadherin-dependent mechanosensing. *Am. J. Physiol. Heart Circ. Physiol.* **300**, H1252–H1266 (2011).
214. Kostetskii, I. et al. Induced deletion of the N-cadherin gene in the heart leads to dissolution of the intercalated disc structure. *Circ. Res.* **96**, 346–354 (2005).
215. Yonemura, S., Wada, Y., Watanabe, T., Nagafuchi, A. & Shibata, M. alpha-Catenin as a tension transducer that induces adherens junction development. *Nat. Cell Biol.* **12**, 533–542 (2010).
216. Vite, A., Zhang, C., Yi, R., Ems, S. & Radice, G. L. alpha-Catenin-dependent cytoskeletal tension controls Yap activity in the heart. *Development* **145**, dev149823 (2018).
217. Sheikh, F. et al. alpha-E-catenin inactivation disrupts the cardiomyocyte adherens junction, resulting in cardiomyopathy and susceptibility to wall rupture. *Circulation* **114**, 1046–1055 (2006).
218. Eher, E. et al. Alterations at the intercalated disk associated with the absence of muscle LIM protein. *J. Cell Biol.* **153**, 763–772 (2001).
219. Zhang, J. Q. et al. Ultrastructural and biochemical localization of N-RAP at the interface between myofibrils and intercalated disks in the mouse heart. *Biochemistry* **40**, 14898–14906 (2001).
220. Hariharan, V. et al. Arrhythmogenic right ventricular cardiomyopathy mutations alter shear response without changes in cell-cell adhesion. *Cardiovasc. Res.* **104**, 280–289 (2014).
221. Yang, Z. et al. Desmosomal dysfunction due to mutations in desmoplakin causes arrhythmogenic right ventricular dysplasia/cardiomyopathy. *Circ. Res.* **99**, 646–655 (2006).
222. Lyon, R. C. et al. Connexin defects underlie arrhythmogenic right ventricular cardiomyopathy in a novel mouse model. *Hum. Mol. Genet.* **23**, 1134–1150 (2014).
223. Pillichou, K. et al. Mutations in desmoglein-2 gene are associated with arrhythmogenic right ventricular cardiomyopathy. *Circulation* **113**, 1171–1179 (2006).
224. Salameh, A. et al. Opposing and synergistic effects of cyclic mechanical stretch and alpha- or beta-adrenergic stimulation on the cardiac gap junction protein Cx43. *Pharmacol. Res.* **62**, 506–513 (2010).
225. Zhuang, J., Yamada, K. A., Saffitz, J. E. & Kleber, A. G. Pulsatile stretch remodels cell-to-cell communication in cultured myocytes. *Circ. Res.* **87**, 316–322 (2000).
226. Wang, Q. et al. Xin proteins and intercalated disc maturation, signaling and diseases. *Front. Biosci.* **17**, 2566–2593 (2012).
227. Chilton, L. et al. K⁺ currents regulate the resting membrane potential, proliferation, and contractile responses in ventricular fibroblasts and myofibroblasts. *Am. J. Physiol. Heart Circ. Physiol.* **288**, H2931–H2939 (2005).
228. Miragoli, M., Gaudesius, G. & Rohr, S. Electrotonic modulation of cardiac impulse conduction by myofibroblasts. *Circ. Res.* **98**, 801–810 (2006).
229. Rohr, S. Myofibroblasts in diseased hearts: new players in cardiac arrhythmias? *Heart Rhythm* **6**, 848–856 (2009).
230. Kohl, P., Camelliti, P., Burton, F. L. & Smith, G. L. Electrical coupling of fibroblasts and myocytes: relevance for cardiac propagation. *J. Electrocardiol.* **38**, 45–50 (2005).
231. Zlochiver, S. et al. Electrotonic myofibroblast-to-myocyte coupling increases propensity to reentrant arrhythmias in two-dimensional cardiac monolayers. *Biophys. J.* **95**, 4469–4480 (2008).
232. Rohr, S. Arrhythmogenic implications of fibroblast-myocyte interactions. *Circ. Arrhythm. Electrophysiol.* **5**, 442–452 (2012).
233. Quinn, T. A. et al. Electrotonic coupling of excitable and nonexcitable cells in the heart revealed by optogenetics. *Proc. Natl Acad. Sci. USA* **113**, 14852–14857 (2016).
234. Ongstad, E. & Kohl, P. Fibroblast-myocyte coupling in the heart: potential relevance for therapeutic interventions. *J. Mol. Cell. Cardiol.* **91**, 238–246 (2016).
235. Roell, W. et al. Overexpression of Cx43 in cells of the myocardial scar: correction of post-infarct arrhythmias through heterotypic cell-cell coupling. *Sci. Rep.* **8**, 7145 (2018).
236. Shyu, K. G., Ko, W. H., Yang, W. S., Wang, B. W. & Kuan, P. Insulin-like growth factor-1 mediates stretch-induced upregulation of myostatin expression in neonatal rat cardiomyocytes. *Cardiovasc. Res.* **68**, 405–414 (2005).
237. Pemberton, C. J., Raudsepp, S. D., Yandle, T. G., Cameron, V. A. & Richards, A. M. Plasma cardiotrophin-1 is elevated in human hypertension and stimulated by ventricular stretch. *Cardiovasc. Res.* **68**, 109–117 (2005).
238. Bowers, S. L. K., Borg, T. K. & Baudino, T. A. The dynamics of fibroblast–myocyte–capillary interactions in the heart. *Ann. NY Acad. Sci.* **1188**, 143–152 (2010).
239. Weinberg, E. O. et al. Sex dependence and temporal dependence of the left ventricular genomic response to pressure overload. *Physiol. Genom.* **12**, 113–127 (2003).
240. Wang, D. et al. Effects of pressure overload on extracellular matrix expression in the heart of the atrial natriuretic peptide-null mouse. *Hypertension* **42**, 88–95 (2003).
241. Miyazaki, H. et al. Comparison of gene expression profiling in pressure and volume overload-induced myocardial hypertrophies in rats. *Hypertens. Res.* **29**, 1029–1045 (2006).
242. Zheng, J. et al. Microarray identifies extensive downregulation of noncollagen extracellular matrix and profibrotic growth factor genes in chronic isolated mitral regurgitation in the dog. *Circulation* **119**, 2086–2095 (2009).
243. Blaxall, B. C., Tschannen-Moran, B. M., Milano, C. A. & Koch, W. J. Differential gene expression and genomic patient stratification following left ventricular assist device support. *J. Am. Coll. Cardiol.* **41**, 1096–1106 (2003).
244. Birks, E. J. et al. Gene profiling changes in cytoskeletal proteins during clinical recovery after left ventricular-assist device support. *Circulation* **112**, 157–64 (2005).
245. Margulies, K. B. et al. Mixed messages: transcription patterns in failing and recovering human myocardium. *Circ. Res.* **96**, 592–599 (2005).
246. Matkovich, S. J. et al. Reciprocal regulation of myocardial microRNAs and messenger RNA in human cardiomyopathy and reversal of the microRNA signature by biomechanical support. *Circulation* **119**, 1263–1271 (2009).
247. Yang, K. C. et al. Deep RNA sequencing reveals dynamic regulation of myocardial noncoding RNAs in failing human heart and remodeling with mechanical circulatory support. *Circulation* **129**, 1009–1021 (2014).
248. Terracciano, C. M. et al. Clinical recovery from end-stage heart failure using left-ventricular assist device and pharmacological therapy correlates with increased sarcoplasmic reticulum calcium content but not with regression of cellular hypertrophy. *Circulation* **109**, 2263–2265 (2004).
249. Weinberg, E. O. et al. Expression and regulation of ST2, an interleukin-1 receptor family member, in cardiomyocytes and myocardial infarction. *Circulation* **106**, 2961–2966 (2002).
250. Kakkar, R. & Lee, R. T. The IL-33/ST2 pathway: therapeutic target and novel biomarker. *Nat. Rev. Drug Discov.* **7**, 827–840 (2008).
251. de Boer, R. A., Daniels, L. B., Maisel, A. S. & Januzzi, J. L. Jr. State of the Art: Newer biomarkers in heart failure. *Eur. J. Heart Fail.* **17**, 559–569 (2015).
252. Frank, D. et al. Gene expression pattern in biomechanically stretched cardiomyocytes: evidence for a stretch-specific gene program. *Hypertension* **51**, 309–318 (2008).
253. McCain, M. L., Sheehy, S. P., Grosberg, A., Goss, J. A. & Parker, K. K. Recapitulating maladaptive, multiscale remodeling of failing myocardium on a chip. *Proc. Natl Acad. Sci. USA* **110**, 9770–9775 (2013).
254. Rysa, J., Tokola, H. & Ruskoaho, H. Mechanical stretch induced transcriptomic profiles in cardiac myocytes. *Sci. Rep.* **8**, 4733 (2018).
255. Kessler, D. et al. Fibroblasts in mechanically stressed collagen lattices assume a “synthetic” phenotype. *J. Biol. Chem.* **276**, 36575–36585 (2001).
256. Driesen, R. B. et al. Reversible and irreversible differentiation of cardiac fibroblasts. *Cardiovasc. Res.* **101**, 411–422 (2014).
257. Haggart, C. R., Ames, E. G., Lee, J. K. & Holmes, J. W. Effects of stretch and shortening on gene expression in intact myocardium. *Physiol. Genomics* **46**, 57–65 (2014).
258. Hirt, M. N. et al. Increased afterload induces pathological cardiac hypertrophy: a new in vitro model. *Bas. Res. Cardiol.* **107**, 307 (2012).
259. Boon, R. A. & Dimmeler, S. MicroRNAs in myocardial infarction. *Nat. Rev. Cardiol.* **12**, 135–142 (2015).
260. van Rooij, E. et al. A signature pattern of stress-responsive microRNAs that can evoke cardiac hypertrophy and heart failure. *Proc. Natl Acad. Sci. USA* **103**, 18255–18260 (2006).
261. Frank, D. et al. MicroRNA-20a inhibits stress-induced cardiomyocyte apoptosis involving its novel target Egn3/PHD3. *J. Mol. Cell. Cardiol.* **52**, 711–717 (2012).
262. van Rooij, E. et al. Control of stress-dependent cardiac growth and gene expression by a microRNA. *Science* **316**, 575–579 (2007).
263. Callis, T. E. et al. MicroRNA-208a is a regulator of cardiac hypertrophy and conduction in mice. *J. Clin. Invest.* **119**, 2772–2786 (2009).
264. Shyu, K. G., Wang, B. W., Wu, G. J., Lin, C. M. & Chang, H. Mechanical stretch via transforming growth factor-beta1 activates microRNA208a to regulate endoglin expression in cultured rat cardiac myoblasts. *Eur. J. Heart Fail.* **15**, 36–45 (2013).

265. Wang, B. W., Wu, G. J., Cheng, W. P. & Shyu, K. G. Mechanical stretch via transforming growth factor-beta1 activates microRNA-208a to regulate hypertrophy in cultured rat cardiac myocytes. *J. Formos. Med. Assoc.* **112**, 635–643 (2013).
266. Ransohoff, J. D., Wei, Y. & Khavari, P. A. The functions and unique features of long intergenic non-coding RNA. *Nat. Rev. Mol. Cell Biol.* **19**, 143–157 (2018).
267. Sallam, T., Sandhu, J. & Tontozog, P. Long noncoding RNA discovery in cardiovascular disease: decoding form to function. *Circ. Res.* **122**, 155–166 (2018).
268. Carrion, K. et al. The long non-coding HOTAIR is modulated by cyclic stretch and WNT/beta-CATENIN in human aortic valve cells and is a novel repressor of calcification genes. *PLOS ONE* **9**, e96577 (2014).
269. Yang, J. H. & Saucerman, J. J. Computational models reduce complexity and accelerate insight into cardiac signaling networks. *Circ. Res.* **108**, 85–97 (2011).
270. Noble, D. Modeling the heart—from genes to cells to the whole organ. *Science* **295**, 1678–1682 (2002).
271. Huxley, A. F. Muscle structure and theories of contraction. *Prog. Biophys. Biophys. Chem.* **7**, 255–318 (1957).
272. Noble, D. Cardiac action and pacemaker potentials based on the Hodgkin-Huxley equations. *Nature* **188**, 495–497 (1960).
273. Jafri, M. S., Rice, J. J. & Winslow, R. L. Cardiac Ca²⁺ dynamics: the roles of ryanodine receptor adaptation and sarcoplasmic reticulum load. *Biophys. J.* **74**, 1149–1168 (1998).
274. Luo, C. H. & Rudy, Y. A dynamic model of the cardiac ventricular action potential. Afterdepolarizations, II. triggered activity, and potentiation. *Circ. Res.* **74**, 1097–1113 (1994).
275. Cortassa, S., Aon, M. A., Marban, E., Winslow, R. L. & O'Rourke, B. An integrated model of cardiac mitochondrial energy metabolism and calcium dynamics. *Biophys. J.* **84**, 2734–2755 (2003).
276. Beard, D. A. A biophysical model of the mitochondrial respiratory system and oxidative phosphorylation. *PLoS Comput. Biol.* **1**, e36 (2005).
277. Saucerman, J. J., Brunton, L. L., Michailova, A. P. & McCulloch, A. D. Modeling beta-adrenergic control of cardiac myocyte contractility in silico. *J. Biol. Chem.* **278**, 47997–48003 (2003).
278. Hund, T. J. & Rudy, Y. Rate dependence and regulation of action potential and calcium transient in a canine cardiac ventricular cell model. *Circulation* **110**, 3168–3174 (2004).
279. Winslow, R. L., Rice, J. J., Jafri, S., Marban, E. & O'Rourke, B. Mechanisms of altered excitation-contraction coupling in canine tachycardia-induced heart failure, II: model studies. *Circ. Res.* **84**, 571–586 (1999).
280. Kang, J. H., Lee, H. S., Kang, Y. W. & Cho, K. H. Systems biological approaches to the cardiac signaling network. *Brief Bioinform.* **17**, 419–428 (2016).
281. Tavi, P. et al. Pacing-induced calcineurin activation controls cardiac Ca²⁺ signalling and gene expression. *J. Physiol.* **554**, 309–320 (2004).
282. Berridge, M. J., Bootman, M. D. & Roderick, H. L. Calcium signalling: dynamics, homeostasis and remodelling. *Nat. Rev. Mol. Cell Biol.* **4**, 517–529 (2003).
283. Colella, M. et al. Ca²⁺ oscillation frequency decoding in cardiac cell hypertrophy: role of calcineurin/NFAT as Ca²⁺ signal integrators. *Proc. Natl Acad. Sci. USA* **105**, 2859–2864 (2008).
284. Saucerman, J. J. & Bers, D. M. Calmodulin mediates differential sensitivity of CaMKII and calcineurin to local Ca²⁺ in cardiac myocytes. *Biophys. J.* **95**, 4597–4612 (2008).
285. Cooling, M. T., Hunter, P. & Crampin, E. J. Sensitivity of NFAT cycling to cytosolic calcium concentration: implications for hypertrophic signals in cardiac myocytes. *Biophys. J.* **96**, 2095–2104 (2009).
286. Cooling, M., Hunter, P. & Crampin, E. J. Modeling hypertrophic IP₃ transients in the cardiac myocyte. *Biophys. J.* **93**, 3421–3433 (2007).
287. Shin, S. Y., Yang, H. W., Kim, J. R., Heo, W. D. & Cho, K. H. A hidden incoherent switch regulates RCAN1 in the calcineurin-NFAT signaling network. *J. Cell Sci.* **124**, 82–90 (2011).
288. Ryall, K. A. et al. Network reconstruction and systems analysis of cardiac myocyte hypertrophy signaling. *J. Biol. Chem.* **287**, 42259–42268 (2012).
289. Molkenkin, J. D. & Robbins, J. With great power comes great responsibility: using mouse genetics to study cardiac hypertrophy and failure. *J. Mol. Cell. Cardiol.* **46**, 130–136 (2009).
290. Cook, S. A., Clerk, A. & Sugden, P. H. Are transgenic mice the 'alkalhest' to understanding myocardial hypertrophy and failure? *J. Mol. Cell. Cardiol.* **46**, 118–129 (2009).
291. Frank, D. U., Sutcliffe, M. D. & Saucerman, J. J. Network-based predictions of in vivo cardiac hypertrophy. *J. Mol. Cell. Cardiol.* **121**, 180–189 (2018).
292. Cheng, B. et al. Cellular mechanosensing of the biophysical microenvironment: A review of mathematical models of biophysical regulation of cell responses. *Phys. Life Rev.* **22–23**, 88–119 (2017).
293. Novak, I. L., Slepchenko, B. M., Mogilner, A. & Loew, L. M. Cooperativity between cell contractility and adhesion. *Phys. Rev. Lett.* **93**, 268109 (2004).
294. Deshpande, V. S., McMeeking, R. M. & Evans, A. G. A bio-chemo-mechanical model for cell contractility. *Proc. Natl Acad. Sci. USA* **103**, 14015–14020 (2006).
295. Chen, K. et al. Role of boundary conditions in determining cell alignment in response to stretch. *Proc. Natl Acad. Sci. USA* **115**, 986–991 (2018).
296. Grosberg, A. et al. Self-organization of muscle cell structure and function. *PLOS Comput. Biol.* **7**, e1001088 (2011).
297. Livne, A. & Geiger, B. The inner workings of stress fibers - from contractile machinery to focal adhesions and back. *J. Cell Sci.* **129**, 1293–1304 (2016).
298. Yuan, H., Marzban, B. & Kit Parker, K. Myofibrils in cardiomyocytes tend to assemble along the maximal principle stress directions. *J. Biomech. Eng.* **139**, 121010 (2017).
299. McCain, M. L., Lee, H., Aratyn-Schaus, Y., Kleber, A. G. & Parker, K. K. Cooperative coupling of cell-matrix and cell-cell adhesions in cardiac muscle. *Proc. Natl Acad. Sci. USA* **109**, 9881–9886 (2012).
300. Lee, L. C., Kassab, G. S. & Guccione, J. M. Mathematical modeling of cardiac growth and remodeling. *Wiley Interdiscip. Rev. Syst. Biol. Med.* **8**, 211–226 (2016).
301. Dingal, P. C. & Discher, D. E. Systems mechanobiology: tension-inhibited protein turnover is sufficient to physically control gene circuits. *Biophys. J.* **107**, 2734–2743 (2014).
302. Sharp, W. W., Terracio, L., Borg, T. K. & Samarel, A. M. Contractile activity modulates actin synthesis and turnover in cultured neonatal rat heart cells. *Circ. Res.* **73**, 172–183 (1993).
303. Schroer, A. K., Ryzhova, L. M. & Merryman, W. D. Network modeling approach to predict myofibroblast differentiation. *Cell. Mol. Bioengineer.* **7**, 446–459 (2014).
304. Dupont, S. et al. Role of YAP/TAZ in mechanotransduction. *Nature* **474**, 179–183 (2011).
305. Sun, M., Spill, F. & Zaman, M. H. A. Computational model of YAP/TAZ mechanosensing. *Biophys. J.* **110**, 2540–2550 (2016).
306. Yang, X. et al. LATS1 tumour suppressor affects cytokinesis by inhibiting LIMK1. *Nat. Cell Biol.* **6**, 609–617 (2004).
307. Zeigler, A. C., Richardson, W. J., Holmes, J. W. & Saucerman, J. J. A computational model of cardiac fibroblast signaling predicts context-dependent drivers of myofibroblast differentiation. *J. Mol. Cell. Cardiol.* **94**, 72–81 (2016).
308. Khalil, H. et al. Fibroblast-specific TGF-beta-Smad2/3 signaling underlies cardiac fibrosis. *J. Clin. Invest.* **127**, 3770–3783 (2017).
309. Tan, P. M., Buchholz, K. S., Omens, J. H., McCulloch, A. D. & Saucerman, J. J. Predictive model identifies key network regulators of cardiomyocyte mechano-signaling. *PLOS Comput. Biol.* **13**, e1005854 (2017).
310. Lu, H. I. et al. Entresto therapy effectively protects heart and lung against transverse aortic constriction induced cardiopulmonary syndrome injury in rat. *Am. J. Transl Res.* **10**, 2290–2305 (2018).
311. von Lueder, T. G. et al. Angiotensin receptor neprilysin inhibitor LCZ696 attenuates cardiac remodeling and dysfunction after myocardial infarction by reducing cardiac fibrosis and hypertrophy. *Circ. Heart Fail.* **8**, 71–78 (2015).
312. Suematsu, Y. et al. LCZ696 (Sacubitril/Valsartan), an angiotensin-receptor neprilysin inhibitor, attenuates cardiac hypertrophy, fibrosis, and vasculopathy in a rat model of chronic kidney disease. *J. Card. Fail.* **24**, 266–275 (2018).
313. Ambrosi, D. et al. Perspectives on biological growth and remodeling. *J. Mech. Phys. Solids* **59**, 863–883 (2011).
314. Witzenburg, C. M. & Holmes, J. W. A. Comparison of phenomenologic growth laws for myocardial hypertrophy. *J. Elast.* **129**, 257–281 (2017).
315. Kerckhoffs, R. C., Omens, J. & McCulloch, A. D. A single strain-based growth law predicts concentric and eccentric cardiac growth during pressure and volume overload. *Mech. Res. Commun.* **42**, 40–50 (2012).
316. Young, A. A., Orr, R., Small, B. H. & Dell'Italia, L. J. Three-dimensional changes in left and right ventricular geometry in chronic mitral regurgitation. *Am. J. Physiol.* **271**, H2689–H2700 (1996).
317. Nagatomo, Y. et al. Translational mechanisms accelerate the rate of protein synthesis during canine pressure-overload hypertrophy. *Am. J. Physiol.* **277**, H2176–H2184 (1999).
318. Rouillard, A. D. & Holmes, J. W. Coupled agent-based and finite-element models for predicting scar structure following myocardial infarction. *Prog. Biophys. Mol. Biol.* **115**, 235–243 (2014).
319. Yamamoto, K. et al. Regulation of cardiomyocyte mechanotransduction by the cardiac cycle. *Circulation* **103**, 1459–1464 (2001).
320. Russell, B., Curtis, M. W., Koshman, Y. E. & Samarel, A. M. Mechanical stress-induced sarcomere assembly for cardiac muscle growth in length and width. *J. Mol. Cell. Cardiol.* **48**, 817–823 (2010).
321. DrugMonkey. Generalization, not "reproducibility". *Scientopia* <http://drugmonkey.scientopia.org/2018/02/26/generalization-not-reproducibility/> (2018).
322. Boerma, M. et al. Microarray analysis of gene expression profiles of cardiac myocytes and fibroblasts after mechanical stress, ionising or ultraviolet radiation. *BMC Genomics* **6**, 6 (2005).

Acknowledgements

The authors acknowledge the following funding sources: US National Science Foundation grant 1252854 (J.J.S.); NIH grants R01 HL137755 (J.J.S.), R01 HL137100 (A.D.M.) and U01 HL127564; and US Department of Defense PR 150090 (supporting J.H.O.).

Author contributions

All the authors researched data for the article, discussed its contents and reviewed and edited the manuscript before submission. J.J.S., A.D.M. and J.H.O. wrote the manuscript.

Competing interests

A.D.M. and J.H.O. are co-founders of and have an equity interest in Insilicomed, and A.D.M. has an equity interest in Vektor Medical. A.D.M. and J.H.O. serve on the scientific advisory board of Insilicomed, and A.D.M. is a scientific adviser to both companies. Some of their research grants have been identified for conflict of interest management on the basis of the overall scope of the project and its potential benefit to these companies. The authors are required to disclose this relationship in publications acknowledging the grant support; however, the research subject and findings reported in this Review did not involve the companies in any way and have no specific relationship with the business activities or scientific interests of either company. The terms of this arrangement have been reviewed and approved by the University of California San Diego in accordance with its conflict of interest policies. J.J.S., P.M.T. and K.S.B. declare no competing interests.

Publisher's note

Springer Nature remains neutral with regard to jurisdictional claims in published maps and institutional affiliations.

Reviewer information

Nature Reviews Cardiology thanks P. Kohl and the other anonymous reviewer(s), for their contribution to the peer review of this work.